TELOMERASE REVERSE TRANSCRIPTASE (TERT) REGULATION BY ACTIVATING PROMOTER MUTATIONS AND ALLELE-SPECIFIC TRANSCRIPTIONAL REGULATION IN THYROID CANCER CELLS

by
Brittany Avin McKelvey

A dissertation submitted to Johns Hopkins University in conformity with the requirements for the degree of Doctor of Philosophy

Baltimore, Maryland
October 2020

Abstract

Telomerase activity is low to absent in somatic cells, but reactivated in over ninety percent of malignancies, allowing for prolonged cellular proliferation which would otherwise be limited by critical telomere shortening. *TERT*, the catalytic subunit of telomerase, is regulated via multiple mechanisms, including activating promoter mutations, promoter methylation, histone modifications, and alternative splicing. However, it remains poorly understood how these regulatory strategies cooperate to activate telomerase or how structural changes such as *TERT* promoter mutations serve to further increase telomerase expression.

Herein, we have characterized *TERT* promoter methylation in differentiated thyroid cancer (DTC) cell lines and normal thyroid tissue by targeted bisulfite sequencing for the first time. Consistent with reports in other cancers, we found localized hypomethylation of the minimal promoter immediately surrounding the transcription start site, including patterns suggesting allele-specific methylation. Further upstream, the promoter was densely methylated, but with foci of hypomethylation harboring previously unreported binding sites for the transcriptional activators MYC and GSC.

To further investigate allele-specific methylation, we utilized nanopore Cas9 targeted sequencing in DTC cell lines heterozygous for the *TERT* promoter mutation, and found the mutant *TERT* promoter allele to be significantly less methylated than the wildtype allele. With chromatin immunoprecipitation followed by Sanger sequencing, we demonstrated that in heterozygous mutant cells, the transcriptional activators GABPA and MYC bind only to the mutant *TERT* allele. In addition, the activating and repressive chromatin marks H3K4me3 and H3K27me3, respectively, exclusively bind mutant and

wildtype alleles. Lastly, utilizing coding SNPs and long read sequencing, we determined that *TERT* is only expressed from the mutant allele.

Future work will continue to further delineate the effect of the *TERT* promoter mutation on activation of *TERT*. Using CRISPR/Cas9 technology to edit the *TERT* promoter mutation status and characterize resulting *TERT* regulation will provide further mechanistic insight. The link between these regulatory strategies could offer additional insight into cellular control of active telomerase in thyroid cancer, and be applied more broadly to other cancer types.

Primary Reader and Advisor: Dr. Christopher B. Umbricht

Secondary Reader: Dr. Winston Timp

Acknowledgements

First and foremost, I would like to thank my advisors, Dr. Christopher Umbricht and Dr. Martha Zeiger. During my entire PhD journey they have both been outstanding mentors. Dr. Umbricht has been my day-to-day support in the lab, helping me to craft new lines of inquiry and problem solve. He is always digging further into the research questions, thinking of all the different avenues a project can take, and wanting to explore them all. Dr. Zeiger, in addition to her scientific insight and authority, has taught me how to be a top-notch communicator- both in writing and in oral presentations. I have honed by writing skills through countless revisions and versions of scientific manuscripts back and forth with her. She has imparted in me the surgeon's mindset that the simplest, most concise communication is best. I will always be thankful for the training and mentorship I have received from them both.

I would also like to wholeheartedly thank my family- my husband, John, and my parents. I would not be where I am today without their countless words of encouragement and support. They willingly read my papers and listened to me practice presentations, even when they had no idea what I was talking about. They always shared excitement for my accomplishments, and were also equally as present to encourage me when my experiments failed or I encountered research setbacks.

I would also be remiss if I did not acknowledge the large contribution my lab mates provided in my PhD journey. I will always look upon the Umbricht lab as a second family. From lab lunch outings at Petit Louis, traditional Chinese hot pot at Yongchun's home, and every celebration in-between, I will greatly miss my lab family. From the

beginning of my thesis, Dr. Sean Cho and Dr. Zeyad Sahli both provided a sounding board for my work, and I had the great pleasure to work with both of these incredible researchers. I would not be anywhere close to finishing my PhD if not for Dr. Yongchun Wang with all of her exceptional lab expertise and help, especially at the conclusion of my thesis and pushing my experiments to the final stretch.

I also had the pleasure of being adopted into a second lab family, the Timp lab, through my time and mentorship by Dr. Winston Timp. Dr. Timp exposed me to a plethora of new techniques outside of my wheelhouse, and gave support and a sounding board throughout my graduate school journey. I am thankful to have been included in their white elephant holiday gift exchanges and other lab outings, which created a second lab home and family. I thank Dr. Isac Lee, Rachael Sparklin, and Timothy Gilpatrick, for all of their expertise, especially Tim, without whom a whole chapter of my thesis would not have been possible.

To my classmates, Hopkins professors and colleagues, and thesis committee, thank you for your expertise, your encouragement, critical thinking about my project, and developing me into the scientist I am today. There is truly no better institution than Johns Hopkins, and I am so blessed to have learned from and with the best.

Lastly, I would like to thank those who first encouraged and cultivated my love of science. I am deeply filled with gratitude for my AP Biology teacher and varsity basketball coach, Coach Smith, for first piquing my interest in biology, and for my undergraduate research PIs, Drs. Kerry and Cheryl Smith, for their nurturing and developing my independent research skills and encouraging my pursuit of my PhD. I am forever thankful for all the mentors I have been so lucky to be mentored by.

Table of Contents

List of Tables

List of Figures

List of Abbreviations

ALT	Alternative lengthening of telomeres
ATC	Anaplastic thyroid cancer
ChIP	Chromatin immunoprecipitation
CpG	Cytosine-guanine dinucleotides
DMR	Differentially methylated regions
DNMT	DNA methyltransferases
DTC	Differentiated thyroid cancer
ETS	E-twenty-six
ETV5	ETS variant 5
FISH	Fluorescence in situ hybridization
FT-UMP	Follicular tumors of uncertain malignant potential
FVPTC	Follicular variant of PTC
GABPA	GA binding protein transcription factor subunit alpha
GSC	Goosecoid homeobox
FTC	Follicular thyroid cancer
HCC	Hürthle cell carcinoma
IHC	Immunohistochemistry
MAE	Monoallelic expression
MAPK	Mitogen-activated protein kinase
MTC	Medullary thyroid cancer
nCATS	nanopore Cas9 targeted sequencing
NIFTP	Non-invasive follicular thyroid neoplasm with papillary-like nuclear features
PDTC	Poorly differentiated thyroid cancer
PRC	Polycomb repressor complex
PTC	Papillary thyroid cancer
RTA	Relative telomerase activity
TERT	Telomerase reverse transcriptase
TR	Telomerase RNA
TSS	Transcription start site

Chapter 1: Telomerase Reverse Transcriptase (TERT) Regulation in Thyroid Cancer

Adapted from: BA. McKelvey, *et al*. Telomerase Reverse Transcriptase (TERT) Regulation in Thyroid Cancer: A Review. *Frontiers in Endocrinology*. 2020 July.

In contrast to stem cells, non-transformed somatic cells have a limited capacity to divide in tissue culture before cell division ceases. This is known as cellular senescence and the number of times a normal human somatic cell population will divide before cell division stops is referred to as the Hayflick limit (1). Cellular senescence results from the progressive shortening of chromosomal ends or telomeres, consisting of identical hexamer repeats, with each cell division. This phenomenon is due to the end replication problem, a shortcoming of semiconservative DNA replication, which cannot complete the synthesis of chromosomal ends (2). This critical shortening of telomeres continues until reactivation of the enzyme, telomerase, facilitates the resynthesizing of telomeres of sufficient length to allow continued cellular replication. Telomere lengthening can also occasionally occur through the alternative lengthening of telomeres (ALT) pathway, which extends telomeres without telomerase activity through recombination-dependent pathways (3).

Telomerase is composed of two subunits: an RNA component, telomerase RNA (TR), serving as a template for telomere hexamer repeat addition onto DNA and, the catalytic component telomerase reverse transcriptase (TERT), responsible for reverse transcribing the hexamer repeats onto chromosomal ends (4). Not only is telomerase active in

embryonic and stem cells, it is also upregulated in over 90% of malignancies, including thyroid cancer, enabling the unlimited replication of cancer cells (5–8).

TERT activation in cancer occurs through a variety of mechanisms. These include activating promoter mutations, alterations in promoter DNA methylation, chromatin remodeling, copy number alterations, and alternative splicing of *TERT* (9–13). Because telomerase plays a key role in carcinogenesis, understanding *TERT* regulation and telomerase activation in thyroid cancer is critical to understanding its pathogenesis. Indeed, two *TERT* regulatory mechanisms, *TERT* promoter mutations and *TERT* promoter methylation status, are implicated in the stratification of thyroid cancer patient prognosis (14–16).

Promoter Mutations

Activation of *TERT* transcription can be achieved by heterozygous point mutations at the *TERT* promoter. The two most common activating mutations are upstream of the *TERT* translation start site at -124 and -146, respectively, and both are cytosine to thymine mutations, -124C>T and -146 C>T (Figure 1) (17–19). These *TERT* promoter mutations are not present in benign thyroid tumors or normal thyroid cells. Their prevalence, however, increases with more aggressive thyroid cancer subtypes and advanced stages of disease. Indeed, *TERT* mutations are present in only 11.3% of well differentiated papillary thyroid cancer (PTC) and 17.1% of follicular thyroid cancer (FTC), but present in 32% of widely invasive Hürthle cell carcinoma (HCC), compared to 5% of minimally invasive HCC, and in 43.2% of poorly differentiated thyroid cancer (PDTC) and 40.1%

of anaplastic thyroid cancer (ATC) (20, 21). Furthermore, the *TERT* promoter mutations are found in almost all thyroid cancer cell lines, even those derived from well-differentiated thyroid cancer (DTC) subtypes, in either the heterozygous or homozygous mutant state, indicative of their important role in cellular proliferation (11).

As seen in the TCGA data, the presence of *TERT* mutation is also strongly associated with high risk of tumor recurrence, older age, higher MACIS (Metastasis, patient Age, Completeness of resection, local Invasion, and tumor Size) scores, and less-differentiated PTC (22). In support of the TCGA data, in a large study of thyroid cancers in which anaplastic carcinoma coexisted with papillary carcinoma, a multivariate comparison between the antecedent papillary carcinoma components and control papillary carcinomas without anaplastic transformation showed that *TERT* mutations were independently associated with anaplastic transformation (23). Further studies have also highlighted the association of the *TERT* promoter mutation and non-radioiodine avidity of metastatic disease (24, 25).

Mechanism of *TERT* Mutation Activation

Likely key to their effect, both *TERT* promoter mutations result in a novel 11 base pair binding site for the E-twenty-six (ETS) transcription factor family. The -124C>T mutation, however, elicits a higher activation of *TERT* compared to the -146C>T mutation and, is more common (20, 26). The activating GA Binding Protein Transcription Factor Subunit Alpha (GABPA), a member of the ETS family, binds at the *TERT* promoter mutation site as a heterotetramer with its counterpart, GABPB, in

multiple cancer types, including thyroid cancer (26, 27). In PTC cell lines, *GABPA* knockdown significantly lowered *TERT* expression in both wildtype and *TERT* promoter mutant cells, and in a luciferase activity assay, *GABPA* knockdown led to significant down regulation of the mutant *TERT* promoter. However, in an analysis of papillary thyroid cancers and TCGA data, an inverse relationship was found between *GABPA* expression and *TERT* expression in *TERT* promoter mutant tumors, highlighting the need for further study of *TERT* mutation activation (28).

Recently, another ETS factor, ETS Variant 5 (ETV5), was also found to bind the mutant *TERT* promoter and, bound at higher levels than GABPA in ATC cell lines. Conversely, GABPA bound at higher levels than ETV5 in well differentiated thyroid cancer-derived cell lines (29), implicating potentially different roles of these specific ETS factors in well-differentiated and poorly differentiated cancers.

Synergistic Effects of *TERT* and *BRAF*V600E Mutation

The *BRAF*V600E mutation is also common in thyroid cancer. The *BRAF*V600E mutation is a single nucleotide mutation at codon 600, resulting in a substitution of glutamic acid for valine in the BRAF protein, a serine/threonine protein kinase that plays a role in the mitogen-activated protein kinase (MAPK) pathway/ERK signaling pathway. The *BRAF*V600E mutation is more abundant in classic PTC (51%) than in the follicular variant of PTC (FVPTC, 24%) or FTC (1.4%) (30). The *BRAF*V600E mutation acts synergistically with *TERT* promoter mutations and the presence of both mutations is associated with greater cancer aggressiveness, lymph node and distant metastasis,

advanced tumor stage, recurrence, and increased mortality in patients with PTC (31–33). The mutation may also be responsible for increased activation of the ETS factor family through activation of the MAPK pathway. There are two prevailing proposed mechanisms for the activation of *TERT* by the *BRAF*V600E mutation and the MAPK pathway. In one study of PTC cell lines, the MAPK pathway activates the transcription factor c-FOS, which can in turn bind to the *GABPB* promoter to increase its expression. This then leads to increase in GABPA-GABPB complex formation, which binds to the mutant *TERT* promoter to activate *TERT* (27). Alternatively, another study in PTCs from the TCGA study cohort shows upregulation of ETS factors ETV1, ETV4, and ETV5 in tumors that concomitantly harbored both *BRAF*V600E and *TERT* mutations and, demonstrated MAPK pathway activation. In cell lines, these ETS factors were found to bind to the mutant *TERT* promoter and upregulate transcription (34).

Epigenetic Alterations

Epigenetic changes are stably inherited during cell division and occur at DNA or chromatin levels, but do not alter the primary base sequence (35). At the DNA level, epigenetic alterations occur by methylation of the cytosine nucleotide in cytosine-guanine dinucleotides (CpGs). In higher eukaryotes, DNA methylation at CpG sites in and around gene promoter regions controls and regulates gene expression. CpG methylation is directed by DNA methyltransferases (DNMTs) which methylate the fifth carbon of the pyrimidine ring of cytosine (36). The principal methyltransferase, DNMT1, adds methyl groups during DNA replication and *de novo* methylates DNA in cancer (37).

Many CpG sites are clustered into CpG islands that are typically one thousand base pairs long and have high GC content. Approximately eighty percent of CpG sites are methylated in mammals, largely in intergenic regions known as heterochromatin, while most sites in promoters and first exons remain unmethylated (38, 39). The promoter and transcription start site (TSS) tends to be unmethylated in actively transcribed genes, since methylated DNA is associated with gene silencing through both interference of transcription factor binding and, by affecting chromatin architecture (40). Importantly, aberrant DNA methylation is a hallmark of cancer cells, and tends to occur early in cancer development (41). In cancer, characteristic changes in methylation patterns involve both genome-wide CpG hypomethylation, which occurs predominantly in intergenic regions, and hypermethylation of CpG islands at promoters. Promoter hypermethylation may result in silencing of tumor suppressors, and promoter hypomethylation can result in activation of proto-oncogenes (42). Intergenic hypomethylation may also lead to expression of dormant non-coding RNA species and otherwise suppressed genetic elements transcribed from normally silent regions of the genome (43–45).

The *TERT* promoter is within a 4 kb CpG island and has a high GC content of approximately 70% (46). The precise pattern of promoter methylation that results in activation of *TERT* in cancer is still under investigation. However, previous studies in a variety of cancer cell lines as well as solid tumors and hematological malignancies show a unique methylation pattern of *TERT*. Its promoter region surrounding the TSS [-200 to +100 relative to TSS] is unmethylated, while the upstream promoter region [-650 to -200]

is hypermethylated (13, 47). The unmethylated TSS allows for transcription to occur by availing its binding sites for activators such as MYC and, when the *TERT* promoter mutation is present, ETS family factors (Figure 1**)** (48). The role of the hypermethylated upstream promoter, and its association with *TERT* expression, however, is unknown.

TERT Upstream Methylation in Thyroid Cancer

A 2016 study of medullary thyroid cancer (MTC) and normal thyroid tissue samples quantified the *TERT* upstream promoter methylation at eight CpG sites. Sporadic MTCs had a significantly higher methylation level (12-90.3%) compared to normal thyroid tissues (approximately 10%). And, this methylation pattern positively correlated with expression of *TERT* and telomerase activation. Further, high methylation of the upstream *TERT* promoter correlated with shortened survival in patients with MTC (16). A 2018 study of follicular neoplasms found the upstream *TERT* promoter was methylated significantly higher in FTC (13%) than follicular adenoma (8%) (49). Lastly, a study of upstream *TERT* promoter methylation patterns in 312 PTC, FTC, MTC, and ATC patients found significantly higher upstream DNA methylation in patients with cancer recurrence than in patients whose tumors did not recur. In patients with a recurrence, upstream *TERT* promoter methylation was also associated with higher tumor stage and the presence of lymph node metastasis (15).

TERT Histone Mark Modifications

In addition to methylation aberrations, epigenetic changes in the histone code can also modify gene expression by altering the chromatin state from a closed, inactive state to an

open, actively transcribed state. The histone mark H3K27me3 maintains heterochromatin and recruitment of the polycomb repressor complex (PRC) for silenced genes (50). Alternatively, the H3K4me3 mark maintains actively transcribed genes in the open confirmation to enable access for transcriptional activators to bind (51). Telomerase negative primary cells exhibit high levels of the silencing H3K27me3 mark at the *TERT* promoter, compared to telomerase positive cancer cell lines (52), which exhibit the activating H3K4me3 mark (53). Further study is needed to determine the chromatin marks associated with the TERT promoter in thyroid cancer.

Allele-Specific Regulation

Recently, in order to further delineate *TERT* transcriptional regulation, studies have been conducted in many cancer subtypes to examine allele-specific regulation and the *TERT* mutation. Allele-specific regulation, resulting in expression of only one allele, is classically described by the well-known phenomenon, inactivation of one of the X chromosomes in all females. This is due to epigenetic effects, in which one of the two X chromosomes is stably transcriptionally silenced by methylation early in development. (54).

A study in 2015 of multiple cancer cell lines showed monoallelic expression of *TERT* in cell lines heterozygous for the *TERT* promoter mutation, although the study did not elucidate which allele was transcribed (55). Further studies expanded upon this by showing allele-specific regulation of the alleles, in which the *TERT* promoter mutant allele exhibits the H3K24me2/3 activating histone modification as well as binding of

RNA polymerase II, the polymerase responsible for actively transcribing genes. The activating ETS factor GABPA has also been shown in multiple cell lines to bind in an allele-specific manner to the mutant *TERT* promoter only. This would be expected since the mutation specifically creates the ETS factor binding site. The wild type *TERT* allele, however, displays the silencing histone mark H3K27me3 and, is associated with the PRC (52, 56).

TERT Allele-Specific Regulation in Thyroid Cancer

Allele-specific regulation in thyroid cancer cell lines has recently been a topic of interest. Bullock *et al.*'s recent study of two heterozygous mutant thyroid cancer cell lines suggested allele-specific regulation of *TERT*, showing monoallelic expression of *TERT* in the ATC and PTC cell lines. In the cell lines H3K4me3 was associated with the mutant allele only, while a majority of H3K27me3 was associated with the wildtype allele. In one ATC line, the ETS factor ETV5 bound in an allele-specific manner (29). Further characterization of allele-specific regulation in thyroid cancer is necessary.

Alternative Splicing

Modulation of alternative splicing is detected in multiple types of cancers, where cancer cells utilize an alternative splicing switch that results in discernible isoform signatures (57). This switching is nonrandom and also seen in tissue development, including the *TERT* splice switch, well characterized in kidney development and various cancer cell types (58–70). This mode of *TERT* regulation has been proposed to be necessary due to the difficulty to completely cease transcription, since even very small amounts of

transcript may have significant cellular effects, given the limited number of cellular targets, *i.e.*, 92 telomeres in the normal human cell (9). Previous studies have shown *TERT* expression is undetectable in normal thyroid tissue, low to absent in benign tumors, and elevated in thyroid cancers (20). Cancer cells with active telomerase have an average of 20 *TERT* transcripts per cell resulting in 100-500 active telomerase complexes (71). Alternative splicing yielding inactive and/or inhibitory forms of *TERT* allows for downregulation of telomerase activity without complete repression of transcription (Figure 1).

Over twenty different isoforms of *TERT* have so far been reported, with the most common being various deletions in the reverse transcriptase domain (72). The most common *TERT* isoforms include the following: 1) full-length transcript, the only isoform resulting in active telomerase (73, 74); 2) the α deletion isoform, an in-frame deletion of 36 base pairs in exon six resulting in a dominant negative inhibitor of telomerase (75); 3) the β deletion isoform, a 182 base pair deletion of exons seven and eight resulting in a reading frame shift forming a truncated *TERT* transcript that is sent for nonsense mediated decay (76) and; 4) the α/β dual deletion isoform. Studies of *TERT* alternative splicing in multiple cancer types have shown the highest expressed isoform in cancer is the full-length isoform, which correlates with higher telomerase activity (59, 60, 68).

TERT **Splicing in MTC**

A study of 42 MTC tumors found *TERT* expression and telomerase activity in 50% (21/42) of the tumors. And, over two-thirds of the telomerase positive cancers (15/21)

showed expression of the full-length *TERT* transcript, higher telomerase activity and were associated with a significantly shorter patient survival time (77).

TERT Splicing in DTC

Our group showed, in a study of 60 malignant tumors (PTC, FVPTC, FTC, and HCC) and 73 benign lesions, that malignant tumors showed a higher amount of the full-length isoform than the inactive *TERT* isoforms, while conversely, the benign tumors showed higher levels of the deletion isoforms (78). Further, only the full-length transcript correlated with telomerase activity (70, 78). By computing the proportion of full-length isoform to the deletion isoforms, we found the percentage score sorted thyroid tumors into subtypes; with the high full-length fractions of *TERT* found in PTC, HCC, and FTC, while intermediate fractions were found in FVPTC, Hürthle cell adenomas, and follicular adenomas and finally, low fractions in adenomatoid nodules (70).

Clinical Significance

In summary, *TERT* is regulated by a variety of mechanisms, indicative of the complex regulatory effort cells exert to control telomerase activity. The majority of malignancies reactivate *TERT* expression, which in turn activates telomerase, to allow for continued proliferation. *TERT* reactivation is important for cancer cells, as cancer cells have significantly shorter telomeres. Shortened telomeres are found in PTC, FTC, HCC and MTC compared to normal thyroid tissue and benign thyroid nodules (70, 77, 79-81). In PTC tumors, short telomeres were significantly correlated with *TERT* promoter mutations and older age (82). While all of these regulatory strategies are altered in thyroid cancer,

and may play a significant role in *TERT* activation, these altered regulatory mechanisms have not yet been leveraged clinically.

TERT mRNA expression has been proposed as a prognostic marker, independent of the *TERT* promoter mutation. A study in PTC found a subset of wildtype *TERT* tumors with high *TERT* expression, which correlated with a higher recurrence rate (83). However, other studies have shown that TERT immunohistochemistry (IHC), or measurement of protein expression is not a useful clinical tool for prognostication. A study in FTC showed no correlation between *TERT* mRNA expression and TERT immunoreactivity (84), and a study in PTC showed no correlation with TERT IHC and clinicopathological traits (85).

Presence of the *TERT* promoter mutation, however, may be promising for future use to guide clinical decision making and treatment. The presence of the *TERT* promoter mutation is indicative of worse clinicopathological factors in thyroid cancer. The thyroid research field has recently begun to embrace the use of molecular markers to help in making clinical decisions. For example, postoperative screening for the *TERT* promoter mutation in follicular tumors of uncertain malignant potential (FT-UMP) was found to inform follow-up and treatment, as the *TERT* mutation was a predictive marker of distant metastases (86). Further, current molecular testing does include the *TERT* promoter mutations in some platforms, including ThyroSeq® and ThyGenX®. Current guidelines, however, do not support using the *TERT* mutation status for initial risk stratification (87). In the new American Association of Endocrine Surgeons Guidelines for the Definitive

Surgical Management of Thyroid Disease in Adults, there is acknowledgement of inclusion of the *TERT* promoter mutation in assessment of the overall mutational burden in thyroid cancers (87). But for many molecular markers, the utility has not been tested given the newly published guidelines, nor has there been an incorporation of the new reclassification of the Non-Invasive Follicular Thyroid neoplasm with Papillary-like nuclear features (NIFTP). The 2015 American Thyroid Association Management Guidelines for Adult Patients with Thyroid Nodules and Differentiated Thyroid Cancer listed *TERT*, alone or in combination with *BRAF*, as potentially helpful to risk stratify patients in conjunction with other clinicopathological risk factors. However, this was considered a weak recommendation with low-quality evidence only (88).

In conclusion, we know much about telomerase regulation. Capitalizing upon our deep understanding of these regulatory mechanisms may lead to crucial and needed therapeutic options in the future. Nevertheless, major gaps in our understanding of telomerase regulation remain. Understanding how *TERT* splicing is regulated is essential to a better understanding the activation of telomerase. Characterization of *TERT* promoter methylation as well as ETS transcriptional activator binding in thyroid cancer cell lines and patient samples is needed. Additionally, the study of chromosomal architecture surrounding *TERT*, and the effect of the *TERT* mutation on 3D chromatin structure in thyroid cancer have yet to be explored. One aspect that remains to be fully understood is how the higher levels of *TERT* expression and activity found in *TERT*-mutant cells provide a proliferative or other competitive advantage, since cancer cells typically have activated *TERT* expression to overcome the Hayflick limit long before *TERT* promoter

mutations arise. Further understanding of how cancer cells that do not harbor the TERT mutation activate *TERT* through various regulatory methods still needs to be elucidated. Further studies are needed to determine the true utility of the *TERT* mutation status in a clinical setting and, how best to target *TERT* regulation.

Figure 1: An overview of *TERT* regulation in thyroid cancer.

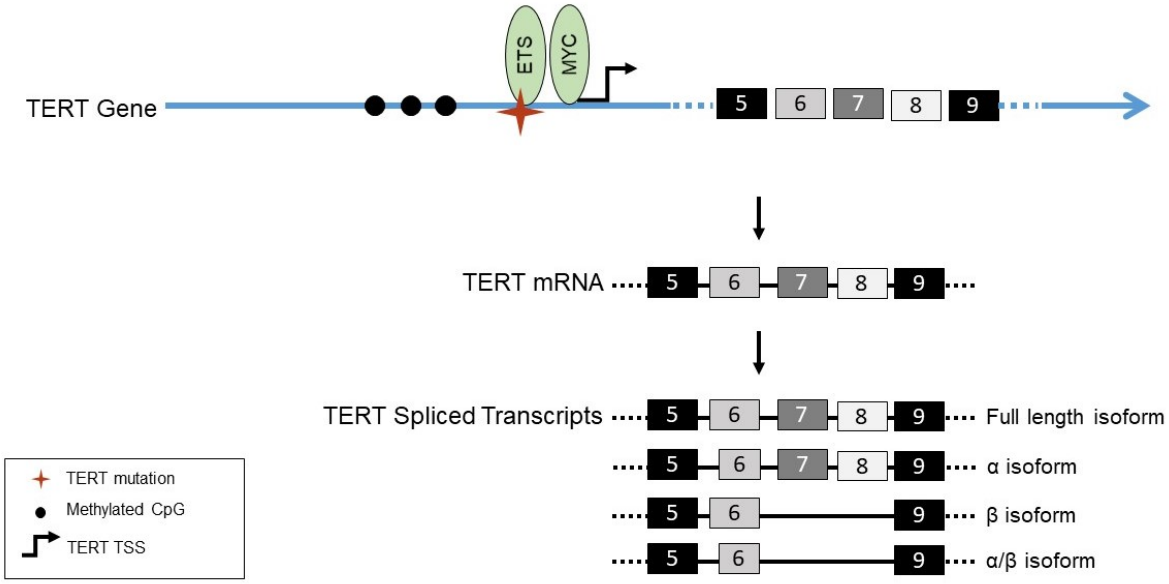

The landscape of the *TERT* promoter in thyroid cancer shows the *TERT* promoter mutation (✦), with hypermethylation (●) further upstream of the TSS (⌐→). Transcriptional activators MYC and ETS family factors bind at the *TERT* promoter, the latter binding in the presence of the *TERT* mutation only. Alternative splicing of *TERT* in thyroid cancer. *TERT* is transcribed into mRNA, containing 16 exons (#5-9 shown). *TERT* can be alternatively spliced, into either the full length, α, β, or α/β isoforms.

Chapter 2*:* Telomerase Reverse Transcriptase Promoter Methylation and Transcription Factor Binding in Differentiated Thyroid Cancer Cell Lines

Adapted from: Avin BA, *et al*. 2019 Characterization of human telomerase reverse transcriptase promoter methylation and transcription factor binding in differentiated thyroid cancer cell lines. Genes, Chromosom Cancer **58**:530-540.

Introduction

TERT upregulation in cancer cells is multifaceted and complex. This transcriptional upregulation occurs via multiple mechanisms, including alteration of chromatin state, promoter hypermethylation, alternative splicing, and novel activator binding sites resultant from mutations (9–12). Previous work has characterized these various mechanisms of regulation in other cancer types, but not thyroid cancer. For this study we focused on characterizing promoter methylation patterns, transcription factor binding, and the resulting *TERT* transcription in thyroid cancer cell lines to better understand the interplay between *TERT* regulatory mechanisms.

The *TERT* promoter is located in a 4 kb CpG island containing approximately 70% GC nucleotides, and exhibits a complex methylation pattern (see Figure 2) (46). The area surrounding the transcription start site (TSS) at -200 to +100 is typically unmethylated, and overlaps the “minimal promoter” at -260 to -75, which also encompasses the binding site for MYC. In contrast, further upstream of the TSS, at -650 to -200, the promoter is hypermethylated in telomerase positive cancer cells as compared to normal tissue. This hypermethylation pattern occurs in a multitude of cancer types, including prostate, medulloblastoma, gastric, esophageal, cervical, and colorectal cancer, and is caused by

currently unknown mechanisms (47, 48, 89, 90). The methylation status of the *TERT* promoter in thyroid cancer is currently unknown.

TERT transcription can also be activated by promoter point mutations, supporting immortalization and tumorigenesis (17–19). These mutations are upstream of the translation start site, at -124C>T and -146C>T, respectively, relative to the ATG (20). Both *TERT* promoter mutations create a new consensus ETS factor binding site. Compared to the -146 C>T mutation, the -124 C>T mutation produces higher levels of TERT promoter transcriptional activation (26). At the -124 C>T mutation, the ETS transcription factor GABPA binds as a heterotetramer in multiple cancer types (26). Investigation into GABPA binding at the *TERT* promoter in thyroid cancer cell lines, which harbor the *TERT* mutation, has not been previously studied.

In order to better understand the connection between promoter methylation and activation of telomerase, we performed tiled amplicon bisulfite sequencing followed by epiallele analysis. Analysis of epialleles, defined as distinctive patterns of methylation over a region of interest as captured in one sequenced amplicon, can allow for more biologically relevant interpretation, as CpG sites function collectively and not in isolation (91). We discovered a dual-methylation pattern at the *TERT* promoter in DTC cell lines, mirroring methylation patterns found in other telomerase positive cancers. Analysis of the hypermethylated upstream promoter led to discovering two putative activator binding sites by chromatin immunoprecipitation (ChIP). Additionally utilizing ChIP, we determined the enrichment of transcription factor binding at the *TERT* promoter in DTC

cell lines, and determined resulting *TERT* expression levels in these cells to further our understanding of the effect of *TERT* regulation on *TERT* activation.

Results

Targeted TERT promoter bisulfite sequencing

DNA from all five DTC cell lines (see Supplemental Table 2 for *BRAF* & *TERT* mutation status) and six normal thyroid tissue samples was bisulfite treated, and the *TERT* promoter region, from –662 to +174 (relative to the transcription start site, TSS), was sequenced in three tiled amplicons. All CpGs in the targeted region had at least 60x coverage (Supplemental Figure 1), and any CpG site that was absent in more than two cell lines was removed from the analysis. The three biological replicates for each cell line were concordant, with a standard deviation of replicates (sd) ranging from 3.7-4.8%. The six normal thyroid tissue samples showed concordant methylation patterns as well (sd = 4.69, see Supplemental Figure 2).

TERT promoter methylation in papillary thyroid cancer cell lines

We focused our attention on two human papillary thyroid cancer (PTC) cell lines, TPC-1 and BCPAP. While TPC-1 is characterized as well differentiated, BCPAP is derived from a poorly differentiated PTC (92). Both PTC cell lines exhibited similar levels of methylation at the *TERT* promoter (Figure 3 and Supplemental Figure 3) with overall high levels of methylation in the sequenced portion of exon 1 (chr5:1,294,996-1,295,047) through just upstream of the TSS (1,295,162). Compared to PTC cell lines, normal thyroid tissue had the lowest methylation at each CpG within the entire region. The

CTCF binding site in exon 1 displayed methylation in the PTC cell lines, with no methylation in normal tissue. In the PTC cell lines, lower levels of methylation were seen upstream of the TSS for approximately 160 bases for the majority of the minimal promoter, including the area containing the ETS binding sites, with TPC-1 maintaining higher levels in this region compared to BCPAP. While the region further upstream, including the MYC binding site (1,295,339-1,295,800), was highly methylated in both PTCs (Figure 3), methylation was mostly absent until 177 bases upstream of the TSS for normal thyroid tissue. The more upstream region was partially methylated in normal tissue (see also epiallele analysis below). Both PTC cell lines and normal tissue showed a significant highly focal decrease in methylation at the upstream CpG at 1,295,547 (illustrated by the arrowhead in Figure 3).

TERT promoter methylation in follicular thyroid cancer cell lines

Next, we characterized three human follicular thyroid cancer (FTC) cell lines, FTC-133, FTC-238, and WRO (Figure 4 and Supplemental Figure 3). FTC-133 and FTC-238 originate from the same patient at different time points and disease stages (93), where FTC-133 is a local lymph node metastasis and FTC-238 is a late distant hematogenous metastasis. WRO is derived from a metastasis from another FTC patient, and is the only DTC cell line analyzed here that does not harbor an activating *TERT* promoter mutation. As in PTC, all three FTC cell lines showed higher levels of methylation at each CpG than normal tissue. Of the three FTC cell lines, FTC-133 showed the least amount of methylation overall, although it exhibited a pattern similar to FTC-238 (Figure 4). While WRO mirrored the methylation pattern of the other FTC cell lines upstream of 1,295,339,

it had much higher levels of methylation in the areas surrounding the TSS and downstream into exon 1 compared to the other two FTC cell lines. The only region of the *TERT* promoter that was not highly methylated in WRO occurred at 1,295,225-1,295,248, less than a hundred bases upstream of the TSS (Figure 4), and this unmethylated region contains the mutation-created ETS binding sites in other DTC cell lines, which are absent in WRO. The drop in methylation at CpG 1,295,547, observed in PTC cell lines, was also noted in FTC cell lines FTC-133 and FTC-238, but not in WRO. Also concurrent with PTC cell lines, FTC cell lines showed partial methylation at the MYC and CTCF binding sites.

Differential methylation between FTC-133 and FTC-238

Studying FTC-133 and FTC-238 provided a direct comparison between early local lymphatic (FTC-133) and later-originating distant hematogenous (FTC-238) thyroid cancer metastases. An analysis of differentially methylated regions (DMRs) within the *TERT* promoter revealed nine DMRs of varying lengths between the two FTC cell lines (Figure 5 and Supplemental Table 1). Overall, FTC-133 was hypomethylated compared to FTC-238 (Figure 5A). The largest DMR, from 1,295,017-1,295,155, ranges from the 5' untranslated region into exon 1 of *TERT* and exhibited significantly more methylation in the distant metastasis, than the lymph node metastasis (Figure 5A, B).

Epiallelic characterization of MYC binding site

Methylation levels at the MYC binding site at the *TERT* minimal promoter in DTC cell lines were approximately 50% for all cell lines, with the exception of FTC-133, which

showed less methylation and more closely mirrored normal thyroid methylation (Figure 6). MYC has been shown to bind in an allele specific manner when there is a methylation difference between the two alleles (94, 95), which may be the case at the *TERT* promoter. Therefore, epiallele analysis for the MYC minimal promoter binding site was conducted. This analysis revealed a methylation pattern where about half the reads were fully methylated and the other half fully unmethylated across CpGs at the binding site (Figure 7), pointing to potential allele specific methylation patterns that may affect MYC binding at the *TERT* locus. This pattern was seen in all DTC cell lines except for the early disease stage cell line FTC-133, which, demonstrated predominantly unmethylated CpGs, similar to normal thyroid tissue.

Epiallelic characterization of TERT upstream promoter

The upstream promoter region, covering 1,295,587 to 1,295,800, was partially or fully methylated at every CpG in all DTC cell lines. As this area has been shown to be characteristically highly methylated in other cancers (13), epiallele analysis was conducted to examine this area further. While in Figure 6, the upstream region of normal thyroid tissue appears partially methylated, epiallele analysis displays the region being mostly unmethylated. Examining the frequency of single allele methylation, the most common pattern across the upstream *TERT* promoter region in normal tissue shows all CpGs unmethylated in 75% of reads (Figure 8). In contrast to normal tissue, the most prominent epialleles in WRO, FTC-238, and TPC-1 show the upstream region fully methylated, while in FTC-133 and BCPAP, the most common epialleles exhibited foci of unmethylated CpGs. Interestingly, and with potential biological relevance, the CpG site

at 1,295,686 showed a marked focal drop in methylation to very low levels, across all DTC cell lines with the exception of WRO, as well as in normal tissue. Other sites, such as 1,295,649-1,295,651, exhibit an unmethylated pattern in PTC cell lines TPC-1 and BCPAP, while the surrounding CpGs are methylated, also pointing to potentially biologically relevant sites.

Motif analysis of upstream TERT promoter

Epiallele analysis of the upstream *TERT* region showed conserved sites of focal lower methylation (Figure 8). A review of transcription factors known to bind this area (96) showed no known factors. Therefore, we conducted motif analysis using the MEME Suite (97) at the 1,295,649-1,295,651 site and at the focal methylation drop at 1,295,547. Motif analysis revealed a potential E-box binding site encompassed in 1,295,649-1,295,651. The *TERT* sequence 'CCGCGTG' is identical except one base pair to the MYC consensus sequence 'CCACGTG'. The 1,295,547 drop in methylation was identified to contain a putative Goosecoid Homeobox (GSC) motif. The consensus sequence for GSC is 'TAATCC', and the *TERT* sequence is 'TAACCC', a one base pair mismatch. This suggests GSC may bind at the *TERT* promoter.

Transcription factor binding at the TERT promoter in DTC cell lines and normal thyroid tissue

Binding of known and predicted transcription factors at the *TERT* promoter was measured. Chromatin immunoprecipitation with a CTCF-specific antibody showed variable binding at the CTCF binding site at *TERT* in all cell lines, while CTCF did not

exhibit binding in normal thyroid tissue (Figure 9A). Transcription factor GABPA was probed by ChIP (Figure 9B), and cell lines BCPAP and WRO had minimal binding compared to TPC-1, FTC-133, and FTC-238. These three cell lines with increased GABPA binding all harbor *TERT* promoter mutations creating the GABPA binding site. TPC-1 and FTC-238 harbor the -124 C>T mutation heterozygously, while FTC-133 is homozygous for the mutation. As expected, normal thyroid tissue showed minimal binding of GABPA at the *TERT* promoter. In probing for MYC binding (Figure 9C), two regions were interrogated by PCR amplification. The MYC binding site in the minimal promoter showed binding in the TPC-1 and FTC-133 cell lines, as well as in normal thyroid tissue. MYC binding in FTC-133 and in normal tissue was expected due to the low levels of methylation, but overall, methylation status did not correlate closely with MYC binding. The potential E-box binding site upstream identified by motif analysis also showed binding of MYC, particularly in the least methylated FTC-133 and normal tissue samples, while all other DTC cell lines exhibited a lesser degree of binding in the upstream region (Figure 9C). Lastly, GSC ChIP was conducted for the identified focal drop in methylation at the 1,295,547 site in the upstream *TERT* region. GSC showed binding relative to input at the upstream *TERT* promoter proposed GSC binding site in all DTC cell lines and normal thyroid tissue (Figure 9D), with the two papillary thyroid cancer cell lines exhibiting the largest amount of binding.

TERT expression in DTC cell lines and normal tissue

TERT transcript levels were measured by quantitative RT-PCR, in triplicate and with two biological replicates, to measure *TERT* expression in the DTC cell lines and normal

thyroid tissue. As shown in Figure 10, all DTC cell lines exhibited variable amounts of *TERT* expression, while normal thyroid tissue did not express *TERT*. WRO showed the lowest *TERT* expression, while FTC-238 exhibited the highest *TERT* levels.

Discussion

While *TERT* promoter methylation patterns have been characterized in various cancer types, only one study has explored the *TERT* promoter methylation pattern in thyroid cancer. In that study, only 8 CpGs spanning 37 base pairs in medullary thyroid cancer was studied in 38 tumors (16). Herein, we interrogated *TERT* promoter methylation patterns in a much larger region (chr5:1,294,996/+166 - 1,295,800/-638) in papillary thyroid cancer cell lines TPC-1 and BCPAP, and in follicular thyroid cancer cell lines WRO, FTC-133, and FTC-238, and in normal thyroid tissue. We also characterized transcription factor binding and *TERT* expression to explore the relationship between promoter methylation and transcriptional activation.

Our characterization of the *TERT* promoter by bisulfite amplicon sequencing revealed that DTC cell lines exhibit the dual-methylation pattern commonly observed in other telomerase positive cancer cell types (13), including medullary thyroid cancer (16), i.e., low levels of methylation in the minimal promoter near the TSS, while the region further upstream was highly methylated. This upstream region of hypermethylation has been shown to be tightly correlated with *TERT* expression, activation of telomerase, and worse clinical outcomes, and is used as a biomarker in pediatric brain tumors and melanoma, specifically with methylation of the region 1,295,647-703 serving as a prognostic marker

for tumor progression and poor prognosis (89). Whereas the lack of methylation at the TSS was similar between normal thyroid tissue and cancer cells, the hypermethylation of only the upstream *TERT* promoter in cancer may be key to transcriptional activation of *TERT*. Absence of methylation within the minimal promoter has been correlated with higher levels of *TERT* transcription (48, 98), but our results suggest a more complex relationship between minimal promoter methylation and transcriptional activity. Comparison of the two FTC cell lines obtained from the same patient at different stages of the disease revealed that the region spanning the 5'UTR to exon 1 exhibited higher levels of methylation in the later distant metastasis-derived line, which also exhibited much higher levels of *TERT* expression than the earlier local lymph node metastasis-derived line with lower levels of methylation. This seems counterintuitive to the conventional expectation that higher DNA methylation levels at the TSS decrease gene expression and suggests a role of areas outside of the minimal promoter in activating *TERT*.

We also considered the binding sites for MYC and CTCF proximal to the TSS, an activator and repressor for *TERT*, respectively (98), which may also play important roles in activation of *TERT*. In normal thyroid tissue, the CTCF binding site was unmethylated, however the factor did not exhibit binding in normal thyroid tissue by ChIP-qPCR, while in all DTC cell lines, the CTCF site was at least partially methylated, and all DTC cell lines showed binding of CTCF. As methylation has been shown to block binding of CTCF to *TERT*, further examination of CTCF binding at the *TERT* promoter is needed (99, 100).

Interestingly, the binding site for MYC within the minimal promoter was also partially methylated in all DTC, as well as normal thyroid tissue. However, hypermethylation in telomerase positive tumor tissue and cell lines at the MYC binding site has been observed previously (101). Through epiallele analysis, it was found that the MYC binding site may be fully methylated in one allele, and fully unmethylated on the other allele- except for in FTC-133 and normal thyroid tissue, which are predominantly unmethylated. ChIP analysis showed that FTC-133, TPC-1, and normal tissue exhibited binding of MYC at the minimal promoter. The low levels of methylation at the site in FTC-133 and normal tissue agree with MYC binding. However the partial methylation at TPC-1 warrants further studies to evaluate its role in activation, possibly in an allele-specific fashion, and its binding in normal tissue suggests MYC may be necessary, but not sufficient, to activate transcription.

The WRO cell line exhibited high levels of methylation throughout the entire *TERT* promoter region, except at the ETS binding sites. The cell line also exhibited the lowest level of *TERT* transcription of the DTC cell lines. WRO may be activating telomerase via a different, less robust mechanism, in which its mutational background may play a role. WRO is also unusual in harboring the BRAF activating heterozygous mutation, which is more typical of PTC than FTC. The significance of overexpression of the GABPA factor by BRAFV600E mutation without a *TERT* promoter mutation is currently unknown. WRO did exhibit low GABPA binding, which is consistent with a lack of binding site in the absence of a *TERT* mutation. BCPAP also exhibited minimal binding of the factor,

which may be due to the unique *TERT* mutation status it carries, with -124/-125 CC>TT, which does not perfectly create the consensus sequence needed for GABPA to bind. The cell lines FTC-133 and TPC-1 showed the most GABPA binding by ChIP-qPCR, and FTC-133 is the only cell line tested which is homozygous for the mutation, while TPC-1 is heterozygous for the *TERT* mutation. The other *TERT* heterozygous mutant, FTC-238, showed intermediate levels of GABPA binding.

The investigation of focal changes in methylation in the hypermethylated upstream region allowed the identification of two additional potential activating sites, a putative E-box and a GSC binding site. This upstream E-box binding site showed binding of MYC in all cell lines, with a high amount of binding in FTC-133 and normal thyroid tissue, which also had the lowest levels of methylation at this binding site. This site may be important for activation, as it is less densely methylated than the surrounding CpGs.

Our motif analysis also identified a GSC factor binding site in the upstream *TERT* promoter, which was less methylated than surrounding CpGs in all cell lines except WRO. ChIP analysis of GSC showed binding of the factor at the upstream *TERT* promoter, with normal thyroid tissue and the two FTC cell lines FTC-133 and FTC-238 showing the least GSC binding. Furthermore, COSMIC data show overexpression and copy number variations of GSC in thyroid cancer (102), which may point to other mutations necessary for activation of GSC. GSC has been shown to be oncogenic in ovarian carcinoma, where overexpression of *TERT* and GSC resulted in chemoresistance and poorer prognosis (103). GSC has also been shown to promote epithelial-

mesenchymal transition in numerous cancers including prostate, breast, and hepatocellular carcinoma (104–106). These findings suggest that further exploration into GSC as an activator of *TERT* is warranted.

In summary, we have characterized the dual-methylation pattern at the *TERT* promoter in DTC cell lines. This pattern mirrors other telomerase positive cancer cell lines, and shows a dysregulation in methylation compared to normal thyroid tissue. Specifically, the upstream *TERT* promoter is hypermethylated in cancer, which may be important for transcriptional activation of *TERT*, and we identified two putative activator binding sites in the upstream region. While the minimal promoter shows variable levels of methylation between DTC cell lines, overall there is a lack of methylation, as seen in normal tissue. The methylation state of the minimal promoter may therefore not play a determining role in *TERT* re-activation. Lastly, *TERT* promoter mutations may cause allele-specific methylation changes at the minimal promoter and affect transcription factor binding, which can be influenced by additional activating mutations. As we observed no simple correlation between promoter methylation status and transcript levels, future work needs to be done to establish a causative role of *TERT* promoter methylation affecting transcriptional activation of the transcript amidst the many regulatory elements.

Table S1: Differentially methylated regions found in FTC cell lines

Start Position	End Position	DMR[a] Width (bp)	Invdensity[b]	DMR Area Tstat[c]	DMR Average Tstat[d]	Max Tstat[e]	Mean Difference[f]	Lymph Node Met Mean	Distant Met Mean	Tstat SD[g]	Direction[h]
1294996	1294996	1	1	3.26	3.26	3.26	0.14	0.48	0.34	0.04	hyper
1295017	1295155	139	6.32	-117.03	-0.84	-3.65	-0.25	0.33	0.58	0.05	hypo
1295171	1295187	17	4.25	-18.92	-1.11	-2.69	-0.24	0.21	0.45	0.05	hypo
1295279	1295279	1	1	1.45	1.45	1.45	0.08	0.16	0.09	0.05	hyper
1295339	1295377	39	5.57	-25.54	-0.65	-3.09	-0.2	0.3	0.49	0.05	hypo
1295405	1295426	22	5.5	-12.42	-0.56	-2.77	-0.18	0.3	0.48	0.06	hypo
1295445	1295491	47	4.7	-35.53	-0.76	-2.96	-0.2	0.28	0.48	0.06	hypo
1295520	1295619	100	12.5	-30.59	-0.31	-2.48	-0.21	0.44	0.64	0.05	hypo
1295762	1295772	11	5.5	3.93	0.36	2.5	0.1	0.84	0.74	0.05	hyper

[a] Differentially methylated region, [b]invdensity= average length in bp per CpG, [c]DMR.Area.Tstat = sum of the T-statistics of the individual methylation loci, [d]DMR.Avg.Tstat = length independent metric of the Tstat for each DMR, [e]Max.Tstat = the maximum T-statistic for an individual CpG, [f]Mean.Difference = the mean difference in methylation loci, [g]standard deviation, [h]direction of methylation change in reference to FTC-133 compared to FTC-238.

Table S2: Mutation status of thyroid cancer cell lines by Sanger sequencing for the *BRAF*V600E mutation and the *TERT* promoter mutations

Cell Lines	Thyroid Cancer Subtype	*BRAF*	*TERT*
TPC-1	Well differentiated papillary	WT	-124 C>T heterozygous mutant
BCPAP	Poorly differentiated papillary	V600E homozygous mutant	-124/-125 CC>TT heterozygous mutant
WRO	Follicular	V600E heterozygous mutant	WT
FTC-133	Follicular (lymph node metastasis)[a]	WT	-124 C>T homozygous mutant
FTC-238	Follicular (distant metastasis)[a]	WT	-124 C>T heterozygous mutant

[a]denotes cell lines derived from the same patient.

Figure 2: *TERT* promoter methylation

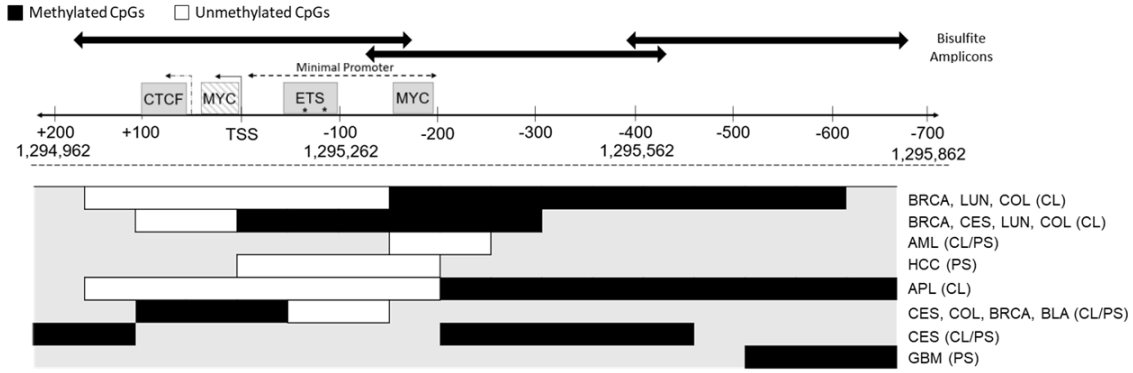

Methylation pattern relative to the transcription start site (TSS) in either cell lines (CL) or patient blood/tumor samples (PS) with positive telomerase expression given in black and white rectangles, with black denoting hypermethylated regions and white denoting hypomethylated regions. Cancer abbreviations are: breast (BRCA), lung (LUN), colon (COL), cervical (CES), acute myeloid leukemia (AML), hepatocellular carcinoma (HCC), acute promyelocytic leukemia (APL), bladder (BLA), and glioblastoma (GBM). Transcription factor binding sites for MYC, ETS, and CTCF are shown, with the minimal promoter represented by a dashed arrow, and *TERT* promoter mutations indicated by *. The proximal MYC site is shaded to denote a lesser importance in transcriptional activation. The translation start site is depicted by a dashed arrow head. The amplicons designed to tile the promoter are shown by the dark double arrowhead.

Figure 3: Characterization of *TERT* promoter methylation by bisulfite sequencing in papillary thyroid cancer cell lines compared to normal thyroid tissue

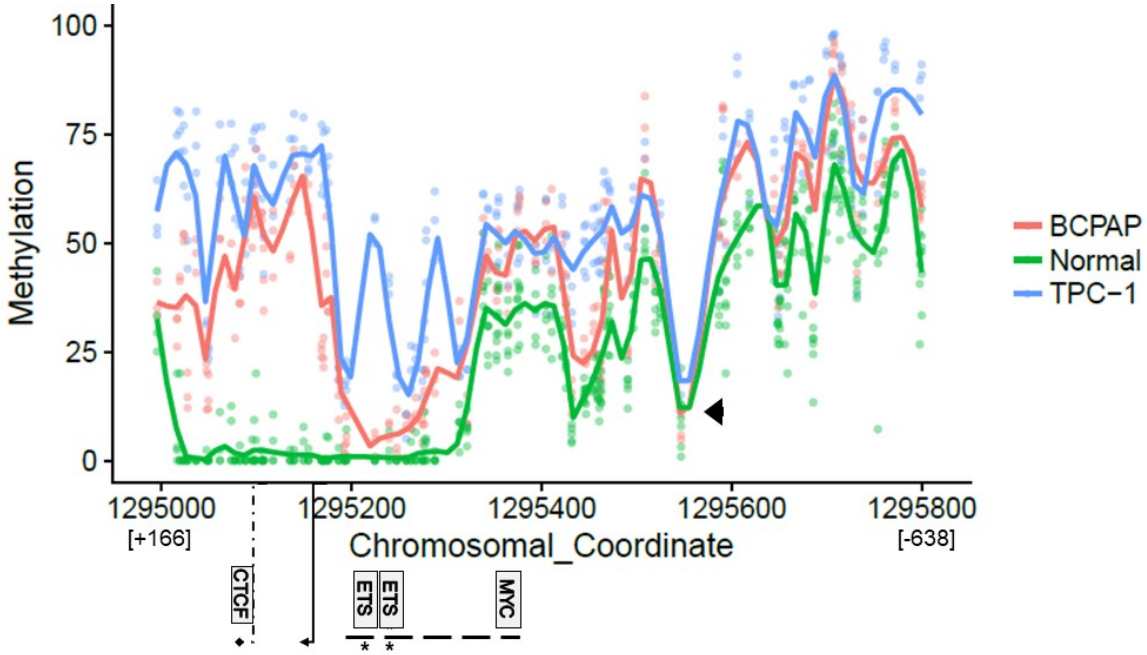

The overall % methylation level at each CpG site over the *TERT* promoter region (chr5:1,294,996/+166 to 1,295,800/-638) in papillary thyroid cancer cell lines TPC-1 (blue) and BCPAP (red), compared to normal thyroid tissue (green). Colored lines represent the average methylation % levels for both TPC-1 and BCPAP. Biological triplicates are represented in different colored dots. Transcription factor binding sites (boxes below), the minimal promoter region (dashed line), the *TERT* promoter mutations (*), methylation drop (arrowhead), and the transcription start site (solid arrow) and translation start site (dashed arrow) are depicted.

Figure 4: Characterization of *TERT* promoter methylation in follicular thyroid cancer cell lines compared to normal thyroid tissue

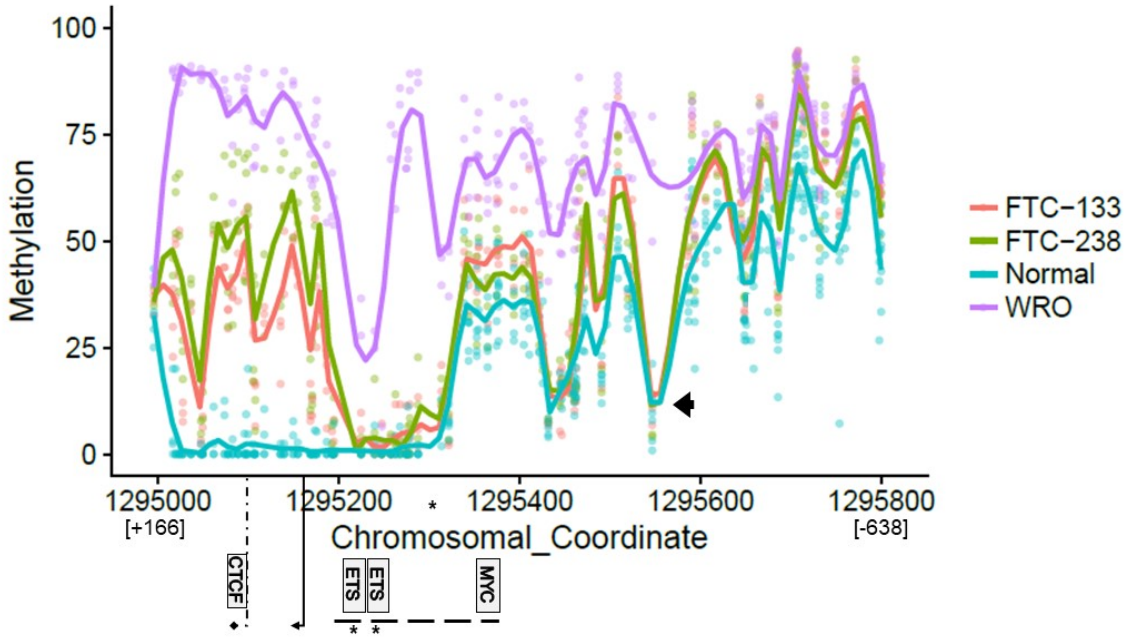

The overall methylation level per CpG locus, as a percentage, over the *TERT* promoter region chr5:1,294,996 (+166) to 1,295,800 (-638) bisulfite sequenced in follicular thyroid cancer cell lines WRO, FTC-133, and FTC-238 compared to normal thyroid tissue. The line represents the average methylation % levels for each cell line. Biological triplicates are represented in different colored dots. Transcription factor binding sites (boxes below), the minimal promoter region (dashed line), the *TERT* promoter mutations (*), methylation drop (arrowhead), and the transcription start site (solid arrow) and translation start site (dashed arrow) are depicted.

Figure 5: Significant differentially methylated regions between cell lines established from the same patient, at different metastatic locations

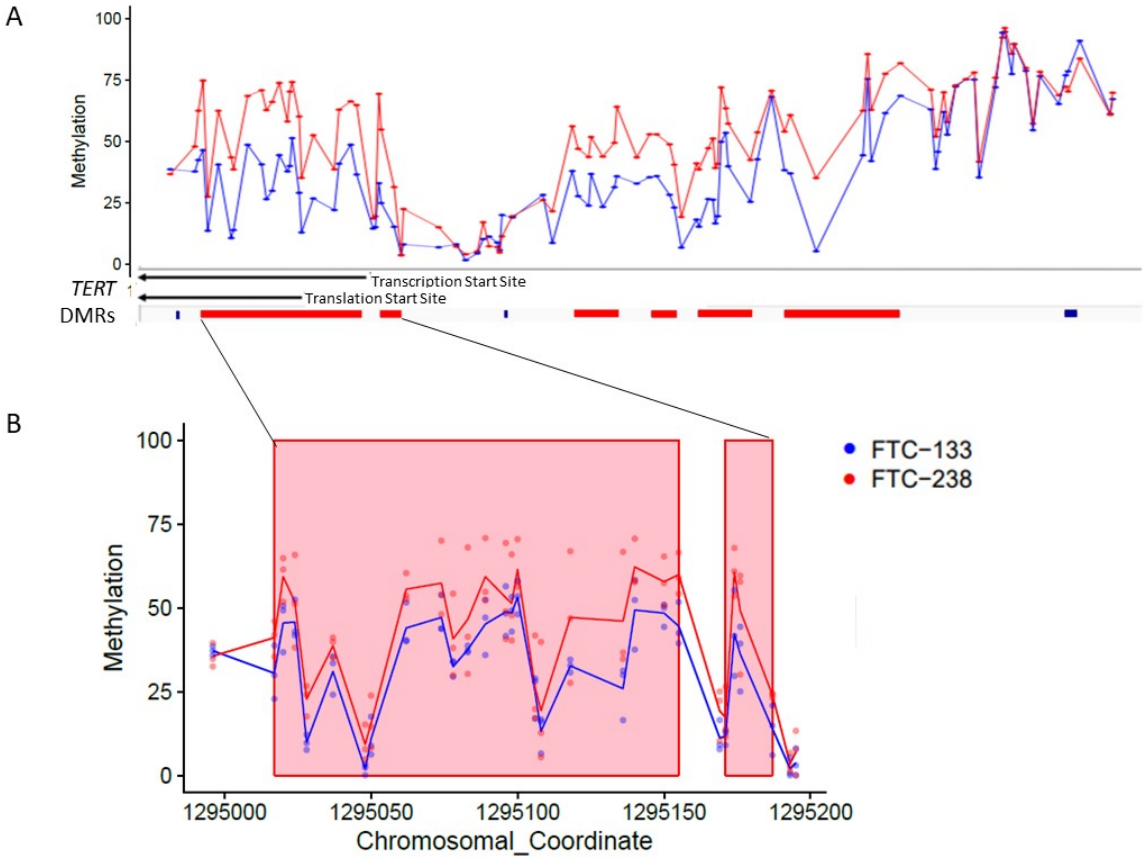

A) Adapted Integrative Genomics Viewer (IGV) visualization of the *TERT* promoter region (build hg19), with black arrows showing the direction of transcription and translation of *TERT*. Line graph illustrates the percentage of methylation per CpG over the region in the lymph node metastasis (FTC-133) and distant metastasis (FTC-238) follicular thyroid cancer cell lines. Differentially methylated regions (DMRs), as determined by the R package bsseq, are defined by blue (distant metastasis is hypomethylated relative to lymph node) or red (distant metastasis is hypermethylated relative to lymph node) blocks covering the DMR between the two cell lines. **B)** Representative plot of the methylation per CpG over an identified DMR region for the differing cell lines, in triplicate. CpGs are represented by tick marks along the x-axis, and the DMRs are highlighted in red.

Figure 6: Overall *TERT* promoter methylation pattern in differentiated thyroid cancer cell lines compared to normal thyroid tissue

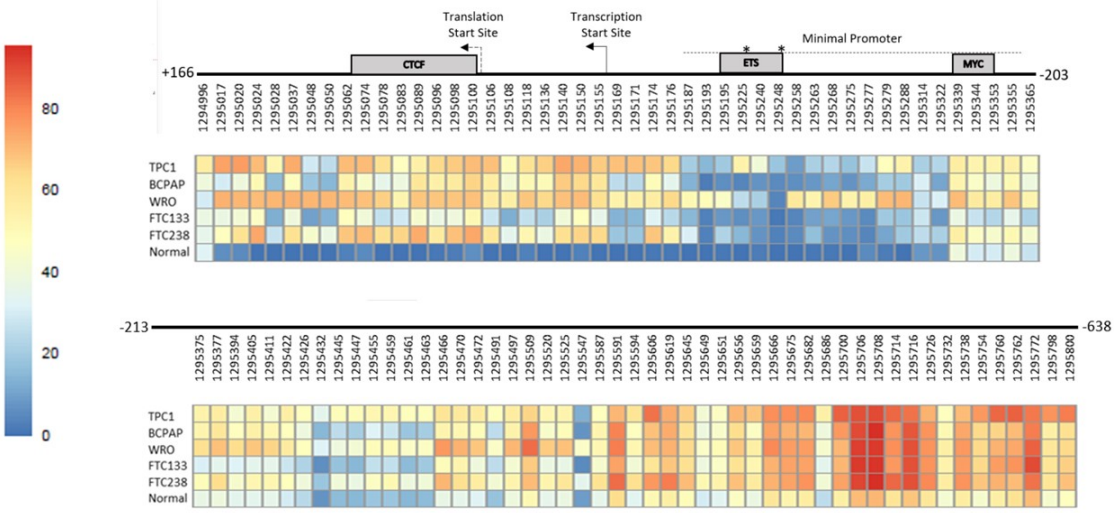

Depiction of the *TERT* promoter from +166 to -638 (relative to the transcription start site) with transcription factor binding sites (CTCF, MYC, ETS), the promoter mutations illustrated by *, and the minimal promoter highlighted at their respective locations. Each cell line tested, along with normal thyroid tissue (Normal), is listed in the leftmost column. Each CpG site is represented as a column, with chromosomal location listed above, in which methylation is a gradient, with blue indicating low levels of methylation, and red as high levels of methylation.

Figure 7: Epiallele analysis of MYC binding site in *TERT* promoter

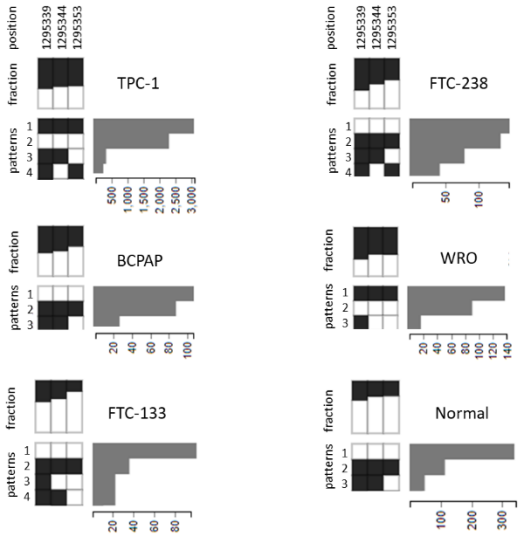

Epiallelic characterization of the *TERT* promoter conducted by MethPat analysis depicting epialleles for the MYC binding region 1,295,339-1,295,353. Each column in the plot is an individual CpG, where the proportion of methylation at each CpG is shown, with methylated CpGs (black) and unmethylated CpGs (white). The amount of reads with a given methylation pattern for all CpGs in the read are shown in order of the most prevalent, with the most prominent patterns shown.

Figure 8: Epiallele analysis of upstream *TERT* promoter hypermethylation in DTC

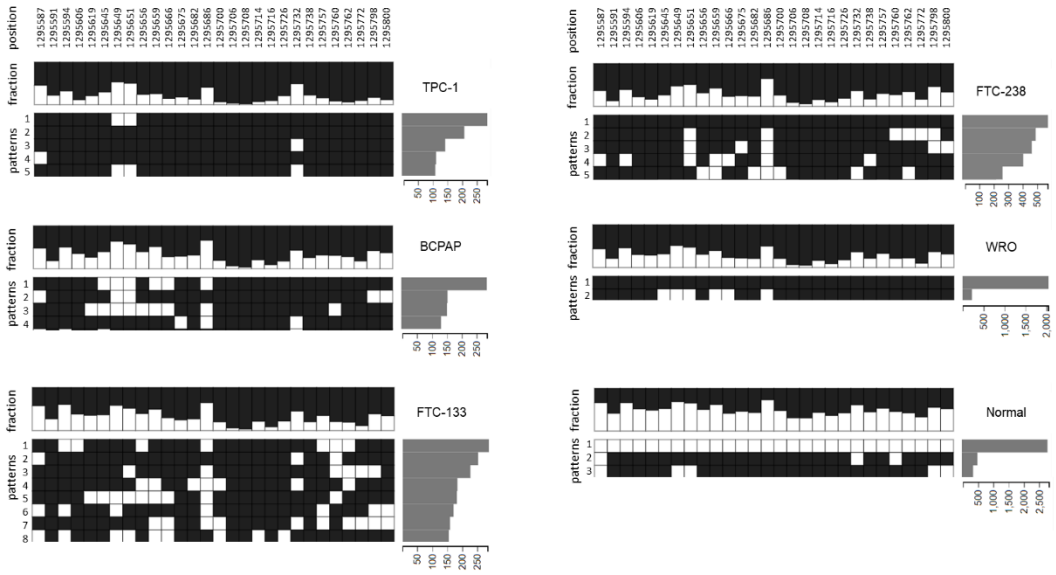

Epiallelic characterization of the *TERT* promoter conducted by MethPat analysis depicting epialleles for the upstream *TERT* region 1,295,587-1,295,800. Each column in the plot is an individual CpG, where the proportion of methylation at each CpG is shown, with methylated CpGs (black) and unmethylated CpGs (white). The amount of reads with a given methylation pattern for all CpGs in the read are shown in order of the most prevalent, with the most prominent patterns shown.

Figure 9: Transcription factor binding varies at the *TERT* promoter in DTC cell lines and normal thyroid tissue

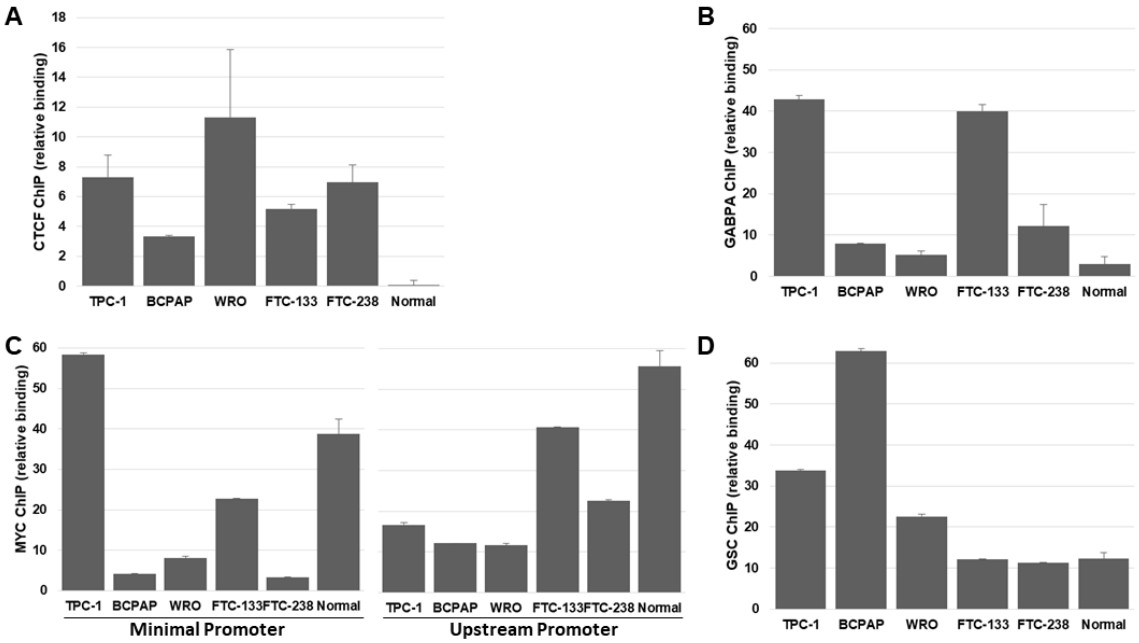

Binding was measured relative to 5% input chromatin, and binding at the *TERT* locus normalized to a positive control locus for each factor in the indicated cell lines and normal thyroid tissue by ChIP-qPCR for **A)** CTCF, **B)** GABPA, **C)** MYC, at two positions- the minimal promoter binding site and the upstream binding site, **D)** GSC. All error bars represent standard error within triplicates.

Figure 10: *TERT* transcript level in thyroid cancer cell lines and normal thyroid tissue

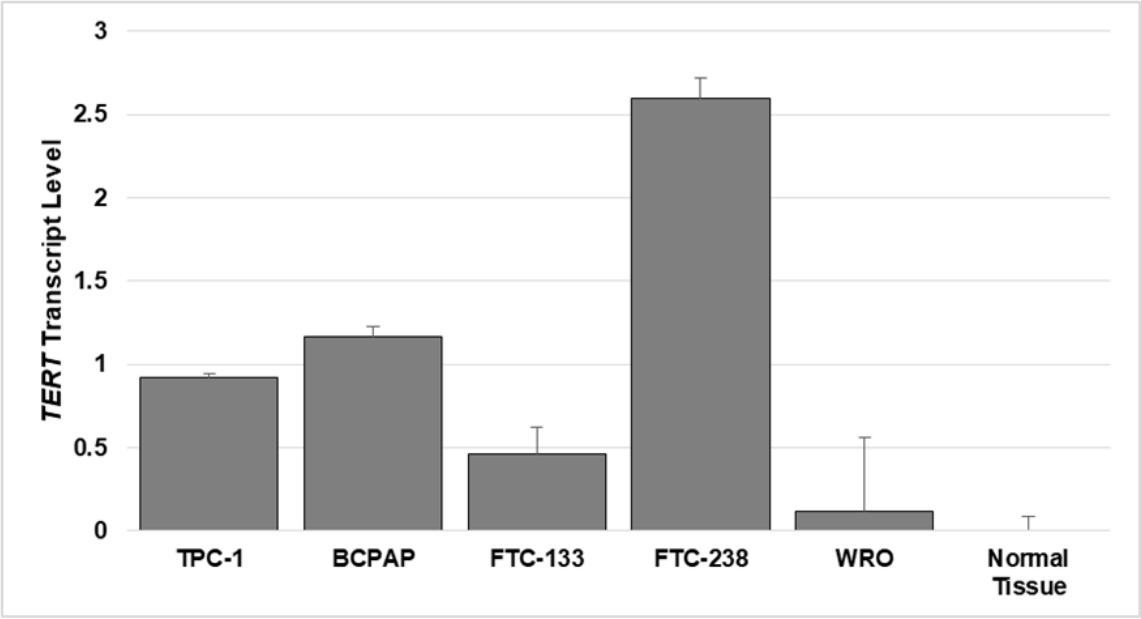

TERT transcript level was assessed by quantitative RT-PCR in thyroid cancer cell lines and six normal thyroid tissue samples (averaged together). *TERT* expression was normalized to *GAPDH* expression, and error bars indicate standard deviation.

Figure S1: Read coverage of amplicon bisulfite sequencing of the *TERT* promoter

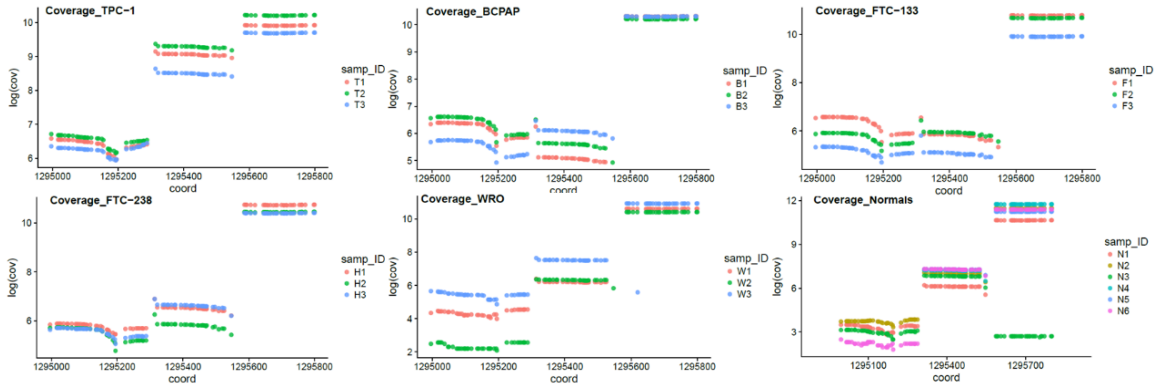

Coverage shown in natural log scale over chr5:1,294,996 to chr5:1,295,800 (hg19 build) in each of the samples. Where in all cancer cell lines (TPC-1, BCPAP, WRO, FTC-133, FTC-238) samples 1-3 are biological replicates. Normal thyroid tissue (Normals) are six different tissue samples. SNPs were filtered on the criteria described in the Methods, and a threshold of more than 60x coverage was required.

Figure S2: Characterization of *TERT* promoter methylation in normal thyroid tissue by bisulfite sequencing

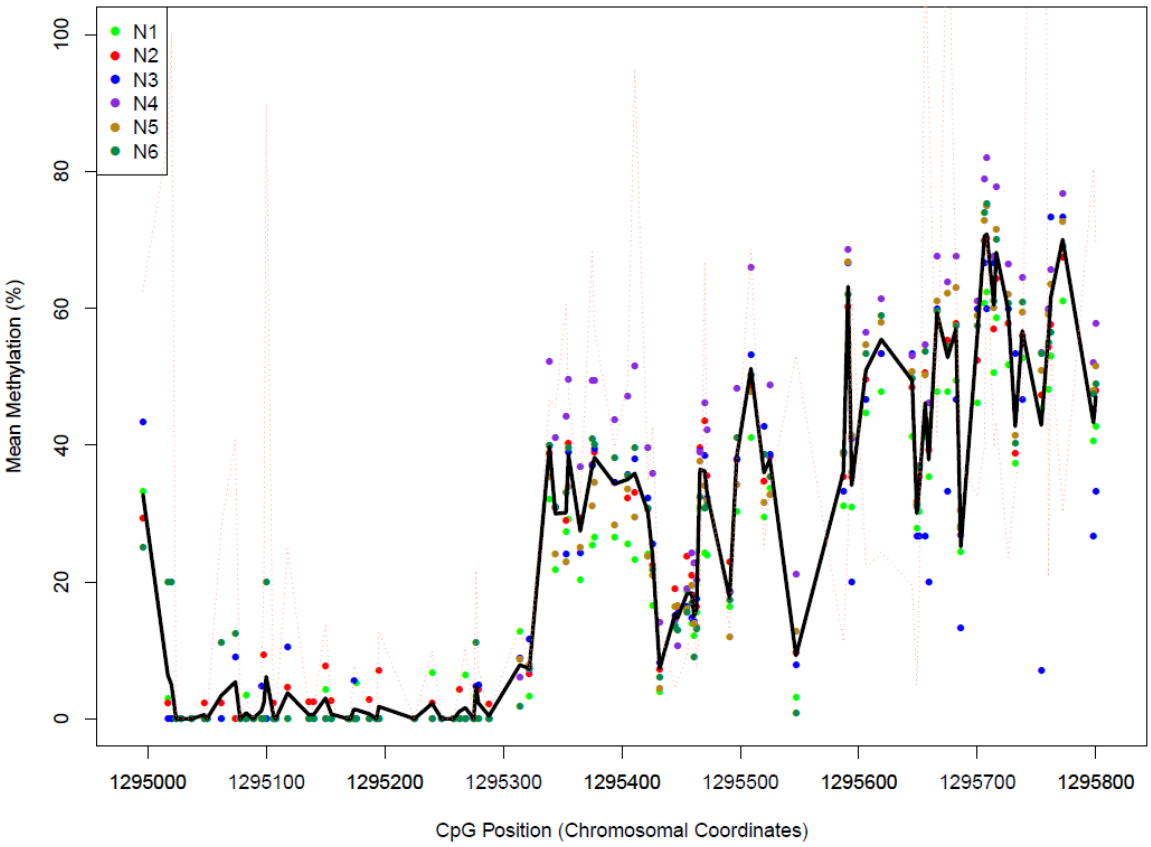

The overall methylation level per CpG locus, as a percentage, over the *TERT* promoter region chr5:1,294,996 (+166) to 1,295,800 (-638) bisulfite sequenced in patient samples from six normal thyroid tissues. Each patient sample is represented in a different color and arbitrarily assigned a number 1-6, with the average of the six samples shown by the black line.

Figure S3: Characterization of *TERT* promoter methylation by bisulfite sequencing in differentiated thyroid cancer cell lines

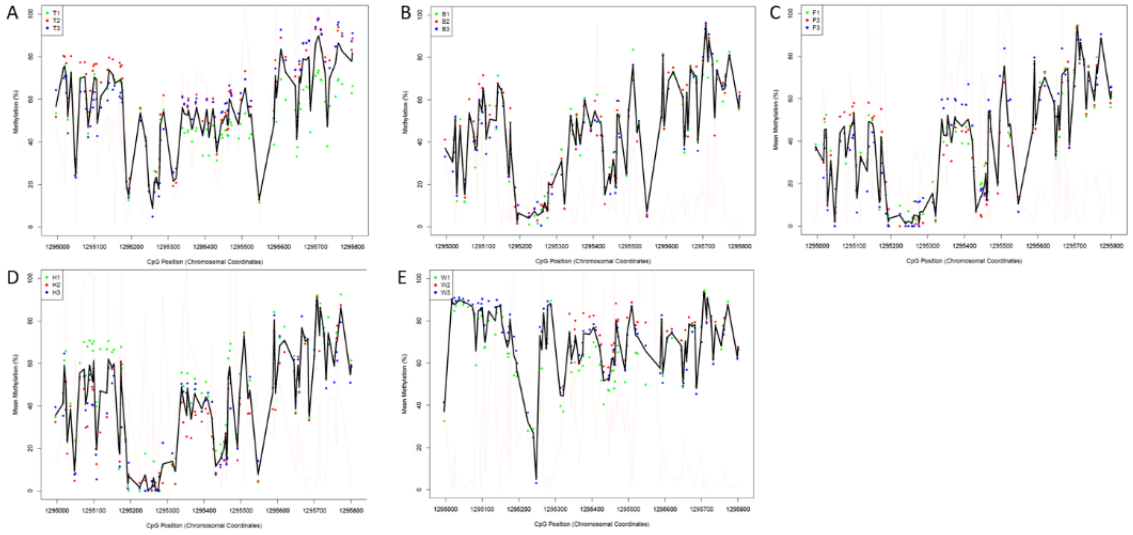

The overall % methylation level at each CpG site over the *TERT* promoter region (chr5:1,294,996/+166 to 1,295,800/-638) in papillary thyroid cancer cell lines TPC-1 (A), BCPAP (B), and follicular thyroid cancer cell lines WRO (C), FTC-133 (D), and FTC-238 (E). Biological triplicates are represented in different colored dots numbered 1-3, with the average of the triplicates shown by the black line, and a red dashed line for the variance between replicates.

Figure S4: Transcription factor binding varies at the *TERT* promoter in DTC cell lines

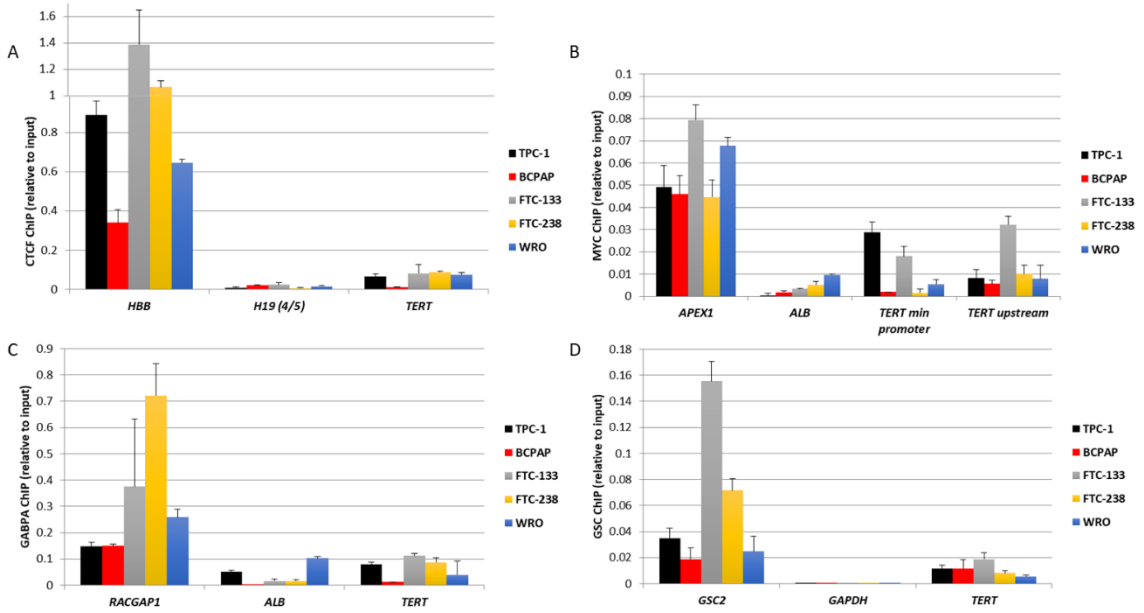

Binding was measured relative to 5% input chromatin in the indicated cell lines by ChIP-qPCR for (A) CTCF. The *HBB* locus was used as a positive control, and the *H19* exon junction as a negative control for CTCF binding, (B) MYC. The *APEX1* locus was used as a positive control, and *ALB* as a negative control, (C) GABPA. The *RACGAP1* locus was used as a positive control, and *ALB* as a negative control, (D) GSC. The *GSC2* locus was used as a positive control, and *GAPDH* as a negative control. All error bars represent standard error within triplicates.

Figure S5: Transcription factor binding varies at the *TERT* promoter in normal thyroid tissue

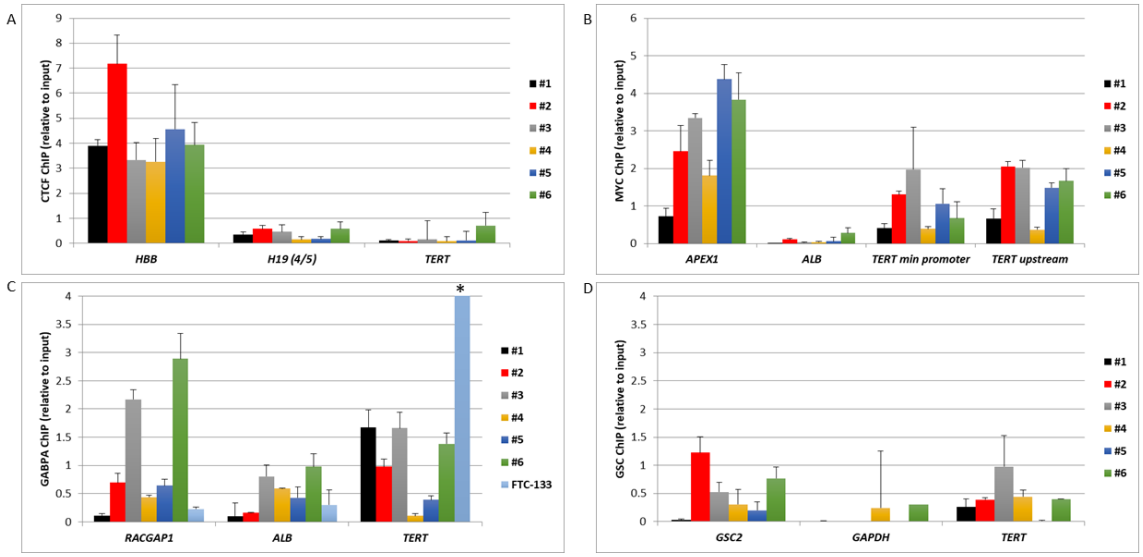

Binding was measured relative to 5% input chromatin in six normal thyroid tissue samples indicated by #1-#6 by ChIP-qPCR for (A) CTCF. The *HBB* locus was used as a positive control, and the *H19* exon junction as a negative control for CTCF binding, (B) MYC. The *APEX1* locus was used as a positive control, and *ALB* as a negative control, (C) GABPA. The *RACGAP1* locus was used as a positive control, and *ALB* as a negative control, (D) GSC. The *GSC2* locus was used as a positive control, and *GAPDH* as a negative control. All error bars represent standard error within triplicates.

Chapter 3: Allele-Specific Regulation of Telomerase Reverse Transcriptase in Promoter Mutant Thyroid Cancer Cell Lines

Adapted from: McKelvey BA, *et al*. 2020 Characterization of Allele-Specific Regulation of Telomerase Reverse Transcriptase in Promoter Mutant Thyroid Cancer Cell Lines. Thyroid Published Online thy.2020.0055.

Introduction

Previously, we characterized *TERT* promoter methylation, transcription factor binding, and their relationship to *TERT* promoter mutations in thyroid cancer cell lines (107). Specifically, we identified a unique methylation pattern suggesting allele-specific methylation in heterozygous *TERT* mutant thyroid cancer cell lines. It is believed that different types of regulation can work in concert and modulate each other's effects on transcription (108). Herein, we investigate the allele-specific effects of *TERT* promoter mutations on promoter methylation, transcription factor binding, chromatin marks, and transcriptional activation.

TERT promoter methylation may play a key regulatory role, including inhibition of transcription factor binding and changing of chromatin state (38, 39, 109). In other genomic locations, DNA methylation blocks binding of the transcriptional activator MYC (95), which also binds to the *TERT* minimal promoter to activate TERT transcription (110). Our previous work demonstrated binding of MYC at the minimal *TERT* promoter, and methylation patterns in heterozygous *TERT* mutant thyroid cancer cell lines in of about 50% methylation (107). This suggested that allele-specific methylation in heterozygous mutant cell lines might play a role in regulation. In support

of this, *TERT* mutant cancers were recently shown to display lower levels of methylation at the *TERT* promoter than wildtype cancers (56). However, allele-specific methylation at the *TERT* promoter, or allele-specific binding of MYC to *TERT* has not been shown. This is in part because standard methylation sequencing has mostly been performed in the context of sodium bisulfite pretreatment of DNA, which reverts both *TERT* promoter mutations back to wild type (C->T). New nanopore sequencing technology (111) relies on Cas9 targeting and cutting at specific genomic locations, allowing for targeted long read sequencing. Unlike Illumina sequencing based on florescence, nanopore sequencing detects nucleotide-specific changes in ionic current as a single molecule of DNA moves through a protein pore inserted into a synthetic polymer membrane (112). Importantly, nanopore sequencing can distinguish cytosine from methyl-cytosine, negating the need for sodium bisulfite pretreatment of DNA. This profiles DNA methylation at the targeted sequence directly, thus enabling one to assess methylation in an allele-specific manner over a much larger genomic region than previously possible.

Further, a subset of cancer cell lines appear to show monoallelic expression (MAE) of *TERT* from the *TERT* mutant promoter (55). Studies have identified heterozygous SNPs in the *TERT* coding region and demonstrated only one allele in the *TERT* cDNA transcript (52, 56). However, since the *TERT* promoter mutation is not represented in the coding sequence, studies have not definitively linked the *TERT* promoter mutation with MAE from the mutated allele.

In this study, we definitively demonstrate for the first time allele-specific methylation at the *TERT* promoter and into the gene body, in which the mutant allele is significantly less methylated at the *TERT* promoter than the wildtype allele, and more methylated into the gene body than the wildtype allele, consistent with the methylation pattern of actively transcribed genes (113, 114). We utilized chromatin immunoprecipitation followed by Sanger sequencing to confirm allele-specific binding of GABPA to the mutant *TERT* allele in thyroid cancer cell lines, and demonstrate for the first time similar allele-specific binding of MYC. Furthermore, we show chromatin marks associated with active transcription (H3K4me3) on only the mutant allele, while repressive chromatin marks (H3K27me3) associate with the wildtype allele. The allele-specific *TERT* promoter methylation, differential histone modifications, and activator binding, all result in monoallelic expression, the latter demonstrated by phasing a SNP present in exon 2 of *TERT* with the allele carrying the *TERT* promoter mutation. In summary, we report the first direct evidence of monoallelic expression by the *TERT* promoter mutation, and confirm previous findings in other cancer types of allele-specific binding of GABPA and chromatin marks in thyroid cancer cell lines.

Results

Allele-Specific Methylation Patterns in Thyroid Cancer Cell Lines

DNA isolated from thyroid cancer cell lines underwent enrichment and nanopore sequencing at the *TERT* promoter by nCATS to determine the methylation status of the *TERT* promoter. Nanopore methylation calls for all cell lines were compared and found comparable to previously published Illumina bisulfite sequencing of the *TERT* promoter

(107) (Supplemental Figure 7). Unlike traditional bisulfite treatment, in which the *TERT* mutation status (C>T) is lost, nanopore sequencing identifies native methylation without bisulfite treatment and thereby maintains the ability to differentiate mutation status between alleles. In the heterozygous *TERT* mutant cell line TPC-1, a significant drop in methylation surrounding the *TERT* TSS occurred on the mutant allele, to under 5% methylation (Figure 11). The mutant allele also showed higher levels of methylation throughout the *TERT* gene body at or above 75%, while the wildtype allele remained comparatively stable at approximately 50-75% methylation over the *TERT* gene body and promoter. The other heterozygous *TERT* mutant cell lines BCPAP and FTC-238 followed the same pattern as TPC-1, in which there was a drop in methylation at the TSS with only 20% and 30% of the mutant allele methylated in BCPAP and FTC-238 respectively (Figure 12, Supplemental Figure 8). The heterozygous mutant cell lines also exhibited the higher levels of methylation in the gene body. In BCPAP, a drop in methylation in the wildtype allele was observed in the gene body, specifically in the intron between exon 2 and 3. The homozygous *TERT* mutant cell line FTC-133 showed a methylation pattern consistent with the mutant alleles of the heterozygous cell lines, showing a drop in methylation to less than 15% at the TSS and high gene body methylation. Conversely, the homozygous wildtype cell line WRO showed no significant drop in methylation at the TSS (above 50%) and lower levels of 50-75% methylation in the gene body, reflective of the wildtype alleles in the heterozygous mutant cell lines (Figure 12). Further examination of *TERT* promoter methylation revealed low methylation surrounding the transcription start site (TSS) in the mutant allele (4.8%, 20%, 31.8% average methylation for TPC-1, BCPAP, and FTC-238 respectively), while high levels of methylation were

seen in the wildtype allele (Figure 13) (79.9%, 73.1%, 75.1% average methylation for TPC-1, BCPAP, and FTC-238 respectively). Furthermore, the regions surrounding the *TERT* promoter mutation at the GABPA binding site, as well as the MYC binding site, also exhibited significantly less methylation on the mutant allele, with the exception of the GABPA site in FTC-238, which exhibited low methylation of both alleles. Homozygous cell lines followed similar patterns of methylation, with the homozygous mutant cell line exhibiting low levels of methylation at the promoter (less than 20% methylation), and the homozygous wildtype cell line showing higher levels of methylation (30-65% methylation) (Figure 13).

Allele-Specific Transcription Factor Binding in Thyroid Cancer Cell Lines

Since the binding sites for GABPA and MYC were differentially methylated in our heterozygous mutant thyroid cancer cell lines, we investigated whether these factors exhibited allele-specific binding as well. ChIP analysis of the two ETS factors known to bind at the *TERT* promoter, ETV5 and GABPA, showed GABPA as the predominant factor binding to the *TERT* promoter in our well differentiated thyroid cancer cell lines (Supplemental Figure 9). We therefore performed Sanger sequencing of the *TERT* promoter on DNA precipitated with either MYC or GABPA antibodies. Sanger sequencing of immunoprecipitated DNA from TPC-1, BCPAP, and FTC-238 cell lines resulted in only the mutant *TERT* allele, indicating selective binding of GABPA and MYC to the mutant allele (Figure 14).

Allele-Specific Chromatin Marks in Thyroid Cancer Cell Lines

To further investigate transcriptional regulation, ChIP followed by Sanger sequencing of the region of the *TERT* promoter encompassing the TERT mutation and TSS, was conducted on DNA immunoprecipitated with antibodies directed against either H3K4me3 (activating) or H3K27me3 (silencing). This revealed the least amount of active chromatin mark, H3K4me3, in the wildtype cell lines Nthy-ori-3 and WRO, an intermediate amount in the heterozygous *TERT* mutant cell lines (TPC-1, BCPAP, and FTC-238), and the highest amount associated with the homozygous *TERT* mutant cell line FTC-133 (Figure 15A). The silent chromatin mark, H3K27me3, displayed the opposite trend, with the highest level in the homozygous wildtype cell lines, and the least abundant in the homozygous *TERT* mutant cell line. To further delineate the effect of the *TERT* mutation on chromatin marks, we conducted Sanger sequencing of the immunoprecipitated DNA at the *TERT* locus. In the heterozygous *TERT* mutant cell lines, we observed an allele-specific association with chromatin marks. The *TERT* mutant allele preferentially bound to the active H3K4me3, while the wildtype allele bound to the silent H3K27me3 (Figure 15B).

Monoallelic Expression of TERT

To determine if monoallelic expression of *TERT* occurs in our heterozygous *TERT* mutant thyroid cancer cell lines, we identified SNPs in the *TERT* coding sequence. As previously described (29), TPC-1 contains a heterozygous G>A SNP in exon 2 (rs2736098). In the heterozygous cell lines BCPAP and FTC-238, a C>T SNP (rs2853690), was identified in the *TERT* 3'UTR by Sanger sequencing of the genomic DNA (Figure 16). Sanger sequencing of cDNA from all three cell lines showed

transcripts with only one of the SNP alleles, confirming monoallelic *TERT* expression (Figure 16). Furthermore, through long sequencing reads obtained by nCATS, we confirmed the *TERT* promoter mutation to be on the same allele as the expressed transcript of exon 2 in TPC-1. This expression of only the 'A' allele at exon 2 (rs2736098) in TPC-1 directly confirms expression of *TERT* only from the mutant *TERT* allele.

Transcriptional Output and Telomerase Activity

To characterize overall telomerase activation, we measured full length *TERT* transcripts, in which the alpha nor beta regions were present, in our thyroid cancer cell lines by quantitative reverse transcriptase PCR (qRT-PCR). We observed that the wildtype normal thyroid cell line, Nthy-ori-3, had no measurable amount of full length *TERT* transcript, and the wildtype WRO showed the least amount of transcript of the cancer cell lines (Figure 17). Interestingly, FTC-133, the homozygous *TERT* mutant thyroid cancer cell line, exhibited less *TERT* transcript than the three heterozygous *TERT* mutant thyroid cancer cell lines. This pattern also correlated with relative telomerase activity (RTA), in which FTC-133 also showed less telomerase activity than the three heterozygous *TERT* mutant cell lines. The wildtype cell lines showed the least telomerase activity.

Discussion

It is already known that *TERT* promoter mutations activate *TERT* transcription and telomerase activity. However, due to limitations in sequencing technology, the allele-

specific effects of the heterozygous *TERT* promoter mutation have not been completely elucidated. Utilizing thyroid cancer cell lines that harbor the *TERT* mutation (11), and nanopore Cas9 targeted sequencing (nCATS), we demonstrated allele-specific methylation at the *TERT* promoter and into the gene body. Specifically, we used ChIP-Sanger sequencing to show both allele-specific GABPA and MYC binding, and allele-specific distribution of both active and silent histone modifications (H3K4me3 and H3K27me3). These allele-specific effects correlated directly with monoallelic expression of *TERT* in the heterozygous *TERT* mutant cell lines as well as overall higher levels of *TERT* transcription and telomerase activity.

Our characterization of *TERT* promoter methylation in thyroid cancer cell lines revealed significantly lower methylation levels at the transcription start site (TSS), *TERT* mutation site, and MYC binding site on the *TERT* mutant allele compared to the wildtype allele. These findings corroborate previous work that showed overall lower levels of *TERT* promoter methylation in *TERT* mutant cancer cell lines (56). Importantly, however, our study extends the work by examining methylation patterns on non-amplified DNA in an allele-specific manner. This demonstrated that only the mutant allele is hypomethylated, with a significant dip (less than 30% methylated in the mutant allele compared to over 70% methylated in the wildtype allele) in methylation restricted to the TSS, and thus, demonstrating for the first time allele-specific methylation of *TERT*. The homozygous wildtype and homozygous *TERT* mutant cell lines follow the same methylation pattern as the heterozygous alleles. This pattern of promoter hypomethylation and gene body methylation is in line with previously reported methylation patterns for genes with active

transcription (113–115). Further, our studies of histone modifications support the activation of the *TERT* mutant allele, as the mutant promoter was associated with activating H3K4me3 marks, while the wildtype allele exhibited silencing H3K27me3 marks, a pattern also seen in other cancer cell types (52).

The *TERT* promoter mutation (-124 C>T) creates a consensus binding site for the ETS family factors, and we previously demonstrated the factor GABPA bound to the *TERT* promoter in our cell lines derived from well-differentiated thyroid cancers (107). After a recent study described ETV5 binding at the *TERT* promoter in thyroid cancer cell lines (29), we investigated ETV5 binding in our thyroid cancer cell lines. We found that ETV5 bound significantly less at the *TERT* promoter than GABPA in our thyroid cancer cell lines. The recent paper functionally characterized ETV5 in three thyroid cancer cell lines, two derived from anaplastic thyroid cancers and one derived from papillary thyroid cancer, finding that ETV5 predominantly bound in the two anaplastic thyroid cancer cell lines, while the papillary thyroid cancer cell line, TPC-1, showed GABPA binding (29). Our GABPA results confirm their findings in TPC-1, and further defines ETS factor involvement in well differentiated thyroid cancer. ETV5 and a different regulatory mechanism may be present in less differentiated cancer cells.

We have confirmed, as seen in other cancer types (26, 52), that GABPA binds to the *TERT* mutant allele in an allele-specific manner in thyroid cancer cell lines. Our previous work showed the highest level of GABPA binding in the *TERT* homozygous mutant, with moderate levels in the heterozygous mutants, and very low levels of binding of GABPA

in the wildtype *TERT* cell line (107). The allele-specific methylation of *TERT* also affected the MYC binding site at the minimal promoter, which exhibits lower levels of methylation on the mutant allele. As with GABPA, we found MYC binding to the *TERT* mutant allele in an allele-specific manner.

Ours is the first study to show allele-specific binding of MYC. MYC is a known direct activator of *TERT* transcription (110). Our previous work showed enrichment for MYC at the TERT promoter in the thyroid cancer cell lines (107). As MYC has been shown to be methylation-sensitive in binding to its consensus site at other gene locations (95), the higher level of methylation at the *TERT* binding site on the wildtype allele may partially prohibit MYC binding, therefore lessening activation. Our results contradict a previous study in cancer cell lines (27) that concluded MYC was a mutation-independent activating factor of *TERT*. The previous study examined the effects on *TERT* expression after MYC knockdown in cancer cell lines, and therefore could be the result of MYC's role at other loci. Conversely, our study specifically interrogated MYC binding to the *TERT* promoter, where we did observe mutation-dependent MYC binding.

In addition to the allele-specific binding of activators MYC and GABPA and the activating chromatin mark H3K4me3, we confirmed monoallelic transcription of *TERT* in the heterozygous *TERT* mutant thyroid cancer cell lines by utilizing SNPs identified in the coding sequence. Analysis of TPC-1 showed that the *TERT* mutation and the SNP on the expressed transcript occur on the same allele, providing the first direct evidence of *TERT* expression solely from the mutant *TERT* allele. Furthermore, this monoallelic

expression resulted from monoallelic transcriptional activation of *TERT* in the thyroid cancer cell lines. As expected, we observed the lowest levels of *TERT* transcription and telomerase activity in the *TERT* wildtype cancer cell line, WRO, and the normal thyroid cell line, Nthy-ori-3. It is important to note that while Nthy-ori-3 is utilized as a normal thyroid cell line, the cell line is immortalized with multiple mutations and chromosomal abnormalities, although none are known to be oncogenic (116). The three heterozygous *TERT* mutant thyroid cancer cell lines showed the highest levels of *TERT* expression and telomerase activity. Surprisingly, the *TERT* homozygous mutant cell line, FTC-133, showed less *TERT* transcript and telomerase activity than the heterozygous cell lines. Previous study of another *TERT* homozygous mutant cell line, SW1736, also showed less *TERT* expression in the cell line than in heterozygous mutant cell lines (29). This may suggest additional post-transcriptional and post-translational regulatory processes affecting telomerase activity.

In summary, we have demonstrated and characterized allele-specific methylation at the *TERT* promoter and into the gene body in heterozygous *TERT* mutant thyroid cancer cell lines. Furthermore, lower levels of methylation at the GABPA and MYC binding site on the *TERT* mutant allele correlated with allele-specific binding of these two transcriptional activators. The chromatin mark H3K4me3 further confirmed activation of only the mutant allele, while the H3K27me3 mark also confirmed silencing of the wildtype allele. These regulatory mechanisms result in monoallelic transcription of *TERT* in heterozygous mutant cell lines, corroborated by unique SNPs that showed TERT transcription originating solely from the mutant *TERT* allele.

Figure 11: DNA methylation assessed by nanopore Cas9 targeted sequencing (nCATS) shows drop in methylation surrounding TSS and higher levels of methylation in the gene body of mutant *TERT* allele in heterozygous TPC-1 thyroid cancer cell line

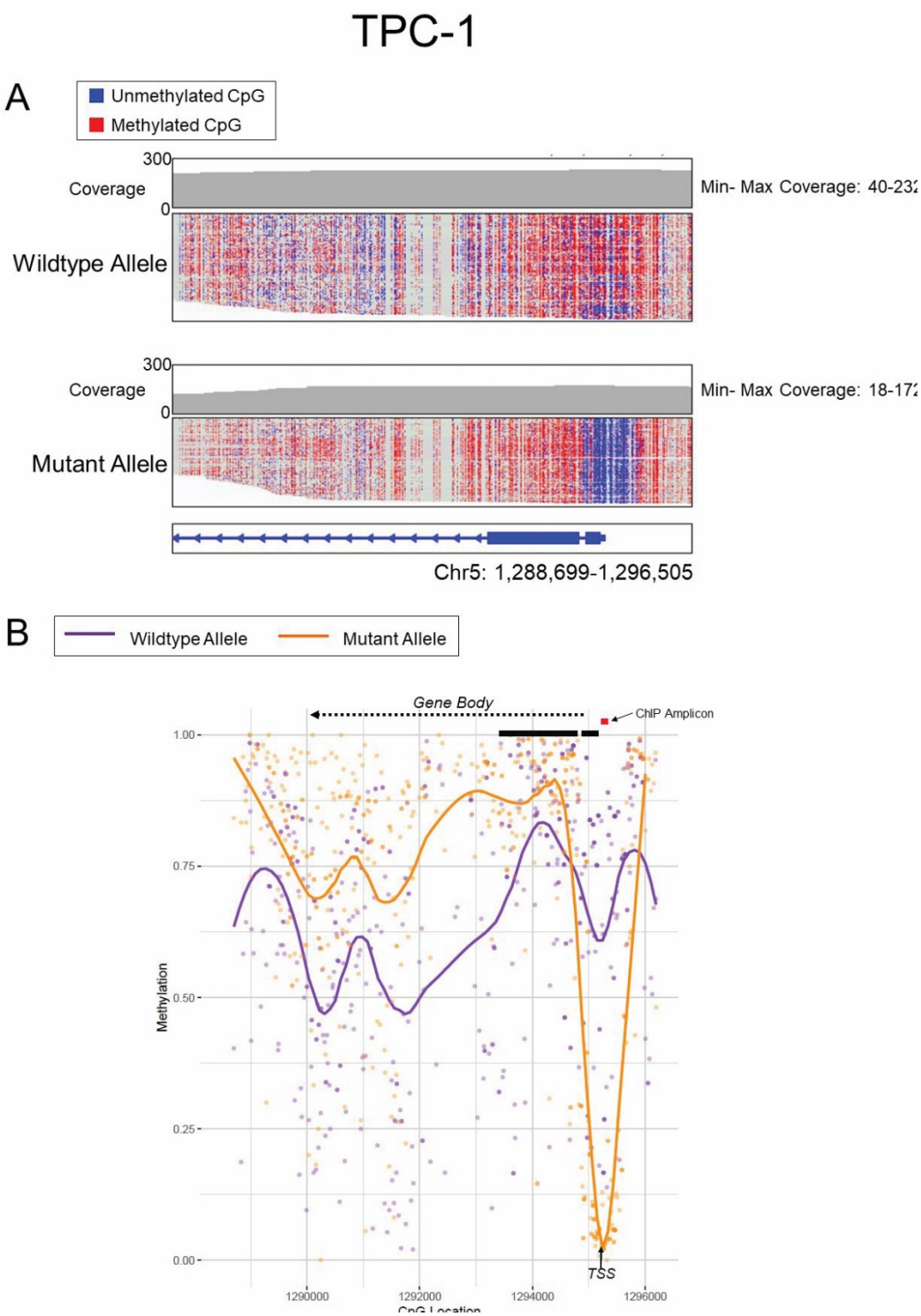

A) Read-level methylation plots using IGV. Depth of coverage at the *TERT* gene is shown in the top graph where the coverage at each base is indicated by the grey line plot with the minimum and maximum CpG coverage stated. Each horizontal line in the wildtype (top) and mutant allele (bottom) plots is a single nCATS read. Red denotes a methylated CpG and blue denotes an unmethylated CpG. The *TERT* chromosomal coordinates are shown at the bottom to designate position. **B)** Average methylation plots. The wildtype allele is depicted in purple and the mutant *TERT* allele in orange. Individual dots represent methylation at an individual CpG site. The orange or purple line represents the smoothened level of methylation over the entire area. The black arrow denotes the transcription start site (TSS). *TERT* exons 1 and 2 are shown by thick black lines. The gene reads from right to left into the gene body, denoted by the dashed arrow. The red line indicates the PCR-amplified region used in subsequent ChIP experiments (Figures 4-5).

Figure 12: Average methylation plots of the *TERT* promoter and gene body in homozygous vs heterozygous *TERT* mutant thyroid cancer cell lines

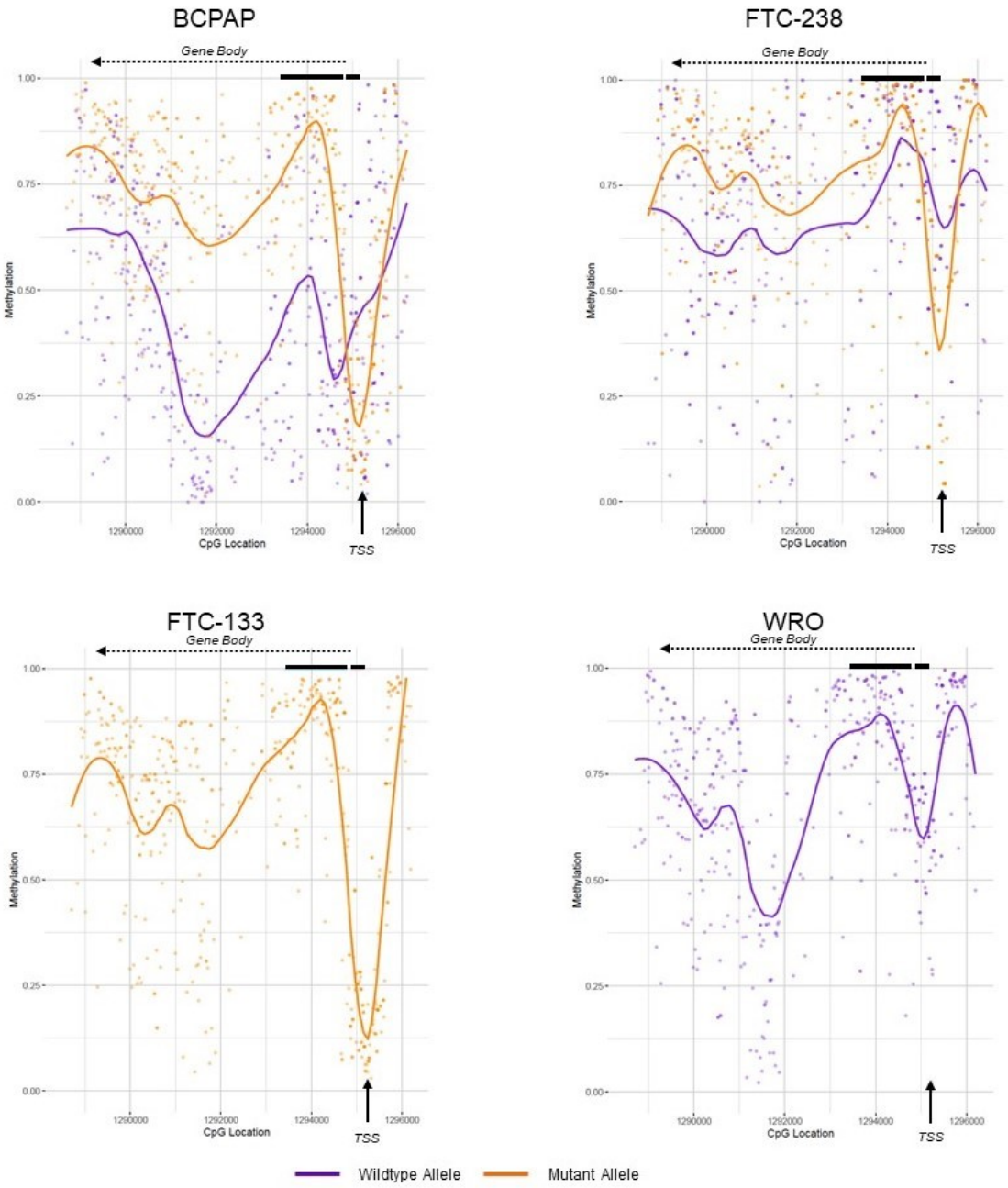

Methylation levels were in the following thyroid cancer cell lines: wildtype cell line WRO, heterozygous TERT mutant cell lines BCPAP and FTC-238, and homozygous mutant cell line FTC-133. The wildtype allele is depicted in purple and the mutant *TERT* allele in orange. Individual dots represent methylation at an individual CpG site. The purple or orange line represents the smoothened methylation over the entire area, showing drops in methylation surrounding the TSS, and higher levels in the gene body, of the mutant allele. The black arrow denotes the transcription start site (TSS). *TERT* exons

1 and 2 are shown by thick black lines. The gene reads from right to left into the gene body, denoted by the dashed arrow.

Figure 13: Allele-specific methylation at the *TERT* promoter in thyroid cancer cell lines by nCATS

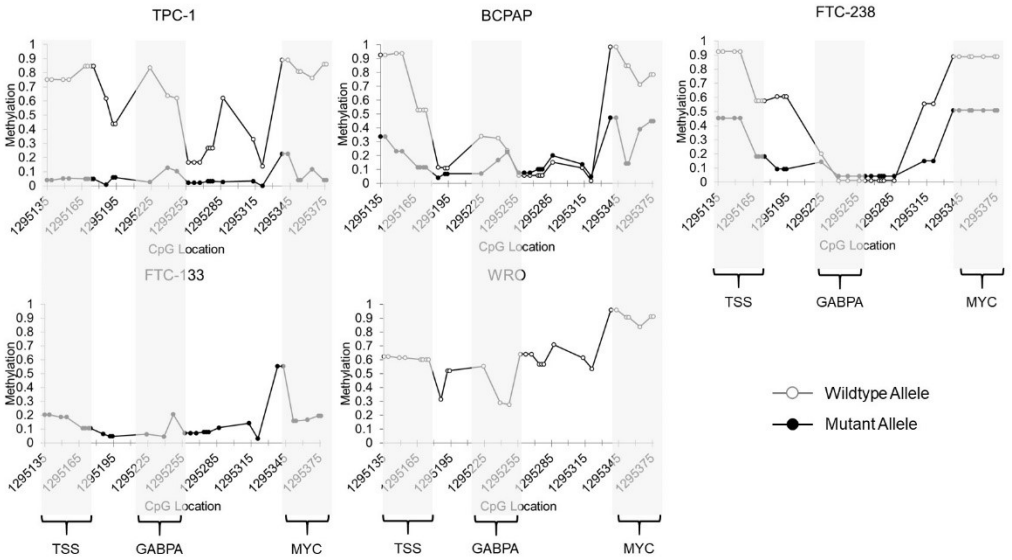

Methylation levels at the *TERT* minimal promoter, including the TSS, GABPA binding site (*TERT* mutation), and MYC binding site in heterozygous *TERT* mutant cell lines TPC-1, BCPAP, and FTC-238, wildtype cell line WRO, and homozygous *TERT* mutant cell line FTC-133. CpG location is denoted by chromosomal location. The wildtype allele is shown in gray with open circles and the mutant allele in black with solid circles.

Figure 14: Allele-specific methylation at the *TERT* promoter in thyroid cancer cell lines by nCATS

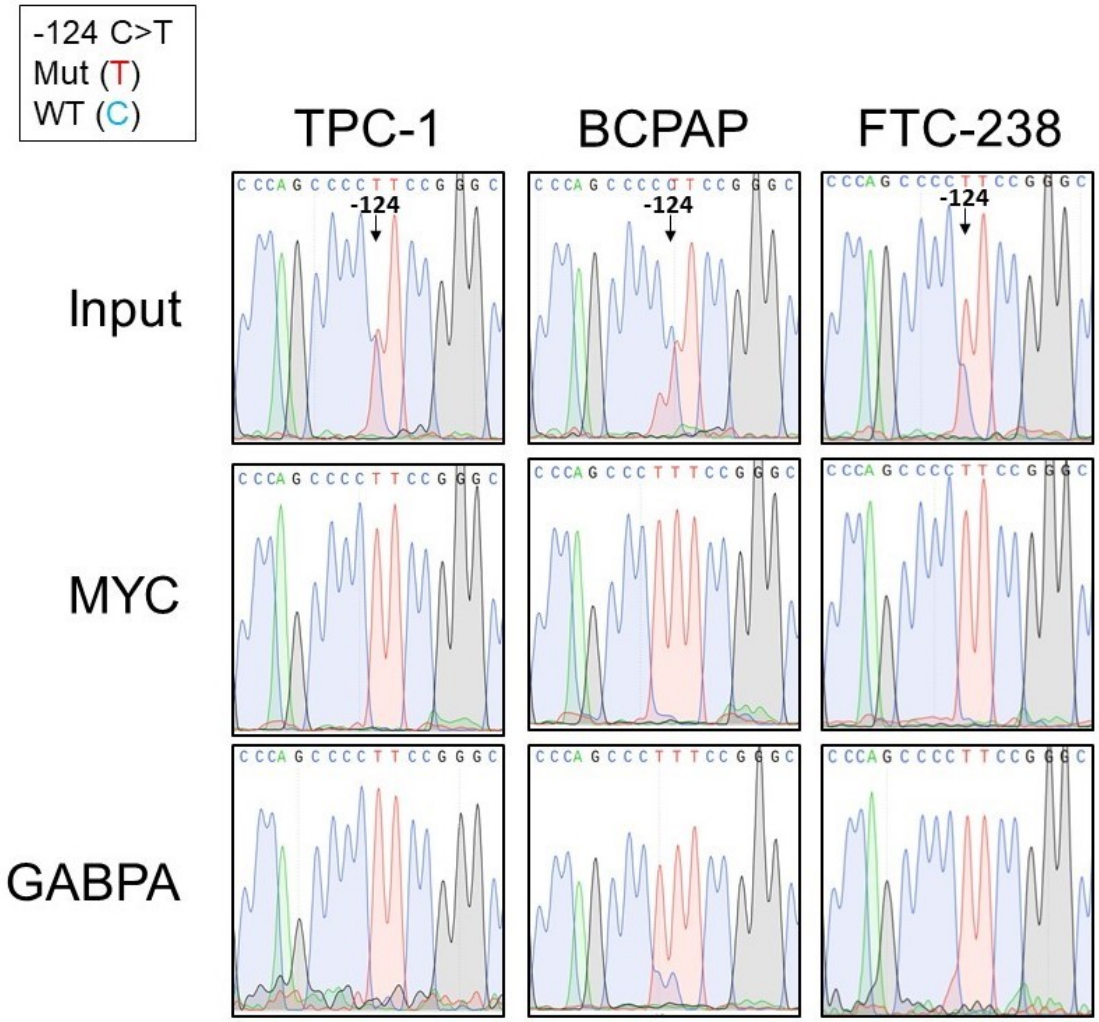

Allele-specific transcription factor binding of MYC and GABPA at the *TERT* promoter in heterozygous *TERT* mutant thyroid cancer cell lines. Chromatin immunoprecipitation (ChIP) in the heterozygous *TERT* mutant thyroid cancer cell lines with either MYC or GABPA antibodies followed by Sanger sequencing of the *TERT* promoter at the -124 C>T *TERT* mutation, compared to input genomic DNA before ChIP. At the -124 *TERT* position, the mutant allele is represented by the red curve (T), while the wildtype allele is represented by the blue curve (C). The input genomic DNA shows the presence of both alleles at the -124 position, while the immunoprecipitated DNA shows only the red curve indicative of the mutant allele.

Figure 15: Allele-specific chromatin marks at the *TERT* minimal promoter in thyroid cancer cell lines

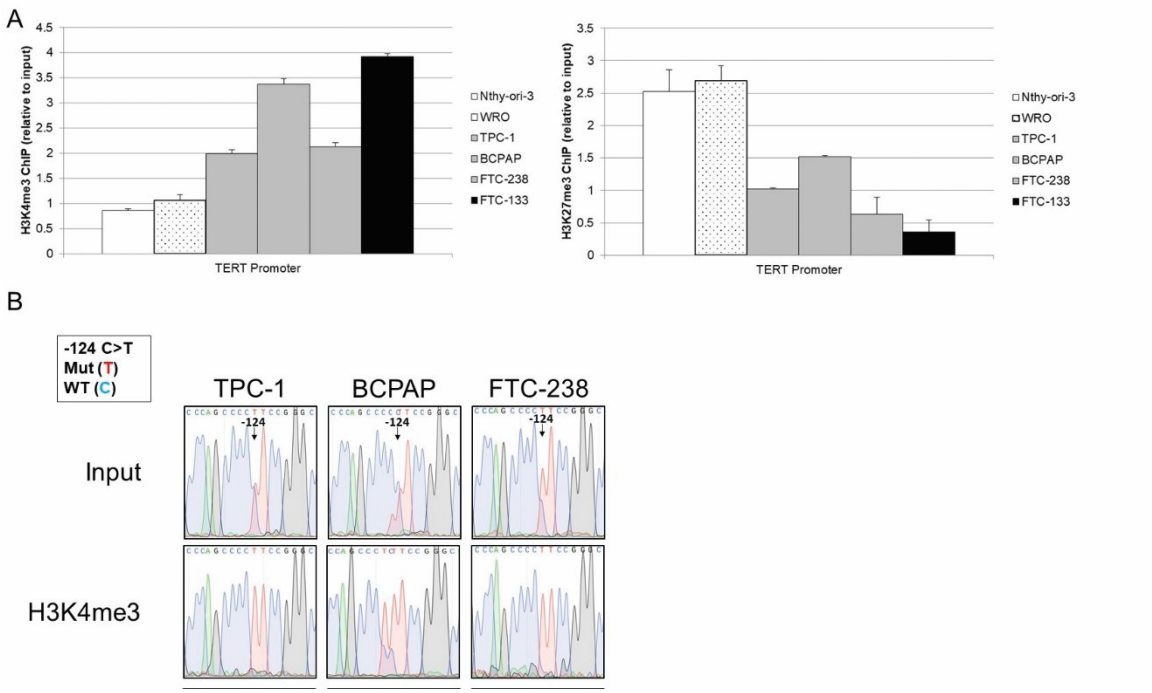

A) ChIP with either H3K4me3 (activating chromatin mark) or H3K27me3 (silencing chromatin mark) antibodies. Binding was measured relative to 5% input chromatin, and binding at the *TERT* locus assessed by qPCR. H3K4me3 binding at the *TERT* promoter was most abundant in the homozygous mutant cell line FTC-133 (black bar), intermediate in the heterozygous mutant cell lines (grey bars), and least abundant in the homozygous wildtype cell lines (white bars with cancer cell line WRO denoted by stipple compared to normal cell line NThy-ori-3). H3K27me3 binding was reciprocal of the H3K4me3 binding. All error bars represent standard error within triplicates. **B)** Sanger sequencing of the *TERT* promoter immunoprecipitated DNA of heterozygous *TERT* mutant thyroid cancer cell lines at the -124 C>T mutation, compared to input genomic DNA before ChIP. At the -124 *TERT* position, the mutant allele is represented by the red curve (T), while the wildtype allele is represented by the blue curve (C). The input genomic DNA shows the presence of both alleles at the -124 position, while the H3K4me3 immunoprecipitated DNA shows only the red curve indicative of the mutant allele. H3K27me3 immunoprecipitated DNA shows only the blue curve indicative of the wildtype allele.

Figure 16: *TERT* monoallelic expression in heterozygous *TERT* mutant thyroid cancer cell lines

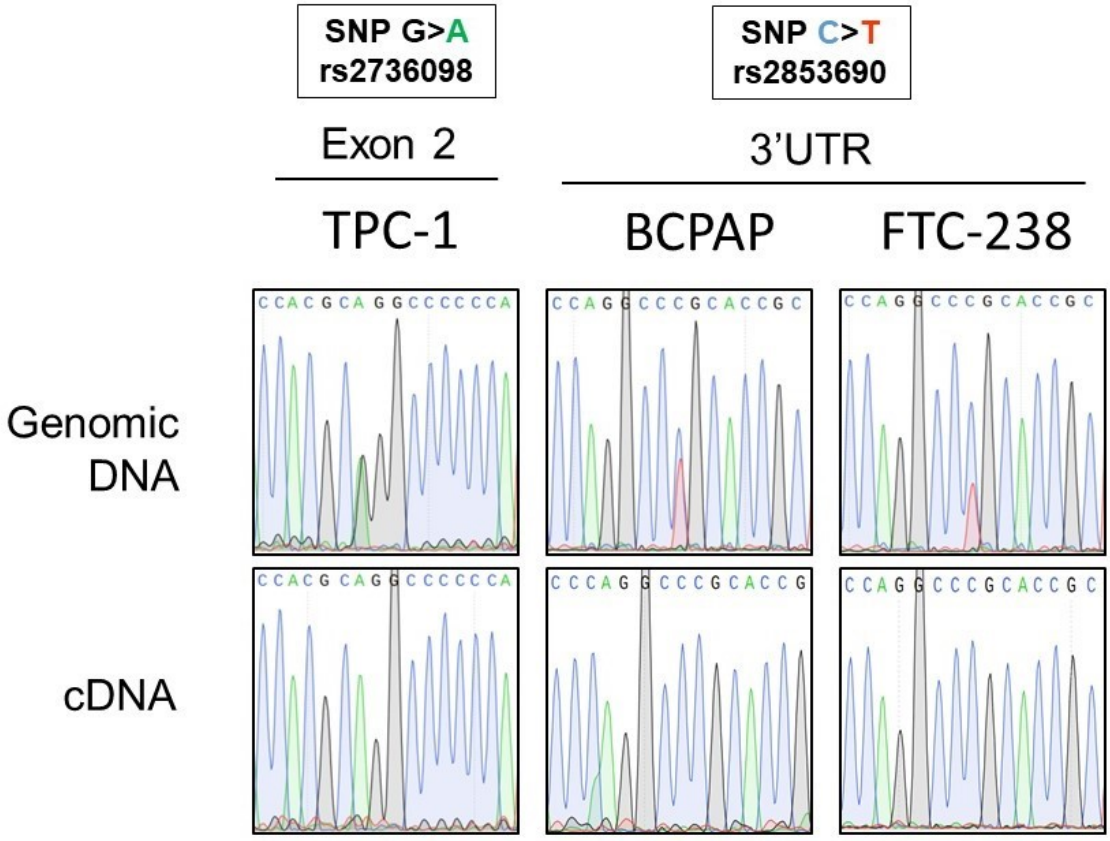

Sanger sequencing analysis of the exon 2 region and 3'UTR region of *TERT* surrounding SNPs rs2736098 and rs2853690 respectively in amplified genomic DNA, as well as cDNA, from *TERT* heterozygous mutant cell lines TPC-1, BCPAP, and FTC-238. While the genomic DNA in all cell lines showed both alleles of the SNP, the cDNA showed only one allele in all cell lines.

Figure 17: Heterozygous *TERT* mutant thyroid cancer cell lines exhibit higher levels of *TERT* transcript and telomerase activity compared to homozygous wildtype or mutant thyroid cancer cell lines

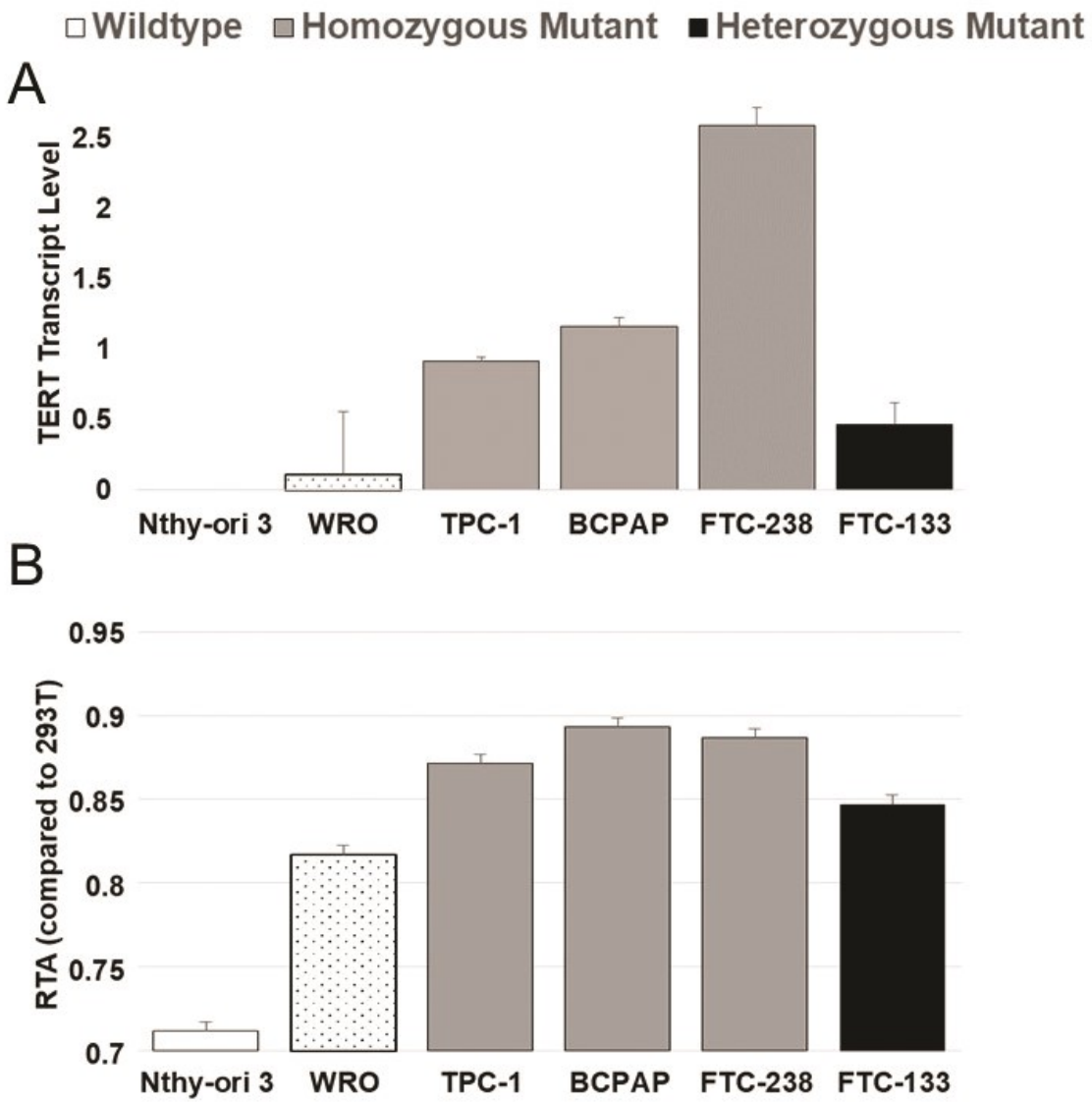

A) *TERT* transcript level measured by qRT-PCR in thyroid cancer cell lines, and **B)** relative telomerase activity (RTA) in thyroid cancer cell lines compared to HEK293T cells. White denotes homozygous wildtype (stippling denotes the *TERT* homozygous wildtype cancer cell line from the normal thyroid cell line), grey denotes heterozygous mutant, and black denotes homozygous mutant thyroid cancer cell lines. Standard deviation is noted.

Figure S6: H3K4me3 and H3K27me3 ChIP-qPCR at control loci

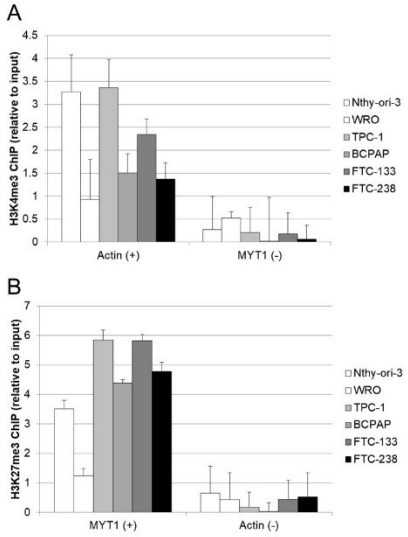

Binding was measured relative to 5% input chromatin in the indicated cell lines by ChIP-qPCR for **A)** H3K4me3. The *Actin* locus was used as a positive control, and *MYT1* as a negative control for H3K4me3 binding, **B)** H3K27me3. The *MYT1* locus was used as a positive control, and *Actin* as a negative control. Both chromatin marks showed robust binding as expected in the positive controls, and low binding in the negative controls. All error bars represent standard error within triplicates.

Figure S7: Methylation calls for Illumina bisulfite sequencing and nCATS are similar

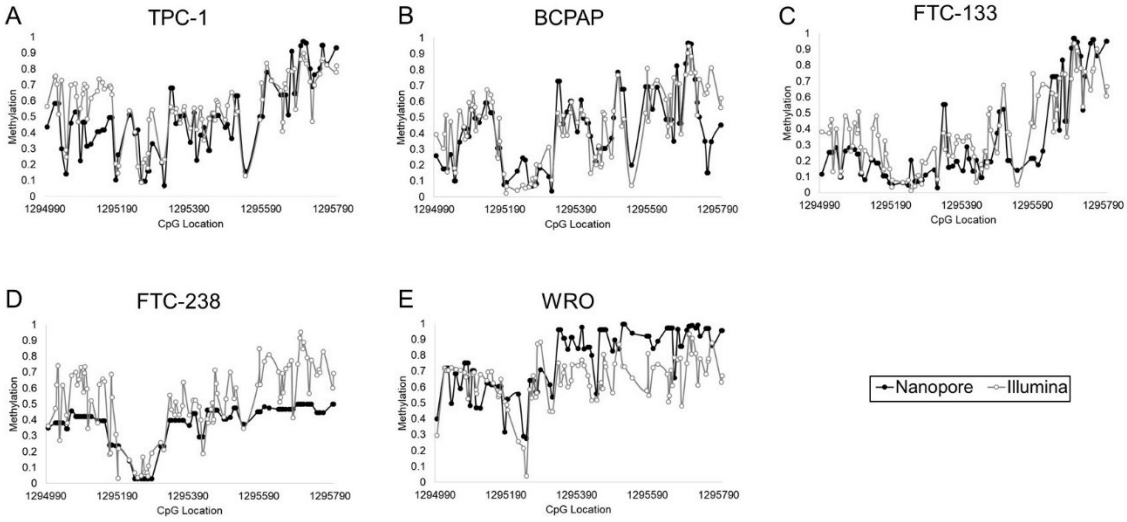

Illumina bisulfite sequencing (gray) at the *TERT* promoter region compared to nCATS (black) in the same region in thyroid cancer cell lines **A)** TPC-1 **B)** BCPAP **C)** FTC-133 **D)** FTC-238 and **E)** WRO show overall concordance in methylation calls.

Figure S8: Thyroid cancer cell lines show TSS methylation level correlated with *TERT* promoter mutation status

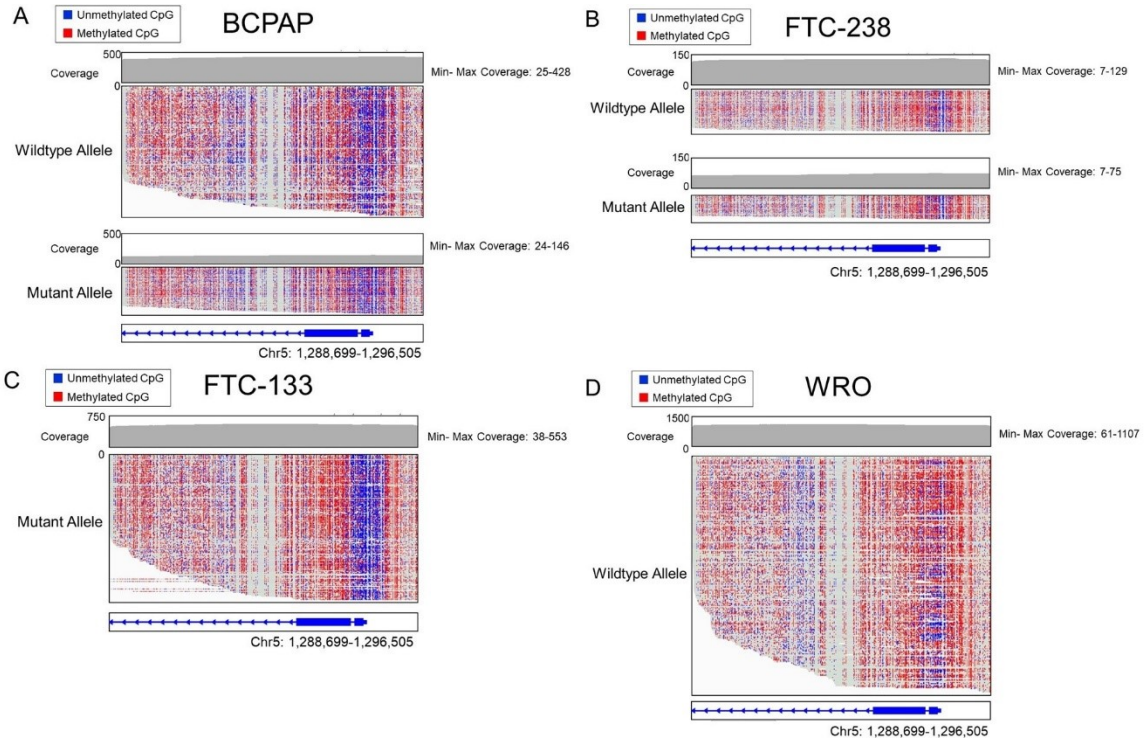

Read-level methylation plots using IGV for heterozygous *TERT* mutant thyroid cancer cell lines **A)** BCPAP and **B)** FTC-238, homozygous mutant **C)** FTC-133, and homozygous wildtype **D)** WRO at the promoter and gene body for *TERT*. Depth of coverage at the *TERT* gene is shown in the top graph where the coverage at each base is shown by the grey line plot with the minimum and maximum CpG coverage stated. Each horizontal line in the mutant and wildtype allele depiction is a single nCATS read sorted based on the *TERT* promoter mutation as mutant or wildtype, where red denotes a methylated CpG and blue denotes an unmethylated CpG. The *TERT* chromosomal coordinates are shown at the bottom to designate position.

Figure S9: GABPA binds more abundantly than ETV5 at the *TERT* promoter in all thyroid cancer cell lines

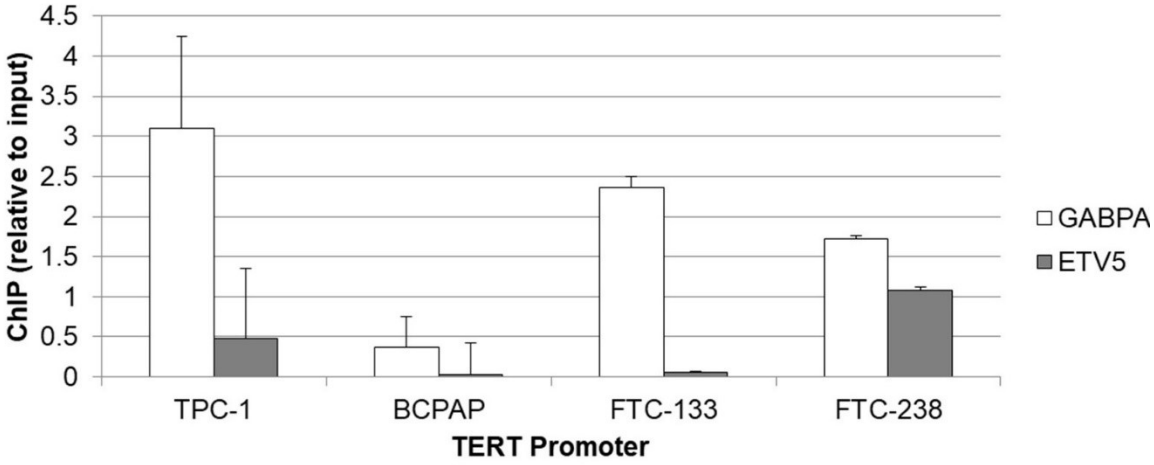

Binding was measured relative to 5% input chromatin in the indicated cell lines by ChIP-qPCR for GABPA and ETV5. All error bars represent standard error within triplicates.

Chapter 4: CRISPR/Cas9 editing the *TERT* promoter

Introduction

Recently, we showed allele-specific methylation, chromatin marks, transcription factor binding, and expression in thyroid cancer cell lines harboring the *TERT* mutation (117). Briefly, the mutant allele showed hypomethylation surrounding the transcription start site (TSS), with the active chromatin mark H3K4me3, and bound transcriptional activators GABPA and MYC. The wildtype allele showed hypermethylation at the TSS, the silencing mark H3K27me3, and no bound transcriptional activators. Further, transcription was mono-allelic, from the mutant allele (117). This allele-specific pattern of methylation, chromatin marks, and transcription factor binding has been demonstrated in other cancer cell types as well (26, 52, 118). Nevertheless, the evidence linking the *TERT* mutation with *TERT* promoter status still remains correlative and not causative. Concluding my thesis, we are further advancing this work by exploring the *causative* role of the mutation and its acute effects on promoter DNA methylation, chromatin marks, and expression.

In our current study, we conducted CRISPR/Cas9 editing of the *TERT* promoter in the heterozygous *TERT* mutant thyroid cancer cell line, TPC-1, to create the full set of possible *TERT* promoter mutation states, in an isogenic background. TPC-1 is a near-diploid PTC derived cell line that carries a RET/PTC1 rearrangement. Through use of the CRISPR/Cas9 editing system, we are creating a controlled study system in a thyroid cancer cell line to study the causative role of the *TERT* promoter mutations on *TERT* transcriptional regulation and telomerase activity, furthering our previous investigations. We will

interrogate the effect of changing the *TERT* promoter mutation status on *TERT* promoter methylation, histone modifications, transcriptional activator binding, and *TERT* expression. This work will further our understanding of the mechanisms of activating *TERT* promoter mutations and their role in telomerase regulation in cancer.

Results

Two-step CRISPR/Cas9 editing of the *TERT* promoter

Given the highly GC-rich status of the *TERT* promoter, the low complexity base composition leads to many potential off-target sites when designing single guide RNAs (sgRNAs) to target *TERT* (19, 119). Previous attempts to target *TERT* with one sgRNA have resulted in great cell toxicity and inefficient editing (19, 119). Therefore, Xi *et al.* devised a two-step CRISPR/Cas9 editing method to modify the *TERT* promoter near the *TERT* mutation, which we adapted to edit our thyroid cancer cell line. Briefly, as shown in Figure 18, the first step involves a single sgRNA targeted to the *TERT* promoter, where Cas9 cuts at -147/148, relative to the translational start site. The homology directed repair (HDR) template also transfected into the cell contains a GFP expression cassette, which is inserted at *TERT* between -139/140 to disrupt the sgRNA recognition site (Figure 18B). In the second editing step, two sgRNAs are used to target and excise the inserted GFP cassette, and an HDR template is provided to repair to the endogenous *TERT* sequence, except that the repair templates contain wildtype or mutant (-124) *TERT* promoter (Figure 18A,B).

Editing of TPC-1 cell line

We utilized this system in the *TERT* heterozygous mutant PTC cell line, TPC-1, to create cell lines with isogenic backgrounds but differing *TERT* mutation states. This cell line was selected from our repertoire of cell lines as it was diploid at the chromosome 5p15 locus where *TERT* is located, which we determined by fluorescence in situ hybridization (FISH) (Supplemental Figure 10). In addition to the HDR template containing wild type or mutant *TERT* sequences, we introduced a SNP in exon 1 in order to track allele-specific transcription and methylation of the edited allele. We identified a SNP occurring at low frequency in the Trans-Omics for Precision Medicine (TOPMED) whole genome sequencing project, SNP rs750133706. We performed site directed mutagenesis of the HDR templates to include the SNP, which does not occur in the TPC-1 cell line, in the introduced template (Supplemental Figure 11).

After screening over 200 single cell-derived clones, we obtained two of the necessary three cell lines with the edited *TERT* promoter and new SNP in exon 1 (Figure 19). We have ongoing work to finish the CRISPR/Cas9 editing to complete our repertoire of isogenic background cell lines with the following mutation states: The parental TPC-1 heterozygous mutant cell line, a homozygous mutant cell line, and a wildtype *TERT* cell line. The necessary control cell lines are also being constructed, such that we can control for the impact of editing the cells on *TERT* regulation (editing the *TERT* promoter and adding a synonymous SNP without changing the mutation status from the parental cell line).

Characterizing *TERT* regulation in edited cell lines

With these engineered cell lines, we will be able to further characterize *TERT* promoter regulation (Figure 20) as a direct consequence of genetic changes we have introduced. Briefly, we will conduct nCATS methylation analysis of the *TERT* promoter in our edited cell lines, and utilizing the *TERT* mutation and exon 1 SNP, be able to determine allele-specific methylation of the *TERT* promoter. This will allow us to determine if altering the *TERT* mutation state affects the *TERT* methylation pattern. We will next conduct ChIP-qPCR, as previously done, to characterize transcriptional activators GABPA and MYC binding at the *TERT* promoter in the edited cell lines. Additionally, ChIP-qPCR for the chromatin marks H3K4me3 and H3K27me3 will be conducted to determine the chromatin state of the edited alleles. Lastly, we will characterize *TERT* expression in the edited cell lines, and again utilizing the exon 1 SNP as allele-specific marker, we will determine the allele-specific expression patterns of the cells.

Discussion

While previous studies have characterized *TERT* promoter regulation in different cancer subtypes with the *TERT* mutation, no study has definitively established a causative relationship between the *TERT* promoter mutation and changes in *TERT* promoter methylation, transcriptional activator binding, histone marks, and expression. The end of my thesis work has been devoted to developing CRISPR/Cas9 edited cell lines as a tool to answer this question regarding *TERT* regulation. Previous correlative studies were conducted in differing cell lines with different mutational backgrounds. Here, we use one cell line, TPC-1, to establish multiple isogenic cell lines that have the same mutational

background except for the *TERT* promoter, providing an excellent system to study the acute effects of the *TERT* promoter mutation on *TERT* regulation. Further, by introducing a synonymous SNP into the first exon, the cell lines will have more utility for the study of allelic expression, and in cell lines homozygous at the *TERT* promoter, the SNP provides a way to track the edited allele to still provide allele-specific context.

We would expect, if the correlation from previous studies holds true, that a wildtype *TERT* allele edited to be a mutant allele would result in a decrease in promoter methylation, increased MYC and GABPA binding, increased H3K4me3 at the *TERT* promoter, and increased expression of the allele. Alternatively, a mutant *TERT* allele edited to remove the mutation would be expected to result in increased promoter methylation, decreased factor binding, increased H3K27me3, and decreased expression. However, one competing scenario would be the artificially introduced mutation would not have immediate epigenetic and/or transcriptional consequences, which would require exploring alternative hypotheses. All of the experiments detailed in Figure 20 have been previously conducted and are described in established protocols which can be completed with minimal optimization by members of the Umbricht lab after completion of my time in lab. Therefore, with the tools created, we will be able to finally answer the question concerning *TERT* promoter mutations causative role in effecting *TERT* promoter regulation and activation.

Figure 18: CRISPR-Cas9 editing of the *TERT* promoter

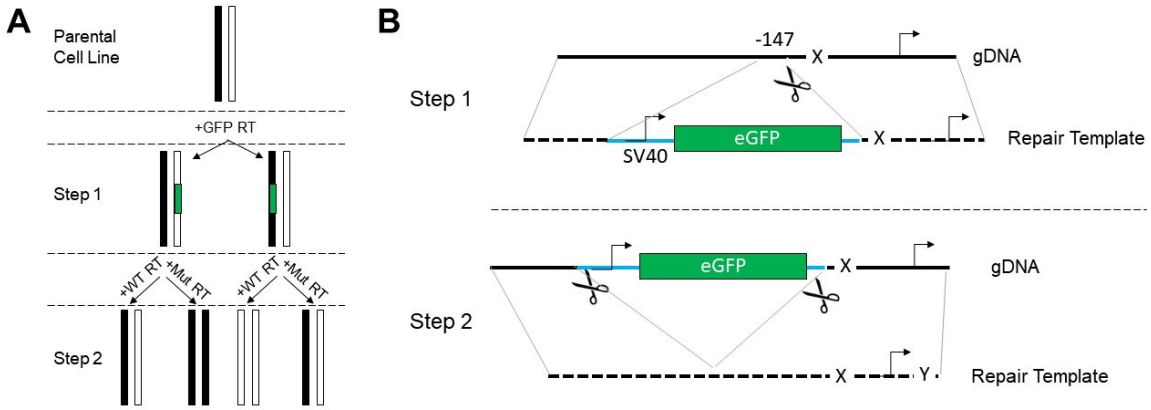

A) Diagram of editing the *TERT* mutation status in a parental, heterozygous mutant cell line. The wildtype (WT) allele is white, the mutant (Mut) is black. In Step 1, the eGFP cassette (green) may insert into either allele. In Step 2, dependent on the repair template (RT) containing the WT or Mut allele, different *TERT* promoter mutation states result. **B)** Schematic of the protocol to edit the *TERT* promoter. In Step 1, a double-stranded break is generated at -147/148 by Cas9 (scissors). A repair template is transfected into cells containing the SV-40 driven eGFP expression cassette surrounded by homology arms to the *TERT* promoter. After selection of cells that contain the modified promoter, in Step 2 the eGFP cassette is removed by two introduced double stranded breaks surrounding the cassette. Different repair templates are provided that include the endogenous *TERT* promoter sequence with WT or Mut *TERT* (depicted by an X) as well as the rs750133706 SNP in exon 1 (depicted by a Y).

Figure 19: Sanger sequencing of the *TERT* promoter in edited cells

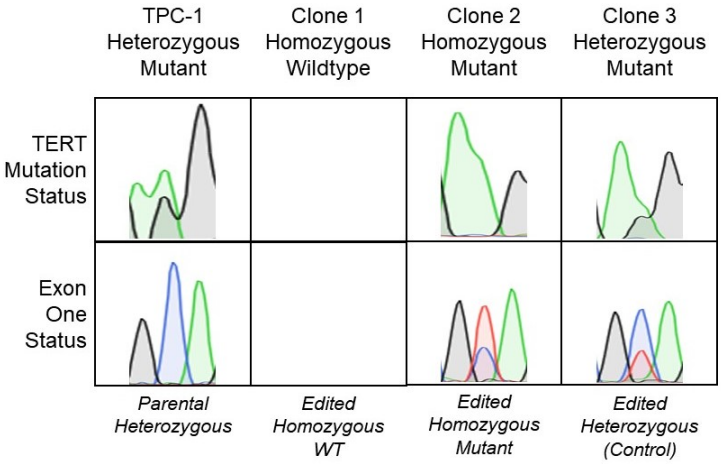

Sanger sequencing analysis of the *TERT* promoter at the -124C>T mutation and the exon 1 region surrounding SNP rs750133706 in amplified genomic DNA from the parental TPC-1 cell line, and the CRISPR/Cas9 edited cell lines. The columns depict each cell line and the cell line's *TERT* mutation status. The base pair of interest is shown in by the middle curve position for both the *TERT* mutation and exon 1 SNP.

Figure 20: Flow chart for characterization of edited cell lines

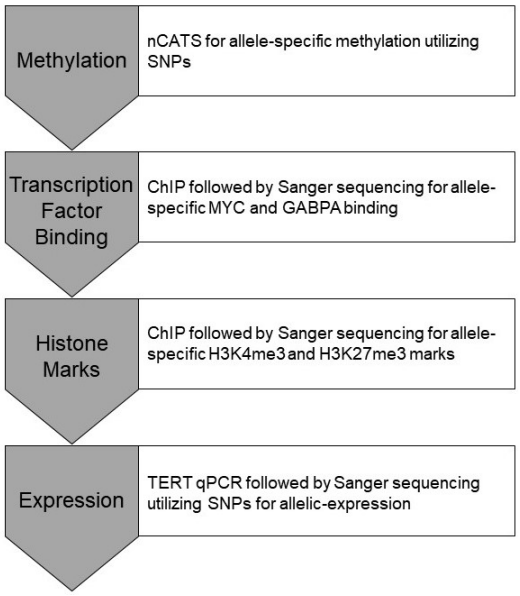

Schematic of characterization elements in gray to be completed with the edited *TERT* promoter cell lines, including methylation, transcription factor binding, histone marks, and expression. White boxes highlight the experimental techniques utilized to achieve the characterization.

Figure S10: Chromosome 5 FISH of thyroid cancer cell lines

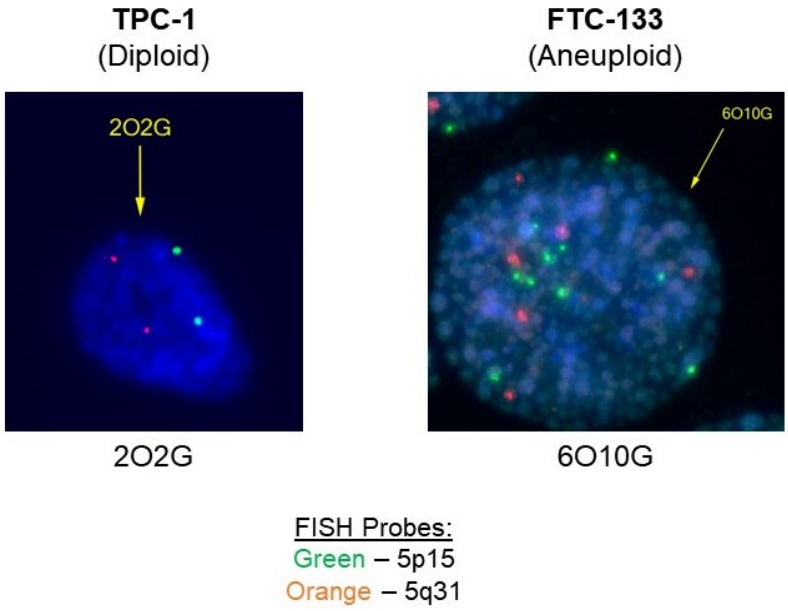

Fluorescence in situ hybridization (FISH) of two representative thyroid cancer cell lines, TPC-1 and FTC-133. FISH analysis was performed with a dual color probe for chromosome 5 that detects a locus on the short arm, 5p15.2 (green signal), and the EGR1 gene on the long arm, 5q31 (orange signal). Counts per cell are shown as the signal number for the orange probe (O) followed by the signal number for the green probe (G), where 2O2G is diploid. FISH analysis was done exclusively on interphase nuclei.

Figure S11: Sanger sequencing of *TERT* exon 1 SNP

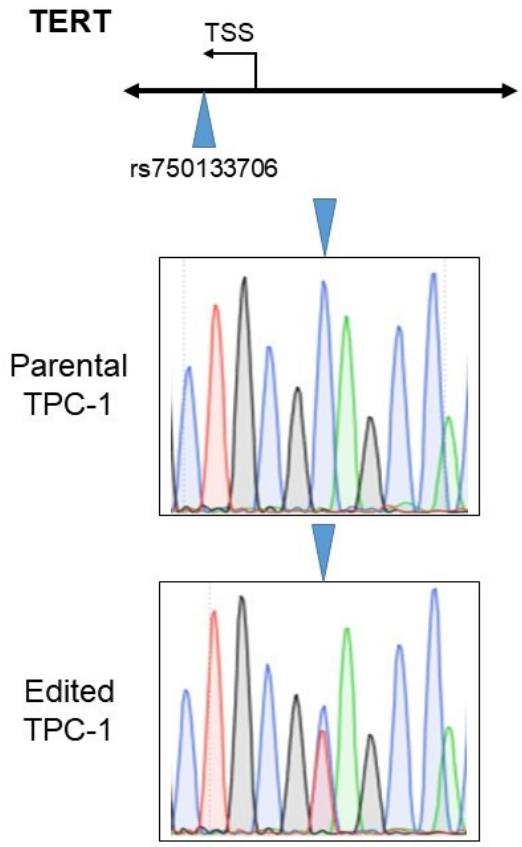

Sanger sequencing analysis of the exon 1 region of *TERT* surrounding SNP rs750133706 in amplified genomic DNA from the cell line TPC-1 and CRISPR-Cas9 edited TPC-1. While the parental DNA showed one allele of the SNP, the edited line showed both alleles.

Chapter 5: Conclusions and Future Directions

In Figure 1, the reader was provided with an overview of the previously known mechanisms of *TERT* regulation in cancer cells. Understanding how these mechanisms activate telomerase, as well as the interplay between the regulatory mechanisms, will allow us to further unravel the ways in which cancer cells manipulate normal cellular machinery and regulation during carcinogenesis. The experiments I have conducted during my PhD have contributed to the body of knowledge surrounding *TERT* regulation in cancer cells. While previous studies in other cancer subtypes have established a pattern of *TERT* promoter methylation, transcription factor binding, and chromatin landscape, previous studies have not explored the pattern of *TERT* regulation in thyroid cancer. As thyroid cancer has one of the least perturbed cancer genomes, with few copy number variations and low mutation density (22), it is an ideal system in which to study telomerase activation.

My experiments, the first comprehensive study of *TERT* promoter methylation in thyroid cancer, demonstrated a pattern consistent with other cancer subtypes, in which the minimal promoter surrounding the TSS is hypomethylated, and the upstream promoter is hypermethylated. Moreover, close investigation of bisulfite sequencing data revealed a pattern consistent with allele-specific methylation. When we followed this path utilizing a novel sequencing technology, nCATS, that did not obscure the *TERT* promoter mutations as bisulfite-based approaches had, we were able to confirm allele-specific methylation in thyroid cancer cells heterozygous for the *TERT* mutation, in which the mutant allele was

significantly less methylated surrounding the TSS than the wildtype allele, mirroring the pattern of an actively transcribed gene. Further, transcriptional activators GABPA and MYC were found to bind only to the mutant allele, with active chromatin mark H3K4me3 associated with the mutant allele and the silencing mark H3K27me3 associated with the wildtype allele. Finally, we were able to prove monoallelic expression of the mutant *TERT* allele for the first time. These data suggest the *TERT* promoter mutation may alter the *TERT* promoter landscape in mutant cells, causing a selection to an activated allele state and active telomerase. This work sheds light on the never before characterized *TERT* regulation in thyroid cancer, and is applicable more broadly in understanding *TERT* regulation in cancer.

The work described here also raises a number of questions regarding the cause and effect relationship between the *TERT* promoter mutations and *TERT* regulation. Previous studies, including ours, have shown a correlation between the *TERT* promoter mutations and less promoter DNA methylation, active chromatin marks, increased activator binding, and higher *TERT* transcription (52, 56, 117). One clear goal, as stated in Chapter 4, is to explore the causative effect of the *TERT* promoter mutation on the other *TERT* regulatory mechanisms. This will help to further delineate the path of immortalization for cancer cells, by understanding what role the *TERT* mutation plays in cancer. As over 90% of immortalized thyroid cancer cell lines harbor the *TERT* mutation (11), there seems to be a clear selection for the mutation to confer a proliferative advantage. However, while understanding the role of the *TERT* mutations will progress our understanding of *TERT* regulation, unlike the immortalized cell lines, the majority of cancers do not harbor the

TERT mutation (141), yet approximately 90% (5) display active telomerase. This is indicative of additional mechanisms that activate telomerase, independent of the *TERT* mutation, that are active in the earliest stages of carcinogenesis. Further work is needed to determine how telomerase is activated without the *TERT* mutation, which could be driven by changes in *TERT* promoter methylation or factor binding.

To better understand dysregulation in cancer, it is imperative to understand regulation in normal somatic cells. Indeed, there is a dearth of information surrounding *TERT* regulation in normal tissue, partly due to problems surrounding its study in non-transformed cells. Most of the work in *TERT* regulation has been conducted in immortalized cell lines, in which the process of immortalization of cell lines may involve activation of *TERT*, thereby confounding its interpretation. Studies in untransformed cells are more challenging, as these cells do not grow in cell culture for a sufficient period of time to be able to complete experiments. However, understanding *TERT* regulation in these normal cells is crucial. Normal tissue that does not express telomerase appears to be hypomethylated throughout the *TERT* promoter, including at the minimal promoter which is also hypomethylated in cancer. This raises the question of the role of the hypomethylated region in cancer, and whether it is necessary but not sufficient to activate *TERT*, as well as how *TERT* is inactivated in normal tissue. These questions should be explored through additional studies involving normal tissue as well as short term cell culture experiments with primary cells.

Lastly, as briefly described above, the role of the *TERT* dual methylation pattern in cancer cells remains to be completely understood, specifically as to what promoter methylation pattern is both necessary and sufficient for *TERT* transcriptional activation. We have found the upstream *TERT* promoter to be hypermethylated in thyroid cancer cell lines, following the same pattern as other cancer types, compared to normal tissue. Further, the methylation of one CpG, cg11625005, in the upstream promoter in glioblastoma is utilized as a prognostic biomarker, where hypermethylation correlates with poor prognosis (10). The role of the hypermethylation in cancer, however, is still poorly understood. Our identification of foci of hypomethylation within the hypermethylated upstream promoter, and further work identifying putative binding sites for activators MYC and GSC at these foci (107), hints at another level of regulation which may be occurring. Recently, an in-depth *TERT* methylation analysis of 833 cancer cell lines also identified foci of lower methylation in the upstream hypermethylated region (142), and warrant further investigation of their role in *TERT* regulation. Experiments such as targeted DNA demethylation by CRISPR/dCas9-mediated epigenome editing at the hypermethylated upstream *TERT* promoter may help elucidate the role of this region on *TERT* regulation.

Overall, understanding *TERT* regulation in thyroid cancer will lead to a better comprehension of the overall mechanism of telomerase activation and immortalization of cancer cells. We recognize that *TERT* regulation is not simple, but rather multifaceted, comprising activating point mutations, DNA methylation changes, altered transcription factor binding, chromatin accessibility alterations, and alternative splicing. These

complex regulatory strategies highlight the importance for somatic cells to keep *TERT* transcriptionally silenced, with multiple regulatory elements to sustain the silencing. While our work has provided a clearer picture of *TERT* regulation in thyroid cancer cells, there is still much work to be done, including establishing a causative role of the *TERT* promoter mutations on regulation, a clearer understanding of *TERT* regulation in normal stem cells and somatic cells, and further exploration into the regulatory role of the dual methylation pattern in cancer. This work will further elucidate the role of *TERT* in oncogenesis.

Materials and Methods

Cell Lines and Culture Conditions: Five differentiated thyroid cancer cell lines (PTC lines TPC-1(120) and BCPAP (121) or FTC lines FTC-133, FTC-238, and WRO) were kindly provided by Dr. Motoyasu Saji (The Ohio State University Wexner Medical Center, Columbus, OH). The SV40-transformed normal thyroid follicular epithelial cell line Nthy-ori-3 (122) was kindly provided by Dr. Thomas Fahey (Weill Cornell Medical Center, New York, NY). All cell lines were authenticated using short tandem repeat profiling. The cell lines BCPAP and Nthy-ori-3 were grown in Roswell Park Memorial Institute-1640 (RPMI-1640; Sigma-Aldrich, St. Louis, MO) medium with 10% heat-inactivated fetal bovine serum (FBS) (GE Healthcare Life Sciences, Marlborough, MA), while TPC1, FTC133, FTC 236, FTC238, and WRO were grown in HyClone Dulbecco's Modified Eagle Medium (DMEM) (GE Healthcare Life Sciences) with 10% FBS. All cultures were supplemented with 1x antibiotic antimycotic solution (Sigma-Aldrich), 2 mM L-glutamine (Life Technologies, Carlsbad, CA), and 1x MEM-Non-Essential Amino Acids (Quality Biological, Gaithersburg, MD) and grown exponentially at 37°C and 5% CO_2.

Patient Samples: Six frozen benign thyroid tissue samples were selected from our thyroid tissue bank, which has been approved by Institutional Review Board at Johns Hopkins Medical Institutions. Samples were immediately placed on ice, prosected and reviewed in the Department of Pathology, snap frozen in liquid nitrogen, and stored at -80˚C until use. Five μm Cryostat H&E sections were obtained to locate tumor-adjacent normal thyroid tissue.

DNA Isolation: Genomic DNA from cell lines and patient tissue was isolated utilizing by Proteinase K digestion, phenol/chloroform extraction, and ethanol precipitation, as described previously (123). DNA was diluted in 1x Low-EDTA TE pH8 (Quality Biological).

Sanger Sequencing: Sanger sequencing was performed to confirm the mutation status of the cell lines for *TERT* and *BRAF*. The target regions surrounding the *TERT* promoter mutation (-124 C>T) and the *BRAF*V600E mutation were amplified by PCR using primers listed in Supplemental Table 3, followed by Sanger sequencing using the sequencing primers (11, 92).

Bisulfite Modification and PCR of *TERT* Promoter: Isolated DNA (100 ng) was used for bisulfite treatment using the EZ DNA Methylation-Lightning Kit, according to manufacturer's guidelines (Zymo Research, Irvine, CA), and eluted in 11 µl H_2O. Bisulfite modified DNA was amplified with three separate tiled primer sets listed in Supplemental Table 3, amplifying the region -662 to +174 relative to the *TERT* TSS. The 50 µl PCR amplification reaction contained 5 µl of bisulfite treated DNA (approximately half of the 100 ng bisulfite-treated input DNA), 300 nM of forward and reverse tile primers, and 25 µl KAPA HiFi HotStart Uracil+ ReadyMix (2X) (KAPA Biosystems, Wilmington, MA) using the ProFlex PCR System (Applied Biosystems, Foster City, CA) [2 minutes 95°C, 35 cycles x (20 seconds 98°C, 20 seconds (T1 58°C/T2 54°C/T3 54°C, 40 seconds 72°C), 2 minutes 72°C].

Bisulfite Library Preparation and Sequencing: PCR products from the bisulfite treated *TERT* tiles were purified with Agencourt AMPure XP beads, using 1.8x beads (Beckman Coulter Life Sciences, Indianapolis, IN) and quantified using the Qubit dsDNA HS Assay Kit (ThermoFisher Scientific, Waltham, MA). The NEBNext Ultra DNA Library Prep Kit for Illumina (New England Biolabs, Ipswich, MA) protocol was followed for library preparation with no size-selection, with DNA input of 20, 40, 200 ng of pooled 3 promoter tiles, T1, T2, T3 respectively. Differences in input was due to differences in the tiles' on-target amplicon amounts, with the tile displaying the least on-target amplicon being the tile with the highest input. Library concentration and size distribution was quantified with the High Sensitivity DNA kit on the 2100 Bioanalyzer (Agilent, Santa Clara, CA) and KAPA Library Quantification Kit for Illumina Platforms (KAPA). A 12 pM sample library for promoter bisulfite sequencing with 30% PhiX control was paired-end sequenced on the MiSeq v3 600 PE system (Illumina, San Diego, CA) for a targeted minimum of 10,000 reads per amplicon.

Data Processing for Bisulfite Sequencing: *TERT* promoter methylation status was analyzed with the Bismark (124) software package. Bisulfite conversion and mapping to the Human Genome Reference Consortium build 37 (GRCh37) was performed on trimmed reads (Trim Galore) with a quality Phred score cutoff of 30 (125). Sequencing coverage for each CpG was analyzed with bsseq (126). A CpG site was included in analysis if the sequencing coverage was over 60 and present in more than two cell lines. Epiallele analysis at the MYC binding site and chr5:1,295,587-1,295,800 was conducted

through MethPat (91), using the settings --amplicons, --filterpartial, --min_cpg_percent 1. Analysis of differentially methylated regions was conducted through software package bsseq (126), with the settings ns=5, h=15. Differentially methylated regions were determined with a quantile-based cutoff, c(0.1,0.9). The Integrative Genomics Viewer (IGV) (127) was utilized to visualize differentially methylated regions.

Chromatin Immunoprecipitation (ChIP) Analysis: DTC cells were grown to 85% confluency in 15 cm plates. ChIP was performed as described previously for cell lines (128). For ChIP analysis in normal thyroid tissue, the Novus Biologicals protocol (129) was followed. Cells were fixed for 8 minutes in 1% formaldehyde. Chromatin was sheared by sonication for 2x [4x 20s on/20s off] by the Bioruptor Pico (Diagenode, Denville, NJ). The following antibodies were used (10 μg per ChIP): anti-CTCF (#2899, Cell Signaling Technology, Danvers, CA), anti-MYC (#9402, Cell Signaling Technology), anti-GABPA (#27795, ThermoFisher), anti-GSC (#40495, ThermoFisher), anti-H3K4me3 (#9727, Cell Signaling Technology), anti-H3K27me3 (#9733, Cell Signaling Technology), and anti-ETV5 (#30023, ThermoFisher). DNA was purified by MinElute PCR Purification Kit (Qiagen, Hilden, Germany). ChIP and input DNA were analyzed by qPCR with Sybr Green and melt curve analysis, with the primer sets listed in Supplemental Table 4. Three replicate PCR reactions were carried out for each sample with two biological replicates, with positive and negative control regions for each antibody. Factor binding was determined by the percent of input normalization method (133), normalizing the binding at the *TERT* locus, encompassing the TERT promoter mutation and TSS, relative to DNA input into ChIP. After ChIP, immunoprecipitated

DNA and input DNA was amplified by PCR surrounding the *TERT* -124 C>T mutation and Sanger sequenced (107).

qRT-PCR for *TERT* Expression: RNA from the DTC cell lines was extracted by Trizol isolation, as described previously (131). RNA from normal thyroid tissue was extracted using the Highpure FFPE RNA kit (Roche, Basel, Switzerland) following the manufacturer's protocol. RNA was reverse transcribed to cDNA using SuperScript III Reverse Transcriptase (ThermoFisher) according to manufacturer instructions. Quantitative PCR was performed as previously described with SYBR Green PCR Master Mix (ThermoFisher), with primers designed to detect the full-length *TERT* transcript levels (70). The expression level of *TERT* was normalized to *GAPDH*.

Nanopore Cas9 Targeted-Sequencing (nCATS) of *TERT*: nCATS was conducted as previously described (111). Briefly, forward and reverse CRISPR RNAs (crRNAs) were designed to target 7.806 kb surrounding the *TERT* region at chr5:1,288,699-1,296,505: F 'AAGGCTTAGGGATCACTAAG', and R 'AGCGGCAGGTGCCCAGAATA'. crRNAs were mixed in equimolar amounts to a final concentration of 100 μM. After duplex formation, dephosphorylation of the genomic DNA, cleavage and dA tailing, adaptor ligation, and clean-up (111), each sample was sequenced on a nanopore flow cell (version 9.4.1) using the GridION sequencer (Oxford Nanopore Technologies, Oxford, UK).

Data Processing for nCATS Methylation: Analysis of the nanopore data was conducted as previously described (111). Base calling to generate FASTQ reads was

performed by the GUPPY algorithm. The resulting reads were aligned to the human genome, hg19, by Minimap2 (132). CpG methylation calling was conducted using nanopolish (133). Reads were phased into wildtype or mutant allele by identifying the promoter motif in fastq reads.

Real-time Quantitative Telomeric Repeat Amplification Protocol (q-TRAP): Cells were lysed in CHAPS lysis buffer (Cell Signaling Technology), and incubated on ice for 20 minutes. Cell debris was removed by centrifugation, and total protein concentration measured. Heat inactivation, no template, and telomerase quantitation controls were performed using serial dilutions of HEK293T cells (ATCC ACS-4500). The 25 µl reaction contained 1x Sybr Green (ThermoFisher), 0.1 µg of TS and ASX primers, and 250 ng of protein extract. Quantitative PCR was performed as previously described (134).

Allele-Specific Transcription Characterization: SNPs in the thyroid cancer cell lines were identified by Sanger sequencing of genomic DNA in the *TERT* 3' untranslated region (UTR), and by IGV examination of the nCATS data in the *TERT* 5' UTR and exons 1 and 2. Isolated RNA from the cell lines was DNase I treated and reverse transcribed as above, then amplified at the SNP location (Supplemental Table 5) and Sanger sequenced utilizing the forward primer to determine genotype.

Plasmid Construction and Transfection: The pX330 plasmid vector containing Cas9 and the sgRNAs (sgRNA sequences in Supplemental Table 6), as described in (135), were kindly provided by Dr. Thomas R. Cech (The University of Colorado Boulder,

Boulder, CO). The repair template with the eGFP expression cassette or the endogenous *TERT* sequence from -589 to +353 in the pUC57-Kan plasmid were also kindly provided by Dr. Thomas R. Cech. Site-directed mutagenesis was performed on the repair template plasmid containing the *TERT* sequence to add the *TERT* promoter mutation (-124C>T) as well as two exon 1 SNPs (rs750133706 and rs1459602769) in different combinations. Briefly, point mutations were introduced by PCR, using the Q5 Site-Directed Mutagenesis Kit (New England Biolabs), according to the manufacturer's protocol. PCRs were run for 25 cycles of 2 min 15 s at 72°C. The resulting mutant plasmids were verified by Sanger sequencing. One million cells were transfected with 1.0 ug pX330 Cas9-gRNA plasmid and 1.0 ug pUC67-Kan repair template plasmid using Lipofectamine 2000 Reagent (ThermoFisher, Waltham, MA) according to the manufacturer's instructions.

Fluorescence Activated Cell Sorting (FACS): Cells were trypsinized and re-suspended to a single cell suspension with cell strainer caps (BD Biosciences, San Jose, CA) in sorting buffer (1x PBS, 1% heat-inactivated FBS, Penicillin-Streptomycin, 2 mM EDTA). Cells were sorted by GFP signal with a 100 uM nozzle on the FACSAria IIu Cell Sorter (BD Biosciences). Cells were collected and single cell seeded into 96 well plates.

Post-CRISPR Editing DNA Extraction and Analysis: DNA was extracted from each well by Extract-N-Amp Blood PCR Kit (Millipore Sigma, Burlington, MA) according to the manufacturer's instructions. Extracted DNA was then PCR amplified surrounding the *TERT* edited locus (primers in Supplemental Table 7) and Sanger sequenced to confirm the correct editing of the *TERT* promoter.

Table S3: Primers for bisulfite and Sanger sequencing analysis

Primer Name	Product Size (bp)	Sequences
***TERT* -124 C>T Sanger amplicon**	162	F 5' GTCCTGCCCCTTCACCTTC 3' R 5' AGCGCTGCCTGAAACTCG 3'
***TERT* -124 C>T Sanger sequencing**	N/A	5' TTCACCTTCCAGCTCCGC 3'
***BRAFV600E* Sanger amplicon**	180	F 5' AACTCTTCATAATGCTTGCTCTGA 3' R 5' CAGACAACTGTTCAAACTGATGGGACC 3'
***BRAFV600E* Sanger sequencing**	N/A	5' AATAGGTGATTTTGGTCTAGCTACAG 3'
BS[a] tile 1 (-662 to -395)[b]	267	F 5' GGGTTTGTGTTAAGGAGTTTAAGT 3' R 5' CATAATATAAAAACCCTAAAAACAAAT 3'
BS tile 2 (-420 to -126)	296	F 5' TTGTTTTTAGGGTTTTTATATTATGGT 3' R 5' AAACTAAAAAATAAAAAAACAAAAC 3'
BS tile 3 (-159 to +174)	333	F 5' GGTATTYGTTTTGTTTTTTTATTTTT 3' R 5' CACCAACCRCCAACCCTAAA 3'

[a]BS- bisulfite sequencing, [b]All *TERT* promoter primer locations are in reference to the TSS.

Table S4: Primers for ChIP-qPCR analysis

Primer Name	Product Size (bp)	Sequences (5'-> 3')
CTCF		
***HBB* (+)**	51	F CACAAGGTGGCAGCATGAAG R GGGATCGAAGCTGTGTCAGG
***H19 4/5* (-)**	164	F CTGACTCAGGAATCGGCTCT R GCTGTTCCGATGGTGTCTTT
TERT	171	F CTGCTGCGCACGTGGGAAGCC R GTCCCCGCGCTGCACCAGCC
MYC		
***APEX1* (+)**	121	F GGCGGGACCTGGTGCGGGGA R ACCGCGTCACCCACCGAAGCA
***ALB* (-)**	194	F CATTGACAAGGTCTTGTGGAGA R CAAACGGAGGGAAATTAGCA
***TERT* 1**	107	F GGGCTCCCAGTGGATTC R CGGAGCTGGAAGGTGAAG
***TERT* 2**	80	F TTCACGTCCGGCATTCG R CCTGATCCGGAGACCCA
GABPA		
***RACGAP1* (+)**	158	F CAAAGGTGGCCATTTTGACT R TAGTCCCGCAGACAGTGAGA
***ALB* (-)**	194	above
TERT	163	F CACCCGTCCTGCCCCTTCA R CTGCCTGAAACTCGCGCC
GSC		
***GSC2* (+)**	95	F CGCCGCAGTCGAGGATTAG R GAGGGAGCGCGCAGTAAT
***ALB* (-)**	194	above
TERT	124	F CCTGGGTCTCCGGATCA R AGCGGAGAGAGGTCGAAT
H3K4me3		
***Actin*(+)**	83	F CGGCCAACGCCAAAACT R CCCTCTCCCCTCCTTTTGC
***MYT1* (-)**	135	F ACAAAGGCAGATACCCAACG R GCAGTTTCAAAAAGCCATCC
TERT	163	F CACCCGTCCTGCCCCTTCA R CTGCCTGAAACTCGCGCC
H3K27me3		

***MYT1* (+)**	135	above
***Actin* (-)**	83	above
TERT	163	above

Citation denotes primers from previously published articles. (+) denotes the positive control gene locus, and (-) denotes the negative control gene locus

Table S5: Primers for Allele-Specific Expression Analysis

Primer Name	Product Size (bp)	Sequences (5'-> 3')
TERT Exon 2	214	F CGTGGTTTCTGTGTGGTGTC R CCTTGTCGCCTGAGGAGTAG
TERT 3'UTR	362	F CACTGCCCTCAGACTTCAA R GGGATGGACTATTCCTATGTGG

Sanger sequencing was conducted utilizing the forward primer for each amplicon.

Table S6: sgRNAs for CRISPR/Cas9 Editing

Cutting Position[a]	sqRNA Sequence (5'-> 3')
-147/-148	GCGCCCCGTCCCGACCCCTCC
Upstream boundary of eGFP	GATTCCACAGGGTCGACCACC
Downstream Boundary of eGFP	GTCTTCGGACCTCGCGGCCC

[a] Denotes position relative to the *TERT* translational start site. sgRNAs from Xi, *et al.* (121)

Table S7: Primers for CRISPR/Cas9 Editing Confirmation

Primer Name	Sequences (5'-> 3')
Step 1 L arm (121)	F CGTCCAGGGAGCAATGCGT R ACTTTCCACACCTGGTTGCTGAC
Step 1 R arm (121)	F CGGCATGGACGAGCTGTACAAGT R ACGCTGGTGGTGAAGGCCTC
Step 2 Exon 1 SNP	F CGCGGCGCGAGTTTCAGGCA R GTGGCCAGCGGCAGCACCTC
Step 2 Final *TERT*	F CACCCGTCCTGCCCCTTCA R CTGCCTGAAACTCGCGCC

Sanger sequencing was conducted utilizing the forward primer for each amplicon.

References

1. Hayflick L 1965 The limited in vitro lifetime of human diploid cell strains. Exp Cell Res **37**:614–636.
2. de Lange T 2009 How telomeres solve the end-protection problem. Science **326**:948–52.
3. Donati B, Ciarrocchi A 2019 Telomerase and Telomeres Biology in Thyroid Cancer. Int J Mol Sci **20**.
4. Greider CW, Blackburn EH 1987 The telomere terminal transferase of tetrahymena is a ribonucleoprotein enzyme with two kinds of primer specificity. Cell **51**:887–898.
5. Koziel JE, Fox MJ, Steding CE, Sprouse AA, Herbert B-S 2011 Medical genetics and epigenetics of telomerase. J Cell Mol Med **15**:457–67.
6. Haugen BR, Nawaz S, Markham N, Hashizumi T, Shroyer AL, Werness B, Shoyer KR 1997 Telomerase Activity in Benign and Malignant Thyroid Tumors. Thyroid **7**:337–342.
7. Yuan X, Larsson C, Xu D 2019 Mechanisms underlying the activation of TERT transcription and telomerase activity in human cancer: old actors and new players. Oncogene **38**:6172–6183.
8. Yoo S-K, Song YS, Lee EK, Hwang J, Kim HH, Jung G, Kim YA, Kim S-J, Cho SW, Won J-K, Chung E-J, Shin J-Y, Lee KE, Kim J-I, Park YJ, Seo J-S 2019 Integrative analysis of genomic and transcriptomic characteristics associated with progression of aggressive thyroid cancer. Nat Commun **10**:2764.
9. Wong MS, Chen L, Foster C, Kainthla R, Shay JW, Wright WE 2013 Regulation of telomerase alternative splicing: a target for chemotherapy. Cell Rep **3**:1028–35.
10. Castelo-Branco P, Choufani S, Mack S, Gallagher D, Zhang C, Lipman T, Zhukova N, Walker EJ, Martin D, Merino D, Wasserman JD, Elizabeth C, Alon N, Zhang L, Hovestadt V, Kool M, Jones DTW, Zadeh G, Croul S, Hawkins C, Hitzler J, Wang JCY, Baruchel S, Dirks PB, Malkin D, Pfister S, Taylor MD, Weksberg R, Tabori U 2013 Methylation of the TERT promoter and risk stratification of childhood brain tumours: an integrative genomic and molecular study. Lancet Oncol **14**:534–42.
11. Liu X, Bishop J, Shan Y, Pai S, Liu D, Murugan AK, Sun H, El-Naggar AK, Xing M 2013 Highly prevalent TERT promoter mutations in aggressive thyroid cancers. Endocr Relat Cancer **20**:603–10.
12. Kyo S, Takakura M, Fujiwara T, Inoue M 2008 Understanding and exploiting hTERT promoter regulation for diagnosis and treatment of human cancers. Cancer Sci **99**:1528–38.
13. Avin B, Umbricht C, Zeiger M 2016 Human telomerase reverse transcriptase regulation by DNA methylation, transcription factor binding and alternative splicing (Review). Int J Oncol **49**: 2199-2205.
14. Cipriani NA 2019 Prognostic Parameters in Differentiated Thyroid Carcinomas. Surg Pathol Clin **12**:883–900.
15. Li J-J, Zheng PCJ-R, Wang Y-Z 2017 The correlations between DNA methylation and polymorphisms in the promoter region of the human telomerase reverse

transcriptase (hTERT) gene with postoperative recurrence in patients with thyroid carcinoma (TC). World J Surg Oncol **15**:114.

16. Wang N, Kjellin H, Sofiadis A, Fotouhi O, Juhlin CC, Bäckdahl M, Zedenius J, Xu D, Lehtiö J, Larsson C 2016 Genetic and epigenetic background and protein expression profiles in relation to telomerase activation in medullary thyroid carcinoma. Oncotarget **7**:21332–46.
17. Huang FW, Hodis E, Xu MJ, Kryukov G V, Chin L, Garraway LA 2013 Highly recurrent TERT promoter mutations in human melanoma. Science **339**:957–9.
18. Horn S, Figl A, Rachakonda PS, Fischer C, Sucker A, Gast A, Kadel S, Moll I, Nagore E, Hemminki K, Schadendorf D, Kumar R 2013 TERT Promoter Mutations in Familial and Sporadic Melanoma. Science (80-) **339**:959–961.
19. Chiba K, Johnson JZ, Vogan JM, Wagner T, Boyle JM, Hockemeyer D, Atkinson S, Saretzki G, Armstrong L, Lako M, Isacson O, Jaenisch R, Mangues R, Batlle E, Lee J, Jaenisch R, Mitalipova M, Mertens F, Netto G, Rasheed B, Riggins G, Rosenquist T, Schiffman M, IeM S, Theodorescu D, Torbenson M, Velculescu V, Wang T, Wentzensen N, Wood L, Zhang M, McLendon R, Bigner D, Kinzler K, Vogelstein B, Papadopoulos N, Yan H, Study AC, Study AOC, (kConFab) KCFC for R into FBC, (GENICA) GEI and BC, (SWE-BRCA) SBCS, (HEBON) HB and OCRGN, (EMBRACE) E study of B& BMC, (GEMO) GM of CR in BMC, Vergote I, Lambrechts S, Despierre E, Risch H, González-Neira A, Rossing M, Pita G, Doherty J, Alvarez N, Larson M, Fridley B, Schoof N, Chang-Claude J, Cicek M, Peto J, Kalli K, Broeks A, Armasu S, Schmidt M, Braaf L, Winterhoff B, Nevanlinna H, Konecny G, Lambrechts D, Rogmann L, Guénel P, Teoman A, Milne R, Garcia J, Cox A, Shridhar V, Burwinkel B, Marme F, Hein R, Sawyer E, Haiman C, Wang-Gohrke S, Andrulis I, Moysich K, Hopper J, Odunsi K, Lindblom A, Giles G, Brenner H, Simard J, Lurie G, Fasching P, Carney M, Radice P, Wilkens L, Swerdlow A, Goodman M, Brauch H, Garcia-Closas M, Hillemanns P, Winqvist R, Dürst M, Devilee P, Runnebaum I, Jakubowska A, Lubinski J, Mannermaa A, Butzow R, Bogdanova N, Dörk T, Pelttari L, Zheng W, Leminen A, Anton-Culver H, Bunker C, Kristensen V, Ness R, Muir K, Edwards R, Meindl A, Heitz F, Matsuo K, Bois A du, Wu A, Harter P, Teo S, Schwaab I, Shu X, Blot W, Hosono S, Kang D, Nakanishi T, Hartman M, Yatabe Y, Hamann U, Karlan B, Sangrajrang S, Kjaer S, Gaborieau V, Jensen A, Eccles D, Høgdall E, Shen C, Brown J, Woo Y, Shah M, Azmi M, Luben R, Omar S, Czene K, Vierkant R, Nordestgaard B, Flyger H, Vachon C, Olson J, Wang X, Levine D, Rudolph A, Weber R, Flesch-Janys D, Iversen E, Nickels S, Schildkraut J, Idos SS, Cramer D, Gibson L, Terry K, Fletcher O, Vitonis A, Schoot C van der, Poole E, Hogervorst F, Tworoger S, Liu J, Bandera E, Li J, Olson S, Humphreys K, Orlow I, Blomqvist C, Rodriguez-Rodriguez L, Aittomäki K, Salvesen H, Muranen T, Wik E, Brouwers B, Krakstad C, Wauters E, Halle M, Wildiers H, Kiemeney L, Mulot C, Aben K, Laurent-Puig P, Altena A, Truong T, Massuger L, Benitez J, Pejovic T, Perez J, Hoatlin M, Zamora M, Cook L, Balasubramanian S, Kelemen L, Schneeweiss A, Le N, Sohn C, Brooks-Wilson A, Tomlinson I, Kerin M, Miller N, Cybulski C, Henderson B, Menkiszak J, Schumacher F, Wentzensen N, Marchand L Le, Yang H, Mulligan A, Glendon G, Engelholm S, Knight J, Høgdall C, Apicella C, Gore M, Tsimiklis H, Song H, Southey M, Jager A, Ouweland A den,

Brown R, Martens J, Flanagan J, Kriege M, Paul J, Margolin S, Siddiqui N, Severi G, Whittemore A, Baglietto L, McGuire V, Stegmaier C, Sieh W, Müller H, Arndt V, Labrèche F, Gao Y, Goldberg M, Yang G, Dumont M, McLaughlin J, Hartmann A, Ekici A, Beckmann M, Phelan C, Lux M, Permuth-Wey J, Peissel B, Sellers T, Ficarazzi F, Barile M, Ziogas A, Ashworth A, Gentry-Maharaj A, Jones M, Ramus S, Orr N, Menon U, Pearce C, Brüning T, Pike M, Ko Y, Lissowska J, Figueroa J, Kupryjanczyk J, Chanock S, Dansonka-Mieszkowska A, Jukkola-Vuorinen A, Rzepecka I, Pylkäs K, Bidzinski M, Kauppila S, Hollestelle A, Seynaeve C, Tollenaar R, Durda K, Jaworska K, Hartikainen J, Kosma V, Kataja V, Antonenkova N, Long J, Shrubsole M, Deming-Halverson S, Lophatananon A, Siriwanarangsan P, Stewart-Brown S, Ditsch N, Lichtner P, Schmutzler R, Ito H, Iwata H, Tajima K, Tseng C, Stram D, Berg D van den, Yip C, Ikram M, Teh Y, Cai H, Lu W, Signorello L, Cai Q, Noh D, Yoo K, Miao H, Iau P, Teo Y, McKay J, Shapiro C, Ademuyiwa F, Fountzilas G, Hsiung C, Yu J, Hou M, Healey C, Luccarini C, Peock S, Stoppa-Lyonnet D, Peterlongo P, Rebbeck T, Piedmonte M, Singer C, Friedman E, Thomassen M, Offit K, Hansen T, Neuhausen S, Szabo C, Blanco I, Garber J, Narod S, Weitzel J, Montagna M, Olah E, Godwin A, Yannoukakos D, Goldgar D, Caldes T, Imyanitov E, Tihomirova L, Arun B, Campbell I, Mensenkamp A, Asperen C van, Roozendaal K van, Meijers-Heijboer H, Collée J, Oosterwijk J, Hooning M, Rookus M, Luijt R van der, Os T, Evans D, Frost D, Fineberg E, Barwell J, Walker L, Kennedy M, Platte R, Davidson R, Ellis S, Cole T, Paillerets BB, Buecher B, Damiola F, Faivre L, Frenay M, Sinilnikova O, Caron O, Giraud S, Mazoyer S, Bonadona V, Caux-Moncoutier V, Toloczko-Grabarek A, Gronwald J, Byrski T, Spurdle A, Bonanni B, Zaffaroni D, Giannini G, Bernard L, Dolcetti R, Manoukian S, Arnold N, Engel C, Deissler H, Rhiem K, Niederacher D, Plendl H, Sutter C, Wappenschmidt B, Borg A, Melin B, Rantala J, Soller M, Nathanson K, Domchek S, Rodriguez G, Salani R, Kaulich D, Tea M, Paluch S, Laitman Y, Skytte A, Kruse T, Jensen U, Robson M, Gerdes A, Ejlertsen B, Foretova L, Savage S, Lester J, Soucy P, Kuchenbaecker K, Olswold C, Cunningham J, Slager S, Pankratz V, Dicks E, Lakhani S, Couch F, Hall P, Monteiro A, Gayther S, Pharoah P, Reddel R, Goode E, Greene M, Easton D, Berchuck A, Antoniou A, Chenevix-Trench G, Dunning A 2015 Cancer-associated TERT promoter mutations abrogate telomerase silencing. Elife **4**:806–823.

20. Liu R, Xing M 2016 TERT promoter mutations in thyroid cancer. Endocr Relat Cancer **23**:R143–55.

21. Ganly I, Makarov V, Deraje S, Dong Y, Reznik E, Seshan V, Nanjangud G, Eng S, Bose P, Kuo F, Morris LGT, Landa I, Carrillo Albornoz PB, Riaz N, Nikiforov YE, Patel K, Umbricht C, Zeiger M, Kebebew E, Sherman E, Ghossein R, Fagin JA, Chan TA 2018 Integrated Genomic Analysis of Hürthle Cell Cancer Reveals Oncogenic Drivers, Recurrent Mitochondrial Mutations, and Unique Chromosomal Landscapes. Cancer Cell **34**:256–270.e5.

22. Cancer Genome Atlas Research Network N, Akbani R, Aksoy BA, Ally A, Arachchi H, Asa SL, Auman JT, Balasundaram M, Balu S, Baylin SB, Behera M, Bernard B, Beroukhim R, Bishop JA, Black AD, Bodenheimer T, Boice L, Bootwalla MS, Bowen J, Bowlby R, Bristow CA, Brookens R, Brooks D, Bryant R, Buda E, Butterfield YSN, Carling T, Carlsen R, Carter SL, Carty SE, Chan TA,

Chen AY, Cherniack AD, Cheung D, Chin L, Cho J, Chu A, Chuah E, Cibulskis K, Ciriello G, Clarke A, Clayman GL, Cope L, Copland J, Covington K, Danilova L, Davidsen T, Demchok JA, DiCara D, Dhalla N, Dhir R, Dookran SS, Dresdner G, Eldridge J, Eley G, El-Naggar AK, Eng S, Fagin JA, Fennell T, Ferris RL, Fisher S, Frazer S, Frick J, Gabriel SB, Ganly I, Gao J, Garraway LA, Gastier-Foster JM, Getz G, Gehlenborg N, Ghossein R, Gibbs RA, Giordano TJ, Gomez-Hernandez K, Grimsby J, Gross B, Guin R, Hadjipanayis A, Harper HA, Hayes DN, Heiman DI, Herman JG, Hoadley KA, Hofree M, Holt RA, Hoyle AP, Huang FW, Huang M, Hutter CM, Ideker T, Iype L, Jacobsen A, Jefferys SR, Jones CD, Jones SJM, Kasaian K, Kebebew E, Khuri FR, Kim J, Kramer R, Kreisberg R, Kucherlapati R, Kwiatkowski DJ, Ladanyi M, Lai PH, Laird PW, Lander E, Lawrence MS, Lee D, Lee E, Lee S, Lee W, Leraas KM, Lichtenberg TM, Lichtenstein L, Lin P, Ling S, Liu J, Liu W, Liu Y, LiVolsi VA, Lu Y, Ma Y, Mahadeshwar HS, Marra MA, Mayo M, McFadden DG, Meng S, Meyerson M, Mieczkowski PA, Miller M, Mills G, Moore RA, Mose LE, Mungall AJ, Murray BA, Nikiforov YE, Noble MS, Ojesina AI, Owonikoko TK, Ozenberger BA, Pantazi A, Parfenov M, Park PJ, Parker JS, Paull EO, Pedamallu CS, Perou CM, Prins JF, Protopopov A, Ramalingam SS, Ramirez NC, Ramirez R, Raphael BJ, Rathmell WK, Ren X, Reynolds SM, Rheinbay E, Ringel MD, Rivera M, Roach J, Robertson AG, Rosenberg MW, Rosenthall M, Sadeghi S, Saksena G, Sander C, Santoso N, Schein JE, Schultz N, Schumacher SE, Seethala RR, Seidman J, Senbabaoglu Y, Seth S, Sharpe S, Shaw KRM, Shen JP, Shen R, Sherman S, Sheth M, Shi Y, Shmulevich I, Sica GL, Simons J V., Sipahimalani P, Smallridge RC, Sofia HJ, Soloway MG, Song X, Sougnez C, Stewart C, Stojanov P, Stuart JM, Tabak B, Tam A, Tan D, Tang J, Tarnuzzer R, Taylor BS, Thiessen N, Thorne L, Thorsson V, Tuttle RM, Umbricht CB, Berg DJ Van Den, Vandin F, Veluvolu U, Verhaak RGW, Vinco M, Voet D, Walter V, Wang Z, Waring S, Weinberger PM, Weinstein JN, Weisenberger DJ, Wheeler D, Wilkerson MD, Wilson J, Williams M, Winer DA, Wise L, Wu J, Xi L, Xu AW, Yang L, Yang L, Zack TI, Zeiger MA, Zeng D, Zenklusen JC, Zhao N, Zhang H, Zhang J, Zhang J (Julia), Zhang W, Zmuda E, Zou. L 2014 Integrated genomic characterization of papillary thyroid carcinoma. Cell **159**:676–90.

23. Oishi N, Kondo T, Ebina A, Sato Y, Akaishi J, Hino R, Yamamoto N, Mochizuki K, Nakazawa T, Yokomichi H, Ito K, Ishikawa Y, Katoh R 2017 Molecular alterations of coexisting thyroid papillary carcinoma and anaplastic carcinoma: identification of TERT mutation as an independent risk factor for transformation. Mod Pathol **30**:1527–1537.
24. Yang X, Li J, Li X, Liang Z, Gao W, Liang J, Cheng S, Lin Y 2017 *TERT* Promoter Mutation Predicts Radioiodine-Refractory Character in Distant Metastatic Differentiated Thyroid Cancer. J Nucl Med **58**:258–265.
25. Meng Z, Matsuse M, Saenko V, Yamashita S, Ren P, Zheng X, Jia Q, Tan J, Li N, Zheng W, Zhao L, Mitsutake N 2019 *TERT* promoter mutation in primary papillary thyroid carcinoma lesions predicts absent or lower ^{131} i uptake in metastases. IUBMB Life **71**:iub.2056.
26. Bell RJA, Rube HT, Kreig A, Mancini A, Fouse SD, Nagarajan RP, Choi S, Hong C, He D, Pekmezci M, Wiencke JK, Wrensch MR, Chang SM, Walsh KM, Myong

S, Song JS, Costello JF 2015 Cancer. The transcription factor GABP selectively binds and activates the mutant TERT promoter in cancer. Science **348**:1036–9.
27. Liu R, Zhang T, Zhu G, Xing M 2018 Regulation of mutant TERT by BRAF V600E/MAP kinase pathway through FOS/GABP in human cancer. Nat Commun **9**:579.
28. Yuan X, Mu N, Wang N, Stråat K, Sofiadis A, Guo Y, Stenman A, Li K, Cheng G, Zhang L, Kong F, Ekblad L, Wennerberg J, Nilsson I-L, Juhlin CC, Larsson C, Xu D 2019 GABPA inhibits invasion/metastasis in papillary thyroid carcinoma by regulating DICER1 expression. Oncogene **38**:965–979.
29. Bullock M, Lim G, Zhu Y, Åberg H, Kurdyukov S, Clifton-Bligh RJ 2019 The ETS Factor ETV5 Activates the Mutant TERT Promoter in Thyroid Cancer. Thyroid thy.2018.0314.
30. Kebebew E, Weng J, Bauer J, Ranvier G, Clark OH, Duh Q-Y, Shibru D, Bastian B, Griffin A 2007 The prevalence and prognostic value of BRAF mutation in thyroid cancer. Ann Surg **246**:466–70; discussion 470–1.
31. Song YS, Lim JA, Choi H, Won J-K, Moon JH, Cho SW, Lee KE, Park YJ, Yi KH, Park DJ, Seo J-S 2016 Prognostic effects of *TERT* promoter mutations are enhanced by coexistence with *BRAF* or *RAS* mutations and strengthen the risk prediction by the ATA or TNM staging system in differentiated thyroid cancer patients. Cancer **122**:1370–1379.
32. Xing M, Liu R, Liu X, Murugan AK, Zhu G, Zeiger MA, Pai S, Bishop J 2014 *BRAF* V600E and *TERT* Promoter Mutations Cooperatively Identify the Most Aggressive Papillary Thyroid Cancer With Highest Recurrence. J Clin Oncol **32**:2718–2726.
33. Liu R, Bishop J, Zhu G, Zhang T, Ladenson PW, Xing M 2017 Mortality Risk Stratification by Combining *BRAF* V600E and *TERT* Promoter Mutations in Papillary Thyroid Cancer. JAMA Oncol **3**:202.
34. Song YS, Yoo S-K, Kim HH, Jung G, Oh A-R, Cha J-Y, Kim S-J, Cho SW, Lee KE, Seo J-S, Park YJ 2019 Interaction of BRAF-induced ETS factors with mutant TERT promoter in papillary thyroid cancer. Endocr Relat Cancer **26**:629–641.
35. Nebbioso A, Tambaro FP, Dell'Aversana C, Altucci L 2018 Cancer epigenetics: Moving forward. PLoS Genet **14**:e1007362.
36. Adams RL 1995 Eukaryotic DNA methyltransferases--structure and function. Bioessays **17**:139–45.
37. Jair K-W, Bachman KE, Suzuki H, Ting AH, Rhee I, Yen R-WC, Baylin SB, Schuebel KE 2006 De novo CpG island methylation in human cancer cells. Cancer Res **66**:682–92.
38. Wan J, Oliver VF, Wang G, Zhu H, Zack DJ, Merbs SL, Qian J 2015 Characterization of tissue-specific differential DNA methylation suggests distinct modes of positive and negative gene expression regulation. BMC Genomics **16**:49.
39. Deaton AM, Bird A 2011 CpG islands and the regulation of transcription. Genes Dev **25**:1010–22.
40. Baylin SB, Jones PA 2011 A decade of exploring the cancer epigenome - biological and translational implications. Nat Rev Cancer **11**:726–34.
41. Stirzaker C, Millar DS, Paul CL, Warnecke PM, Harrison J, Vincent PC, Frommer M, Clark SJ 1997 Extensive DNA Methylation Spanning the Rb Promoter in

Retinoblastoma Tumors. Cancer Res **57**:2229–2237.
42. Smith IM, Glazer CA, Mithani SK, Ochs MF, Sun W, Bhan S, Vostrov A, Abdullaev Z, Lobanenkov V, Gray A, Liu C, Chang SS, Ostrow KL, Westra WH, Begum S, Dhara M, Califano J 2009 Coordinated activation of candidate proto-oncogenes and cancer testes antigens via promoter demethylation in head and neck cancer and lung cancer. PLoS One **4**:e4961.
43. Jones PA, Baylin SB 2002 The fundamental role of epigenetic events in cancer. Nat Rev Genet **3**:415–28.
44. Tahira AC, Kubrusly MS, Faria MF, Dazzani B, Fonseca RS, Maracaja-Coutinho V, Verjovski-Almeida S, Machado MCC, Reis EM 2011 Long noncoding intronic RNAs are differentially expressed in primary and metastatic pancreatic cancer. Mol Cancer **10**:141.
45. Hangauer MJ, Vaughn IW, McManus MT 2013 Pervasive transcription of the human genome produces thousands of previously unidentified long intergenic noncoding RNAs. PLoS Genet **9**:e1003569.
46. Choi J-H, Park SH, Park J, Park BG, Cha S-J, Kong K-H, Lee K-H, Park AJ 2007 Site-specific methylation of CpG nucleotides in the hTERT promoter region can control the expression of hTERT during malignant progression of colorectal carcinoma. Biochem Biophys Res Commun **361**:615–20.
47. Zinn RL, Pruitt K, Eguchi S, Baylin SB, Herman JG 2007 hTERT is expressed in cancer cell lines despite promoter DNA methylation by preservation of unmethylated DNA and active chromatin around the transcription start site. Cancer Res **67**:194–201.
48. Lopatina NG, Poole JC, Saldanha SN, Hansen NJ, Key JS, Pita MA, Andrews LG, Tollefsbol TO 2003 Control mechanisms in the regulation of telomerase reverse transcriptase expression in differentiating human teratocarcinoma cells. Biochem Biophys Res Commun **306**:650–659.
49. Paulsson JO, Mu N, Shabo I, Wang N, Zedenius J, Larsson C, Juhlin CC 2018 TERT aberrancies: a screening tool for malignancy in follicular thyroid tumours. Endocr Relat Cancer **25**:723–733.
50. Bannister AJ, Kouzarides T 2011 Regulation of chromatin by histone modifications. Cell Res **21**:381–95.
51. Salgado C, Roelse C, Nell R, Gruis N, Doorn R van, Velden P van der 2019 Interplay between TERT promoter mutations and methylation culminates in chromatin accessibility and TERT expression. bioRxiv 859892.
52. Stern JL, Theodorescu D, Vogelstein B, Papadopoulos N, Cech TR 2015 Mutation of the TERT promoter, switch to active chromatin, and monoallelic TERT expression in multiple cancers. Genes Dev **29**:2219–24.
53. Zhao Y, Cheng D, Wang S, Zhu J 2014 Dual roles of c-Myc in the regulation of hTERT gene. Nucleic Acids Res **42**:10385–10398.
54. Panning B 2008 X-chromosome inactivation: the molecular basis of silencing. J Biol **7**:30.
55. Huang FW, Bielski CM, Rinne ML, Hahn WC, Sellers WR, Stegmeier F, Garraway LA, Kryukov G V 2015 TERT promoter mutations and monoallelic activation of TERT in cancer. Oncogenesis **4**:e176.
56. Stern JL, Paucek RD, Huang FW, Ghandi M, Nwumeh R, Costello JC, Cech TR

2017 Allele-Specific DNA Methylation and Its Interplay with Repressive Histone Marks at Promoter-Mutant TERT Genes. Cell Rep **21**:3700–3707.
57. Sebestyen E, Zawisza M, Eyras E 2015 Detection of recurrent alternative splicing switches in tumor samples reveals novel signatures of cancer. Nucleic Acids Res **43**:1345–1356.
58. Ulaner GA, Hu JF, Vu TH, Giudice LC, Hoffman AR 2001 Tissue-specific alternate splicing of human telomerase reverse transcriptase (hTERT) influences telomere lengths during human development. Int J cancer **91**:644–9.
59. Lincz LF, Mudge L-M, Scorgie FE, Sakoff JA, Hamilton CS, Seldon M 2008 Quantification of hTERT Splice Variants in Melanoma by SYBR Green Real-time Polymerase Chain Reaction Indicates a Negative Regulatory Role for the β Deletion Variant. Neoplasia **10**:1131–1137.
60. Mavrogiannou E, Strati A, Stathopoulou A, Tsaroucha EG, Kaklamanis L, Lianidou ES 2007 Real-time RT-PCR quantification of human telomerase reverse transcriptase splice variants in tumor cell lines and non-small cell lung cancer. Clin Chem **53**:53–61.
61. Listerman I, Sun J, Gazzaniga FS, Lukas JL, Blackburn EH 2013 The major reverse transcriptase-incompetent splice variant of the human telomerase protein inhibits telomerase activity but protects from apoptosis. Cancer Res **73**:2817–28.
62. Kolquist KA, Ellisen LW, Counter CM, Meyerson M, Tan LK, Weinberg RA, Haber DA, Gerald WL 1998 Expression of TERT in early premalignant lesions and a subset of cells in normal tissues. Nat Genet **19**:182–6.
63. Meyerson M, Counter CM, Eaton EN, Ellisen LW, Steiner P, Caddle SD, Ziaugra L, Beijersbergen RL, Davidoff MJ, Liu Q, Bacchetti S, Haber DA, Weinberg RA 1997 hEST2, the Putative Human Telomerase Catalytic Subunit Gene, Is Up-Regulated in Tumor Cells and during Immortalization. Cell **90**:785–795.
64. Yi X 2001 Quantitation of telomerase components and hTERT mRNA splicing patterns in immortal human cells. Nucleic Acids Res **29**:4818–4825.
65. Kotoula V, Hytiroglou P, Pyrpasopoulou A, Saxena R, Thung SN, Papadimitriou CS 2002 Expression of human telomerase reverse transcriptase in regenerative and precancerous lesions of cirrhotic livers. Liver Int **22**:57–69.
66. Ohyashiki JH, Hisatomi H, Nagao K, Honda S, Takaku T, Zhang Y, Sashida G, Ohyashiki K 2005 Quantitative relationship between functionally active telomerase and major telomerase components (hTERT and hTR) in acute leukaemia cells. Br J Cancer **92**:1942–7.
67. Barclay JY, Morris AG, Nwokolo CU 2005 hTERT mRNA Partially Regulates Telomerase Activity in Gastric Adenocarcinoma and Adjacent Normal Gastric Mucosa. Dig Dis Sci **50**:1299–1303.
68. Rha SY, Jeung HC, Park KH, Kim JJ, Chung HC 2009 Changes of Telomerase Activity by Alternative Splicing of Full-Length and β Variants of hTERT in Breast Cancer Patients. Oncol Res Featur Preclin Clin Cancer Ther **18**:213–220.
69. Liu Y, Wu B, Zhong H, Tian X, Fang W 2012 Quantification of alternative splicing variants of human telomerase reverse transcriptase and correlations with telomerase activity in lung cancer. PLoS One **7**:e38868.
70. Wang Y, Meeker AK, Kowalski J, Tsai H-L, Somervell H, Heaphy C, Sangenario LE, Prasad N, Westra WH, Zeiger MA, Umbricht CB 2011 Telomere length is

related to alternative splice patterns of telomerase in thyroid tumors. Am J Pathol **179**:1415–24.
71. Wong MS, Wright WE, Shay JW 2014 Alternative splicing regulation of telomerase: a new paradigm? Trends Genet **30**:430–8.
72. Kilian A, Bowtell DDL, Abud HE, Hime GR, Venter DJ, Keese PK, Duncan EL, Reddel RR, Jefferson RA 1997 Isolation of a Candidate Human Telomerase Catalytic Subunit Gene, Which Reveals Complex Splicing Patterns in Different Cell Types. Hum Mol Genet **6**:2011–2019.
73. Liu L, Liu C, Fotouhi O, Fan Y, Wang K, Xia C, Shi B, Zhang G, Wang K, Kong F, Larsson C, Hu S, Xu D 2017 TERT Promoter Hypermethylation in Gastrointestinal Cancer: A Potential Stool Biomarker. Oncologist **22**:1178–1188.
74. Ulaner GA, Hu JF, Vu TH, Giudice LC, Hoffman AR 1998 Telomerase activity in human development is regulated by human telomerase reverse transcriptase (hTERT) transcription and by alternate splicing of hTERT transcripts. Cancer Res **58**:4168–72.
75. Colgin LM, Wilkinson C, Englezou A, Kilian A, Robinson MO, Reddel RR 2000 The hTERTalpha splice variant is a dominant negative inhibitor of telomerase activity. Neoplasia **2**:426–32.
76. Bounacer A, Wicker R, Caillou B, Cailleux AF, Sarasin A, Schlumberger M, Suárez HG 1997 High prevalence of activating ret proto-oncogene rearrangements, in thyroid tumors from patients who had received external radiation. Oncogene **15**:1263–1273.
77. Wang N, Xu D, Sofiadis A, Höög A, Vukojević V, Bäckdahl M, Zedenius J, Larsson C 2014 Telomerase-dependent and independent telomere maintenance and its clinical implications in medullary thyroid carcinoma. J Clin Endocrinol Metab **99**:E1571–9.
78. Wang Y, Kowalski J, Tsai H-L, Marik R, Prasad N, Somervell H, Lo P-K, Sangenario LE, Dyrskjot L, Orntoft TF, Westra WH, Meeker AK, Eshleman JR, Umbricht CB, Zeiger MA 2008 Differentiating alternative splice variant patterns of human telomerase reverse transcriptase in thyroid neoplasms. Thyroid **18**:1055–63.
79. Capezzone M, Cantara S, Marchisotta S, Busonero G, Formichi C, Benigni M, Capuano S, Toti P, Pazaitou-Panayiotou K, Caruso G, Carli AF, Palummo N, Pacini F 2011 Telomere Length in Neoplastic and Nonneoplastic Tissues of Patients With Familial and Sporadic Papillary Thyroid Cancer. J Clin Endocrinol Metab **96**.
80. Kammori M, Takubo K, Nakamura K, Furugouri E, Endo H, Kanauchi H, Mimura Y, Kaminishi M 2000 Telomerase activity and telomere length in benign and malignant human thyroid tissues. Cancer Lett **159**:175–81.
81. Sugishita Y, Kammori M, Yamada O, Yamazaki K, Ito K, Fukumori T, Yoshikawa K-I, Yamada T 2014 Biological differential diagnosis of follicular thyroid tumor and Hürthle cell tumor on the basis of telomere length and hTERT expression. Ann Surg Oncol **21**:2318–25.
82. Liu T, Wang N, Cao J, Sofiadis A, Dinets A, Zedenius J, Larsson C, Xu D 2014 The age- and shorter telomere-dependent TERT promoter mutation in follicular thyroid cell-derived carcinomas. Oncogene **33**:4978–4984.

83. Tanaka A, Matsuse M, Saenko VA, Nakao T, Yamanouchi K, Sakimura C, Yano H, Nishihara E, Hirokawa M, Suzuki K, Miyauchi A, Eguchi S, Yoshiura K, Yamashita S, Nagayasu T, Mitsutake N 2019 TERT mRNA expression as a novel prognostic marker in papillary thyroid carcinomas. Thyroid **29**:1105-1114.
84. Paulsson JO, Olander A, Haglund F, Zedenius J, Juhlin CC 2018 TERT Immunohistochemistry Is a Poor Predictor of TERT Promoter Mutations and Gene Expression in Follicular Thyroid Carcinoma. Endocr Pathol **29**:380.
85. Cacciato Insilla A, Proietti A, Borrelli N, Macerola E, Niccoli C, Vitti P, Miccoli P, Basolo F 2017 TERT promoter mutations and their correlation with BRAF and RAS mutations in a consecutive cohort of 145 thyroid cancer cases. Oncol Lett **15**:2763–2770.
86. Hysek M, Paulsson JO, Jatta K, Shabo I, Stenman A, Höög A, Larsson C, Zedenius J, Juhlin CC 2019 Clinical Routine TERT Promoter Mutational Screening of Follicular Thyroid Tumors of Uncertain Malignant Potential (FT-UMPs): A Useful Predictor of Metastatic Disease. Cancers (Basel) **11**.
87. Patel KN, Yip L, Lubitz CC, Grubbs EG, Miller BS, Shen W, Angelos P, Chen H, Doherty GM, Fahey TJ, Kebebew E, Livolsi VA, Perrier ND, Sipos JA, Sosa JA, Steward D, Tufano RP, McHenry CR, Carty SE 2020 The American Association of Endocrine Surgeons Guidelines for the Definitive Surgical Management of Thyroid Disease in Adults. Ann Surg **271**:e21–e93.
88. Smallridge RC, Ain KB, Asa SL, Bible KC, Brierley JD, Burman KD, Kebebew E, Lee NY, Nikiforov YE, Rosenthal MS, Shah MH, Shaha AR, Tuttle for the American Thyroid Ass RM, American Thyroid Association Anaplastic Thyroid Cancer Guidelines Taskforce 2012 American Thyroid Association Guidelines for Management of Patients with Anaplastic Thyroid Cancer. Thyroid **22**:1104–1139.
89. Lee S, Borah S, Bahrami A 2017 Detection of Aberrant TERT Promoter Methylation by Combined Bisulfite Restriction Enzyme Analysis for Cancer DiagnosisThe Journal of Molecular Diagnostics.
90. Pettigrew KA, Armstrong RN, Colyer HAA, Zhang S-D, Rea IM, Jones RE, Baird DM, Mills KI 2012 Differential TERT promoter methylation and response to 5-aza-2'-deoxycytidine in acute myeloid leukemia cell lines: TERT expression, telomerase activity, telomere length, and cell death. Genes Chromosomes Cancer **51**:768–80.
91. Wong NC, Pope BJ, Candiloro IL, Korbie D, Trau M, Wong SQ, Mikeska T, Zhang X, Pitman M, Eggers S, Doyle SR, Dobrovic A 2016 MethPat: a tool for the analysis and visualisation of complex methylation patterns obtained by massively parallel sequencing. BMC Bioinformatics **17**:98.
92. Saiselet M, Floor S, Tarabichi M, Dom G, Hébrant A, van Staveren WCG, Maenhaut C 2012 Thyroid cancer cell lines: an overview. Front Endocrinol (Lausanne) **3**:133.
93. Rao AS, Goretzki PE, Kohrle J, Brabant G 2005 Letter re: Id1 Gene Expression in Hyperplastic and Neoplastic Thyroid Tissues. J Clin Endocrinol Metab **90**:5906.
94. Barsyte-Lovejoy D, Lau SK, Boutros PC, Khosravi F, Jurisica I, Andrulis IL, Tsao MS, Penn LZ 2006 The c-Myc oncogene directly induces the H19 noncoding RNA by allele-specific binding to potentiate tumorigenesis. Cancer Res **66**:5330–7.
95. Prendergast G, Ziff E 1991 Methylation-sensitive sequence-specific DNA binding

by the c-Myc basic region. Science (80-) **251**:186–189.
96. Ramlee M, Wang J, Toh W, Li S 2016 Transcription Regulation of the Human Telomerase Reverse Transcriptase (hTERT) Gene. Genes (Basel) **7**:50.
97. Bailey TL, Boden M, Buske FA, Frith M, Grant CE, Clementi L, Ren J, Li WW, Noble WS 2009 MEME SUITE: tools for motif discovery and searching. Nucleic Acids Res **37**:W202–W208.
98. Renaud S, Loukinov D, Bosman FT, Lobanenkov V, Benhattar J 2005 CTCF binds the proximal exonic region of hTERT and inhibits its transcription. Nucleic Acids Res **33**:6850–60.
99. Renaud S, Loukinov D, Abdullaev Z, Guilleret I, Bosman FT, Lobanenkov V, Benhattar J 2007 Dual role of DNA methylation inside and outside of CTCF-binding regions in the transcriptional regulation of the telomerase hTERT gene. Nucleic Acids Res **35**:1245–56.
100. Shukla S, Kavak E, Gregory M, Imashimizu M, Shutinoski B, Kashlev M, Oberdoerffer P, Sandberg R, Oberdoerffer S 2011 CTCF-promoted RNA polymerase II pausing links DNA methylation to splicing. Nature **479**:74–9.
101. Guilleret I, Benhattar J 2004 Unusual distribution of DNA methylation within the hTERT CpG island in tissues and cell lines. Biochem Biophys Res Commun **325**:1037–43.
102. Forbes SA, Bindal N, Bamford S, Cole C, Kok CY, Beare D, Jia M, Shepherd R, Leung K, Menzies A, Teague JW, Campbell PJ, Stratton MR, Futreal PA 2011 COSMIC: mining complete cancer genomes in the Catalogue of Somatic Mutations in Cancer. Nucleic Acids Res **39**:D945–50.
103. Kang K-W, Lee M-J, Song J-A, Jeong J-Y, Kim Y-K, Lee C, Kim T-H, Kwak K-B, Kim O-J, An HJ 2014 Overexpression of goosecoid homeobox is associated with chemoresistance and poor prognosis in ovarian carcinoma. Oncol Rep **32**:189–198.
104. Xue T-C, Ge N-L, Zhang L, Cui J-F, Chen R-X, You Y, Ye S-L, Ren Z-G 2014 Goosecoid promotes the metastasis of hepatocellular carcinoma by modulating the epithelial-mesenchymal transition. PLoS One **9**:e109695.
105. Ju X, Casimiro MC, Gormley M, Meng H, Jiao X, Katiyar S, Crosariol M, Chen K, Wang M, Quong AA, Lisanti MP, Ertel A, Pestell RG 2014 Identification of a cyclin D1 network in prostate cancer that antagonizes epithelial-mesenchymal restraint. Cancer Res **74**:508–19.
106. Taube JH, Herschkowitz JI, Komurov K, Zhou AY, Gupta S, Yang J, Hartwell K, Onder TT, Gupta PB, Evans KW, Hollier BG, Ram PT, Lander ES, Rosen JM, Weinberg RA, Mani SA 2010 Core epithelial-to-mesenchymal transition interactome gene-expression signature is associated with claudin-low and metaplastic breast cancer subtypes. Proc Natl Acad Sci U S A **107**:15449–54.
107. Avin BA, Wang Y, Gilpatrick T, Workman RE, Lee I, Timp W, Umbricht CB, Zeiger MA 2019 Characterization of human telomerase reverse transcriptase promoter methylation and transcription factor binding in differentiated thyroid cancer cell lines. Genes, Chromosom Cancer **58**:530-540.
108. Conaway JW 2012 Introduction to Theme “Chromatin, Epigenetics, and Transcription.” Annu Rev Biochem **81**:61–64.
109. Hashimshony T, Zhang J, Keshet I, Bustin M, Cedar H 2003 The role of DNA

methylation in setting up chromatin structure during development. Nat Genet **34**:187–192.
110. Wu K-J, Grandori C, Amacker M, Simon-Vermot N, Polack A, Lingner J, Dalla-Favera R 1999 Direct activation of TERT transcription by c-MYC. Nat Genet **21**:220–224.
111. Gilpatrick T, Lee I, Graham JE, Raimondeau E, Bowen R, Heron A, Sedlazeck FJ, Timp W 2019 Targeted Nanopore Sequencing with Cas9 for studies of methylation, structural variants and mutations. bioRxiv 604173.
112. Feng Y, Zhang Y, Ying C, Wang D, Du C 2015 Nanopore-based Fourth-generation DNA Sequencing Technology. Genomics Proteomics Bioinformatics **13**:4–16.
113. Ball MP, Li JB, Gao Y, Lee J-H, LeProust EM, Park I-H, Xie B, Daley GQ, Church GM 2009 Targeted and genome-scale strategies reveal gene-body methylation signatures in human cells. Nat Biotechnol **27**:361–8.
114. Chen Y-C, Elnitski L 2019 Aberrant DNA methylation defines isoform usage in cancer, with functional implications. PLoS Comput Biol **15**:e1007095.
115. Suzuki MM, Bird A 2008 DNA methylation landscapes: provocative insights from epigenomics. Nat Rev Genet **9**:465–476.
116. Landa I, Pozdeyev N, Korch C, Marlow LA, Smallridge RC, Copland JA, Henderson YC, Lai SY, Clayman GL, Onoda N, Tan AC, Garcia-Rendueles MER, Knauf JA, Haugen BR, Fagin JA, Schweppe RE 2019 Comprehensive Genetic Characterization of Human Thyroid Cancer Cell Lines: A Validated Panel for Preclinical Studies. Clin Cancer Res **25**:3141–3151.
117. McKelvey BA, Gilpatrick T, Wang Y, Timp W, Umbricht CB, Zeiger MA 2020 Characterization of Allele-Specific Regulation of Telomerase Reverse Transcriptase in Promoter Mutant Thyroid Cancer Cell Lines. Thyroid Published Online thy.2020.0055.
118. Esopi D, Graham MK, Brosnan-Cashman JA, Meyers J, Vaghasia A, Gupta A, Kumar B, Haffner MC, Heaphy CM, De Marzo AM, Meeker AK, Nelson WG, Wheelan SJ, Yegnasubramanian S 2020 Pervasive promoter hypermethylation of silenced TERT alleles in human cancers. Cell Oncol 1–15.
119. Xi L, Schmidt JC, Zaug AJ, Ascarrunz DR, Cech TR 2015 A novel two-step genome editing strategy with CRISPR-Cas9 provides new insights into telomerase action and TERT gene expression. Genome Biol **16**:231.
120. Tanaka J, Ogura T, Sato H, Hatano M 1987 Establishment and biological characterization of an in vitro human cytomegalovirus latency model. Virology **161**:62–72.
121. Fabien N, Fusco A, Santoro M, Barbier Y, Dubois PM, Paulin C 1994 Description of a human papillary thyroid carcinoma cell line. Morphologic study and expression of tumoral markers. Cancer **73**:2206–12.
122. Lemoine N, Mayall E, Jones T, Sheer D, McDermid S, Kendall-Taylor P, Wynford-Thomas D 1989 Characterisation of human thyroid epithelial cells immortalised in vitro by simian virus 40 DNA transfection. Br J Cancer **60**:897–903.
123. Nagarajan RP, Zhang B, Bell RJA, Johnson BE, Olshen AB, Sundaram V, Li D, Graham AE, Diaz A, Fouse SD, Smirnov I, Song J, Paris PL, Wang T, Costello JF

2014 Recurrent epimutations activate gene body promoters in primary glioblastoma. Genome Res **24**:761–74.
124. Krueger F, Andrews SR 2011 Bismark: a flexible aligner and methylation caller for Bisulfite-Seq applications. Bioinformatics **27**:1571–2.
125. Krueger F 2015 Babraham Bioinformatics - Trim Galore! Available at http://www.bioinformatics.babraham.ac.uk/projects/trim_galore/. Accessed July 6, 2018.
126. Hansen KD, Langmead B, Irizarry RA 2012 BSmooth: from whole genome bisulfite sequencing reads to differentially methylated regions. Genome Biol **13**:R83.
127. Robinson JT, Thorvaldsdóttir H, Winckler W, Guttman M, Lander ES, Getz G, Mesirov JP 2011 Integrative genomics viewer. Nat Biotechnol **29**:24–26.
128. Delmore JE, Issa GC, Lemieux ME, Rahl PB, Shi J, Jacobs HM, Kastritis E, Gilpatrick T, Paranal RM, Qi J, Chesi M, Schinzel AC, McKeown MR, Heffernan TP, Vakoc CR, Bergsagel PL, Ghobrial IM, Richardson PG, Young RA, Hahn WC, Anderson KC, Kung AL, Bradner JE, Mitsiades CS 2011 BET Bromodomain Inhibition as a Therapeutic Strategy to Target c-Myc. Cell **146**:904–917.
129. Novus Biologicals Chromatin Immunoprecipitation Protocol.
130. Haring M, Offermann S, Danker T, Horst I, Peterhansel C, Stam M 2007 Chromatin immunoprecipitation: optimization, quantitative analysis and data normalization. Plant Methods **3**:11.
131. Rio DC, Ares M, Hannon GJ, Nilsen TW 2010 Purification of RNA using TRIzol (TRI reagent). Cold Spring Harb Protoc **2010**:pdb.prot5439.
132. Li H 2018 Minimap2: pairwise alignment for nucleotide sequences. Bioinformatics **34**:3094–3100.
133. Simpson JT, Workman RE, Zuzarte PC, David M, Dursi LJ, Timp W 2017 Detecting DNA cytosine methylation using nanopore sequencing. Nat Methods **14**:407–410.
134. Jiang S, Tang M, Xin H, Huang J 2017 Assessing Telomerase Activities in Mammalian Cells Using the Quantitative PCR-Based Telomeric Repeat Amplification Protocol (qTRAP). Humana Press, New York, NY, pp 95–101.
135. Cong L, Ran FA, Cox D, Lin S, Barretto R, Habib N, Hsu PD, Wu X, Jiang W, Marraffini LA, Zhang F 2013 Multiplex Genome Engineering Using CRISPR/Cas Systems. Science **339**.
136. Yo J, Hay KSL, Vinayagamoorthy D, Maryanski D, Carter M, Wiegel J, Vinayagamoorthy T 2015 Detection of BRAF mutations from solid tumors using Tumorplex™ technology. MethodsX **2**:316–322.
137. Hou C, Dale R, Dean A 2010 Cell type specificity of chromatin organization mediated by CTCF and cohesin. Proc Natl Acad Sci U S A **107**:3651–6.
138. Barrilleaux BL, Cotterman R, Knoepfler PS 2013 Chromatin immunoprecipitation assays for Myc and N-Myc. Methods Mol Biol **1012**:117–33.
139. Iliopoulos D, Satra M, Drakaki A, Poultsides GA, Tsezou A 2009 Epigenetic regulation of hTERT promoter in hepatocellular carcinomas. Int J Oncol **34**:391–399.
140. Odrowaz Z, Sharrocks AD 2012 The ETS Transcription Factors ELK1 and GABPA Regulate Different Gene Networks to Control MCF10A Breast Epithelial

Cell Migration. PLoS One **7**:e49892.
141. Guterres A, Villanueva J 2020 Targeting telomerase for cancer therapy. Oncogene **39**:5811–5824.
142. Rowland T, Bonham A, Cech TR 2020 Allele-specific proximal promoter hypomethylation of the telomerase reverse transcriptase gene (TERT) associates with TERT expression in multiple cancers. Mol Oncol Published Online.

Curriculum Vitae

EDUCATION

Johns Hopkins University School of Medicine Baltimore, Maryland — Entered Fall 2015
Biochemistry, Cellular, and Molecular Biology PhD Program — Graduation October 2020
PhD Candidate

Clemson University Clemson, South Carolina — May 2015
Bachelor of Science, Genetics — Summa Cum Laude
Bachelor of Science, Biochemistry
Minor: Science and Technology in Society — GPA: 3.95/4.0
Calhoun Honors College
National Scholars Program

Cambridge University Cambridge, United Kingdom — Summer 2012
Courses in History of Science, Islam in the Middle Ages and the Effect on Western Medicine

GRANTS AND AWARDS

St. Jude National Graduate Student Symposium (NGSS) Selected Attendee 2020
One of 38 out of over 1,500 students selected by a faculty review committee to attend

Johns Hopkins' Martin Luther King, Jr. Award for Community Service 2019
Recognizes outstanding commitment to volunteer service by members of the Johns Hopkins community

GameChanger Award 2018
Recognizes excellence in profession, commitment to the community, and displayed leadership

National Science Foundation (NSF) Graduate Research Fellowship Program Fellowship 2017
Recognizes and supports outstanding graduate students in STEM obtaining PhDs

Thomas J. Kelly, MD, PhD and Mary L. Kelly Young Scholar Fund 2015-2016
Outstanding first-year graduate student at Johns Hopkins School of Medicine

Norris Medal Award 2015
Clemson University's most prestigious award for best all-around graduating student

Barry M. Goldwater National Award 2014
Support STEM college sophomores and juniors who show exceptional promise of being research leaders

Clemson University National Scholar 2011-2015
Full-tuition academic scholarship and enrichment program

Outstanding Senior in the Major of Genetics 2015
Awarded to one student in genetics at Clemson University

Phi Kappa Phi Merit Award 2015
Awarded to College of Agriculture Forestry and Life Sciences graduate on merit

RESEARCH EXPERIENCE

PhD Thesis, Department of Surgery Johns Hopkins University School of Medicine
PhD Student, PI- Dr. Christopher Umbricht and Dr. Martha Zeiger — Spring 2016-October 2020

— Understanding the role of the telomerase reverse transcriptase (TERT) promoter mutation on methylation and transcriptional activation and alternative splicing of the transcript in normal and cancer cells

— Discerning the allele-specific effects of the TERT promoter mutation on promoter methylation, chromatin marks, transcription factor binding, and mono-allelic expression through CRISPR/Cas9 editing and new sequencing technology- nanopore Cas9 targeted sequencing

Departmental Honors Study, Department of Genetics and Biochemistry Clemson University
Undergraduate Researcher, PI- Dr. Kerry Smith and Dr. Cheryl Ingram-Smith Fall 2011-2015

— Understanding the biochemical pathways associated with acetate production in eukaryotic microbial pathogens, specifically *Cryptococcus neoformans*
— Create knockouts of the three putative acetate transporters in the fungal pathogen to be characterized
— Investigation of acetate production by acetylated acetyl-CoA synthetase in the pathogen through creation of the modified enzyme and assaying production of acetate

National Cancer Institute's Integrative Cancer Biology Program, Department of Cancer Biology Vanderbilt University, Nashville, TN
Summer Intern, PI- Dr. Vito Quaranta, Mentor- Dr. Katherine Jameson Summer 2014

— Identification of biomarkers correlating with drug response in non-small cell lung cancer
— Employed fluorescent live-cell microscopy to quantitatively measure drug response heterogeneity in cancer cell lines using R programming
— Analyzed molecular correlates identified in broad-scale proteomic analysis for potential biomarkers indicative of drug response
— Assayed tumor volume growth dynamics through ultrasound measurements of xenografts in mice

Summer Undergraduate Research Experience (SURE) Program, Department of Biochemistry Emory University, Decatur, GA
Summer Intern, PI- Dr. Anita Corbett, Mentor- Dr. Katherine Mills-Lujan Summer 2013

— Molecular modeling of neurodegenerative disease pontocerebellar hypoplasia type 1
— Experimentally mutated the yeast exosome subunit mimicking patient mutations through site-directed mutagenesis
— Applied various assays to observe effect of mutations on transcript (qRT-PCR), protein (Western Blot), and organismal (spot growth) level

CONFERENCE PRESENTATIONS

BA. McKelvey, T. Gilpatrick, Y. Wang, W. Timp, C.B. Umbricht, and M.A. Zeiger. Characterization of Allele-Specific Regulation of Telomerase Reverse Transcriptase in Promoter-Mutant Thyroid Cancer Cell Lines. **Invited Session Panelist** October 2020 American Society of Human Genetics Annual Meeting.

BA. McKelvey, T. Gilpatrick, Y. Wang, W. Timp, C.B. Umbricht, and M.A. Zeiger. Allele-Specific Regulation of Telomerase Reverse Transcriptase (TERT) In TERT Promoter-Mutant Thyroid Cancer Cell Lines. **Invited Oral Presentation** May 2020 for The Sidney Kimmel Comprehensive Cancer Center Fellows' Research Day.

BA. McKelvey, T. Gilpatrick, Y. Wang, W. Timp, C.B. Umbricht, and M.A. Zeiger. Characterization of Telomerase Reverse Transcriptase Promoter Regulation in Thyroid Cancer Cell Lines. **Invited Oral Presentation** January 2020 at the NIH Surgery Oncology Program.

B. Avin, T. Gilpatrick, Y. Wang, W. Timp, C.B. Umbricht, and M.A. Zeiger. Allele-Specific Effects of the TERT Mutation in Thyroid Cancer Cell Lines. **Selected Oral Presentation** October 2019 at the Annual Meeting of American Thyroid Association.

B. Avin, Y. Wang, T. Gilpatrick, I. Lee, R. Workman, W. Timp, C.B. Umbricht, and M.A. Zeiger. Characterization of Telomerase Reverse Transcriptase Promoter Regulation in Thyroid Cancer Cell Lines. **Selected Oral Presentation** August 2019 at International Association of Endocrine Surgeons Meeting. Presented by M.A. Zeiger.

B. Avin, T. Gilpatrick, Y. Wang, W. Timp, C.B. Umbricht, and M.A. Zeiger. Transcription Factor Binding at the Telomerase Promoter in Thyroid Cancer. **Selected Oral Presentation** October 2018 at the Annual Meeting of American Thyroid Association.

B. Avin, Y. Wang, T. Gilpatrick, W. Timp, C.B. Umbricht, and M.A. Zeiger. The Effect of the Telomerase Reverse Transcriptase Promoter Mutation on Promoter Methylation, Transcription Factor Binding, and Transcriptional Activation in Thyroid Cancer. Poster presented June 2019 at the Johns Hopkins Department of Surgery's Research Day. **1st Place Poster Presentation Award for Student Presenter**.

B. Avin, Y. Wang, I. Lee, R. Workman, L. Florea, W. Timp, C.B. Umbricht, and M.A. Zeiger. Understanding the Epigenetic Regulation of Alternative Splicing of Human Telomerase Reverse Transcriptase. Poster presented October 2017 at the Annual Meeting of the American Thyroid Association.

B. Avin, Y. Wang, I. Lee, R. Workman, L. Florea, W. Timp, C.B. Umbricht, and M.A. Zeiger. Understanding the Epigenetic Regulation of Alternative Splicing of Human Telomerase Reverse Transcriptase. Poster presented May 2017 at the Johns Hopkins Department of Surgery's Research Day.

B. Avin, Y. Wang, I. Lee, R. Workman, L. Florea, W. Timp, C.B. Umbricht, and M.A. Zeiger. The Link between Human Telomerase Reverse Transcriptase (hTERT) Promoter Methylation Status and Alternative Splicing in Thyroid Cancer. Poster presented September 2016 at the Annual Meeting of American Thyroid Association. **Chosen as a Featured Poster for the Trainee Poster Contest.**

B. Avin, K. Jameson, P. Frick, D. Tyson, L. Estrada, and V. Quaranta. Identification of Biomarkers Correlating with Drug Response in Non-Small Cell Lung Cancer. Poster presented April 2015 at the Annual Meeting of the American Association for Cancer Research, Undergraduate Student Caucus. **3rd Place Award for National Undergraduate AACR Poster Competition.**

B. Avin, K. Jameson, P. Frick, D. Tyson, L. Estrada, and V. Quaranta. Identification of Biomarkers Correlating with Drug Response in Non-Small Cell Lung Cancer. Poster presented August 2014 at NCI's ICBP Summer Cancer Research Virtual Poster Session.

B. Arnson, **B. Avin**, J. Tumolo, M. Reinhart, C. Ingram-Smith, K. Smith. Characterization of the *Cryptococcus neoformans* Acetyl-CoA Synthetase. Poster presented October 2013 at the Cell Biology of Eukaryotic Pathogens Symposium, Clemson University.

B. Avin, S. Brutus, K. Mills Lujan and A.H. Corbett. Molecular Modeling of Neurodegenerative Disease Pontocerebellar Hypoplasia Type 1: Functional Studies of *S. cerevisiae* Rrp40. Poster presented August 2013 at the Emory University SURE Poster Session. **Awarded Most Popular Poster Award for Summer Undergraduate Research Experience Program.**

REVIEW ARTICLES

BA. McKelvey, C. Umbricht, M. Zeiger. Telomerase Reverse Transcriptase (TERT) Regulation in Thyroid Cancer: A Review. *Frontiers in Endocrinology*. 2020 July. doi: 10.3389/fendo.2020.00485

B. Avin, C. Umbricht, M. Zeiger. Human Telomerase Reverse Transcriptase (hTERT) Regulation by DNA Methylation, Transcription Factor Binding and Alternative Splicing. *International Journal of Oncology*. 2016;49(6):2199-2205. doi: 10.3892/ijo.2016.3743

PEER-REVIEWED PUBLICATIONS

BA. McKelvey, MA. Zeiger, and CB. Umbricht. Exploring the Epigenetic Regulation of Telomerase Reverse Transcriptase (TERT) in Human Cancer Cell Lines: Invited Commentary. *Molecular Oncology*. Accepted September 2020. doi: 10.1002/1878-0261.12798

BA. McKelvey, T. Gilpatrick, Y. Wang, W. Timp, C.B. Umbricht, and M.A. Zeiger. Characterization of Allele-Specific Regulation of Telomerase Reverse Transcriptase in Promoter Mutant Thyroid Cancer Cell Lines. *Thyroid.* Published Online 2020 Mar. doi: 10.1089/thy.2020.0055

B. Avin, Y. Wang, T. Gilpatrick, R. Workman, I. Lee, W. Timp, C.B. Umbricht, and M.A. Zeiger. Characterization of Human Telomerase Reverse Transcriptase Promoter Methylation and Transcription Factor Binding in Differentiated Thyroid Cancer Cell Lines. *Genes Chromosomes and Cancer.* 2019 Aug;58(8):530-540. doi: 10.1002/gcc.22735

M.B. Fasken, J.S. Losh, S.W. Leung, S. Brutus, **B. Avin**, J.C. Vaught, J. Potter-Birriel, T. Craig, G.L. Conn, K. Mills-Lujan, A.H. Corbett, A. van Hoof. Insight into the RNA Exosome Complex Through Modeling Pontocerebellar Hypoplasia Type 1b Disease Mutations in Yeast. *Genetics*. 2017; 205(1):221-237. doi: 10.1534/genetics.116.195917

BOOK CHAPTERS

B. Avin, Z. Sahli, M.A. Zeiger. "Molecular Biology of Endocrine Tumors" *11th edition of Principles and Practice of Oncology.* 2018.

LEADERSHIP

American Thyroid Association Diversity, Equity and Inclusion Task Force	2019-Present
American Thyroid Association Strategic Planning Participant	2019
American Thyroid Association Women in Thyroidology Task Force	2017-2019

WRITING OUTREACH

Author for NCI's "Patient Sensitivity Guidelines for Principal Investigators"	2020
Author for NCI DCCPS "Evidence-Based Approaches for Survivorship Care"	2020
Author for FDA's "Histology Agnostic Drug Development"	2020
Writer for OncoBites, a blog focused on cutting-edge cancer research without jargon	2019-Present
Writer for the Biomedical Odyssey, the Hopkins graduate student blog	2017-2018
Designer of an online teaching module for the Epigenetics course for Hopkins graduate students	2017
Writer for *Tigra Scientifica,* Clemson University's popular science journal	2013
Writer for CancerQuest, a cancer education scientific research resource	2013

PATIENT- RESEARCH ADVOCACY

Association for Clinical Oncology: Improving Access to Clinical Trials Speaker	2020
Accelerating Anticancer Agent Development Validation: Drug Development Panelist	2019
ThyCa: Thyroid Cancer Survivors' Association Person to Person Network Advocate	2019-Present
NCI Technology Research Advocacy Partnership (NTRAP) Advocate	2016-Present
One Voice Against Cancer's On the Horizon Opportunities &Challenges in Cancer Research Speaker	2018
American Cancer Society Cancer Action Network Lead Advocate	2017-Present
ThyCa National Representative at AACR Scientist to Survivor Program	2016

SCIENCE POLICY OUTREACH

Johns Hopkins Science Policy Group President	2019-2020
Selected American Association for Cancer Research (AACR) Early-Career Hill Day Participant	2019
AACR Panelist- How to Effectively Advocate for Cancer Research and Science-Based Policy	2019
Johns Hopkins Science Policy Group Advocacy Chair	2017-2019
Selected Representative for the AAAS Catalyzing Advocacy in Science Engineering Program	2019

PROFESSIONAL ASSOCIATIONS

American Association for the Advancement of Science
American Society of Human Genetics
American Association for Cancer Research
American Thyroid Association